Supporting Information for

Enantiopure nanohoops through racemic resolution of diketo[n]CPPs by chiral derivatization as precursors to DBP[n]CPPs

Contents

1 Materials and Methods S3
2 Synthetic Manipulations S6
2.1 Synthesis of DBP[6]CPP hoop **1** S6
2.2 Synthesis of DBP[7]CPP hoop **2** S14
2.3 Chiral Resolution of **3** and Synthetic Transformation to **(*M*)-1** and **(*P*)-1** S20
2.3.1 Assignment of Stereodescriptors in Enantiopure Nanohoops **1** S26
2.3.2 HPLC Elugrams S27
3 NMR Spectra S29
3.1 NMR Spectra of Synthesized Title Compounds S29
3.2 NMR Spectra of Sulfoximine Adducts S49
4 Mass Spectrometry S66
5 Absorption Spectra S74
6 Solvatochromic Effects in Emission Spectra S75
7 Cyclic Voltammograms S76
8 Circular Dichroism and Circularly Polarized Luminescence S77
9 Thermodynamics of *ortho*-Tolyl-Rotation at the 5,10-Positions of DBP S80
10 Single Crystal X-Ray Diffraction S81
10.1 General Experimental Setup and Solution S81
10.2 Refinement Details for Each Crystal S85
10.2.1 Crystal Structure of **1**•(cyclohexane) (pentane) S85
10.2.2 Crystal Structure of **2**•(pentane) S86
10.2.3 Crystal Structure of **2**•(PhCl)2 (i PrOH)0.5 ..... S87
10.2.4 Crystal Structure of **(S,S)-3**•(PhCl) S88

10.2.5 Crystal Structure of **9** S89
10.2.6 Crystal Structure of **8a** S89
10.2.7 Crystal Structure of **5** S90
10.2.8 Crystal Structure of **S6** S90
10.2.9 Crystal structure of **S7** S90
11 DFT Calculations S91
11.1 Strain Energies S91
11.2 Calculation of Racemization Barriers S94
11.3 NICS Calculations S95
11.4 TD-DFT Calculations S96
12 References S100

1 Materials and Methods

All **solvents** and **chemicals** were purchased from commercial sources and used directly without further purification unless otherwise stated. Moisture or oxygen-sensitive reactions were carried out in dried glassware, heated under vacuum (10^{-3} mbar), using standard Schlenk techniques in a dry argon atmosphere (Argon 5.0 from SAUERSTOFFWERKE FRIEDRICHSHAFEN). Anhydrous solvents (CH_2Cl_2, THF) were obtained from an M. BRAUN solvent purification system (MB-SPS-800) and stored over molecular sieves (3 Å). Anhydrous 1,4-Dioxane was purchased from ACROS-ORGANICS (extra dry, < 50 ppm H_2O) and further stored over activated molecular sieves (3 Å). Cyclohexane for flash chromatography was purchased in technical grade and purified by distillation using a rotary evaporator. Other solvents were purchased and used in analytical or HPLC grade.

Analytical thin layer chromatography was carried out using silica gel-coated aluminium plates with a fluorescence indicator (MERCK 60 F_{254}). Detection was carried out by using short wave UV light (λ_{max} = 254 nm) and long wave UV light (λ_{max} = 356 nm).

Flash column chromatography was carried out using silica gel 60, grain size 40-63 µm (230-400 mesh) from MACHERY-NAGEL. In some cases, an automated flash chromatography system (GRACE Reveleris X2) was employed using prepacked columns (silica gel, 25 g to 80 g, 30 µm grain size) from INTERCHIM (INTERCHIM Puriflash Silica HP 30 µm flash column).

NMR spectra were recorded at 300 K, unless otherwise stated, on the following spectrometers: BRUKER *Avance III HD 300* [300.1 MHz (1H)], BRUKER *Avance II 400* [400.1 MHz (1H), 100.6 MHz (13C)], BRUKER *Avance Neo 400* with a *Prodigy CryoProbe* [400.1 MHz (1H), 100.6 MHz (13C)] and BRUKER *Avance III HD 500* [500.3 MHz (1H), 125.8 MHz (13C)]. Chemical shifts are reported in parts per million (ppm, δ scale) relative to the signal of tetramethylsilane (δ = 0.00 ppm). ^{1}H NMR spectra are referenced to tetramethylsilane as an internal standard or the residual solvent signal of the respective solvent: $CDCl_3$: δ = 7.26 ppm; CD_2Cl_2: δ = 5.32 ppm, C_6D_6: δ = 7.16 ppm, DMSO-d_6: δ = 2.50 ppm, toluene-d_8: δ = 2.03 ppm. ^{13}C NMR spectra are referenced to the following signals: $CDCl_3$: δ = 77.16 ppm; CD_2Cl_2: δ = 53.84 ppm, C_6D_6: δ = 128.06 ppm, DMSO-d_6: δ = 39.52 ppm, toluene-d_8: δ = 20.43 ppm.[1] Analysis followed first order, and the following abbreviations for multiplets were used: singlet (s), broad singlet (br. s), doublet (d), triplet (t), quartet (q), septet (sept), multiplet (m) and combinations thereof i.e. doublet of doublets (dd). Coupling constants (*J*) are given in Hertz [Hz].

High resolution mass spectra were measured on a THERMO FISHER SCIENTIFIC Exactive via electrospray ionization (ESI) or atmospheric pressure chemical ionization (APCI) with an orbitrap analyzer.

UV/Vis absorption spectra were measured on a SHIMADZU UV-1800 using Quartz (*Suprasil*) cuvettes (1 cm path length) from HELLMA ANALYTICS. Extinction coefficients were measured by serial dilution. Spectra were measured in 10 steps from 10^{-6} to 10^{-5} M. Extinction coefficient values were then averaged over all measurements.

Fluorescence spectra were measured on a JASCO FP-8300 Spectrofluorometer in 10 mm Quartz cuvettes and with the spectral correction (combined spectral correction data created with a rhodamine B solution and a JASCO calibrated light source) turned on. A JASCO STR-812 water thermostated cell holder was used

with the temperature set to 298 Kelvin. Higher-order light effects are cancelled out with a built-in filter. Excitation and emission bandwidth were set to 5 nm. Analyte concentrations were below 10^{-6} M **Photoluminescence Quantum Yields** were measured on the same fluorimeter using an JASCO ILF-835 100 mm integrating sphere and 1 mm quartz cuvettes. The PLQYs are corrected for indirect excitation and incident light spectra. The given values always refer to the internal quantum efficiency which is defined as the ratio of the number of photons in the emission from the sample to the number of photons in the excitation light absorbed by the sample.

Cyclic voltammograms (CVs) and differential pulse voltammograms (DPVs) were measured inside an argon-filled glovebox using a PGSTAT128N or PGSTAT302N potentiostat by METROHM AUTOLAB. As working electrode, a glassy carbon disc electrode (2 mm diameter) was used, as counter electrode a platinum rod was used, as reference electrode a silver wire was used. The analyte solution contained 10 mL of solvent (anhydrous degassed CH_2Cl_2 or THF) with 0.1 M *n*-Bu_4NPF_6 and the analyte in a 1 mM concentration. The ferrocene/ferrocenium redox couple was used as an internal reference. HOMO and LUMO levels were calculated using the following equations: E_{LUMO} (eV) = -($E_{i,Fc}$+x_{Red}) (with $E_{i,Fc}$ = 4.8 eV (ionization energy of ferrocene[2]); x_{Red} = onset of the first reduction peak, calibrated vs Fc/Fc^+ in eV), E_{HOMO} (eV) = -($E_{i,Fc}$+x_{Ox}) with x_{Ox} = onset of the first oxidation peak, calibrated vs Fc/Fc^+ in eV).

Analytical HPLC was performed using an AGILENT TECHNOLOGIES 1290 Infinity II with a G1311B-1260 Quat pump, a G7117A-1290 DAD FS detector, a G7129A-1260 Vialsampler autosampler, a G7116B-1290 MCT column oven using AGILENT Open LAB CDS (EZChrome Edition) software version A.04.07. A chiral column, DAICEL Chiralpak IA (250 mm × 4.6 mm, 5 µm) was used.

Circular Dichroism (CD) spectra were recorded on a JASCO J-815 spectropolarimeter equipped with a Peltier thermostated cell holder and Xe laser. Data were recorded in distilled CH_2Cl_2 or toluene (analytical grade) at 20 °C using a 1 × 10 mm cell. The obtained signals were processed by subtracting solvent and cell contribution.

The **Circularly Polarized Luminescence** (CPL) measurements were performed using a commercialized instrument JASCO CPL-300 at room temperature in 10 × 10 mm cell. Data pitch was set at 1 nm, scanning speed was set at 100 nm/min and spectra displayed are mean values of a minimum of 10 accumulations. Beforehand CPL measurement, absorption spectra were recorded on a UV-CARY 50 and optical density was checked to be below 0.1 for the first absorption transition for **3**. Then emission spectra were recorded with Fluoromax-3 (HORIBA) spectrofluorometer.

Absorbance dissymmetry factor is defined as follow[3]:

$$g_{abs}(\lambda) = \frac{\Delta\varepsilon(\lambda)}{\varepsilon(\lambda)}$$

where $\Delta\varepsilon(\lambda)$ and $\varepsilon(\lambda)$ correspond to the ECD and the molar extinction coefficient, respectively, at the wavelength λ.

Luminescence dissymmetry factor is defined as follow[3]:

$$g_{lum}(\lambda) = 2 \times \frac{\Delta I(\lambda)}{I(\lambda)} = 2 \times \frac{I_L(\lambda) - I_R(\lambda)}{I_L(\lambda) + I_R(\lambda)}$$

Where I_L (λ)and I_R (λ) are respectively the left and right intensity of the spontaneous emission of circularly polarized light, Δ*I* (λ) the intensity difference between them and *I* (λ) the total luminescence intensity.

2 Synthetic Manipulations

2.1 Synthesis of DBP[6]CPP hoop 1

5[4], **6a**[5] and **6b**[6] were synthesized according to previously reported procedures.

2,7-Bis(4,4,5,5-tetramethyl-1,3,2-dioxaborolan-2-yl)-4b,9b-dihydroindeno[2,1-*a*]indene-5,10-dione (5)

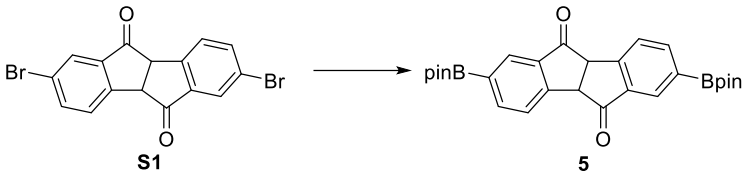

Diketone **S1** (1.00 g, 2.55 mmol, 1.00 eq.), bis(pinacolato)diboron (1.43 mg, 5.61 mmol, 2.2 eq.), KOAc (1.50 g, 15.3 mmol, 6.0 eq.) and $PdCl_2$(dppf) (22 mg, 30 µmol, 10 mol%) were dissolved in degassed, anhydrous 1,4-dioxane (25 mL) and stirred at 90°C for 19 h. The dark-brown solution was cooled to room temperature and quenched with H_2O. The mixture was extracted with CH_2Cl_2 (3 × 30 mL), dried over Na_2SO_4, and the solvents were removed under reduced pressure. The crude product was washed with EtOH to yield the title compound as an off-white solid (1.00 g, 81%).

***R*$_f$** 0.40 (cyclohexane/EtOAc: 6/1); **^{1}H NMR** (400 MHz, $CDCl_3$): δ 8.17 (dd, *J* = 1.2, 0.9 Hz, 2H), 8.08 (dd, *J* = 7.7, 1.2 Hz, 2H), 7.90 (dd, *J* = 7.7, 0.9 Hz, 2H), 4.40 (s, 2H), 1.32 (s, 12H), 1.31 (s, 12H); **^{13}C NMR** (101 MHz, $CDCl_3$): δ 201.2, 152.5, 142.0, 134.5, 131.7, 126.0, 84.4, 53.0, 25.0, 25.0; **HRMS** (pos. ESI): *m/z* calcd for $C_{28}H_{33}{}^{11}B_2O_6$ 487.2457 $[M+H]^+$, found 487.2456.

2,7-Bis(4-((1s,4s)-4-(4-bromophenyl)-1,4-bis(methoxymethoxy)cyclohexyl)phenyl)-4b,9b-dihydroindeno[2,1-*a*]indene-5,10-dione (7a)

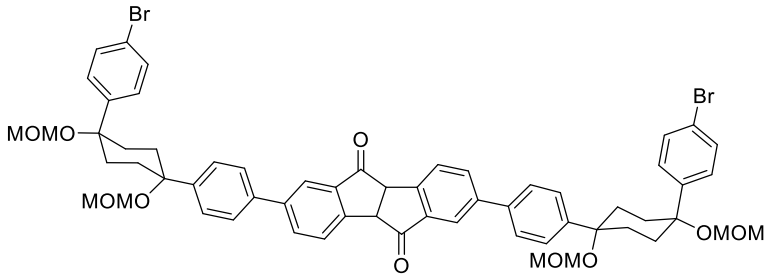

MOM = $-CH_2OCH_3$

Borylated diketone **5** (0.40 g, 0.82 mmol, 1.00 eq.), corner unit **6a** (1.88 g, 3.29 mmol, 4.00 eq.), K_2CO_3 (1.14 g, 8.23 mmol, 10.0 eq.) and $Pd(dppf)Cl_2$ (30 mg, 0.04 mmol, 5 mol%) were added to a mixture of toluene (40 mL), dioxane (40 mL) and water (8 mL). The mixture was purged with argon for 1 h and then refluxed for 48 h under an argon atmosphere. Water was added and the mixture was extracted with CH_2Cl_2. The combined organic layers were washed with brine and dried over Na_2SO_4. The solvents were removed under reduced pressure and the crude product was purified by column chromatography (silica gel, cyclohexane/EtOAc, 10/1 to 2/1). The title compound (0.50 g, 0.45 mmol, 55%) was obtained as a white solid.

***R*$_f$** 0.13 (cyclohexane/EtOAc: 2/1); ^{1}**H NMR** (500 MHz, $CDCl_3$): δ 8.00–7.97 (m, 2H), 7.91–7.88 (m, 4H), 7.53–7.47 (m, 8H), 7.46–7.42 (m, 4H), 7.34–7.29 (m, 4H), 4.48 (s, 2H), 4.45 (s, 4H), 4.42 (s, 4H), 3.41 (s, 6H), 3.40 (s, 6H), 2.39 – 2.26 (m,8H), 2.19 – 1.98 (m, 8H).; ^{13}**C NMR** (126 MHz, $CDCl_3$): δ 201.5, 148.8, 142.1, 138.8, 135.7, 135.0, 131.6, 128.8 (bs), 127.6 (bs), 127.2, 127.0, 122.9, 121.8, 92.4, 92.3, 78.1, 78.0, 56.2, 56.2, 52.9, 33.0 (bs); The compound could not be detected in mass spectrometric measurements.

8a

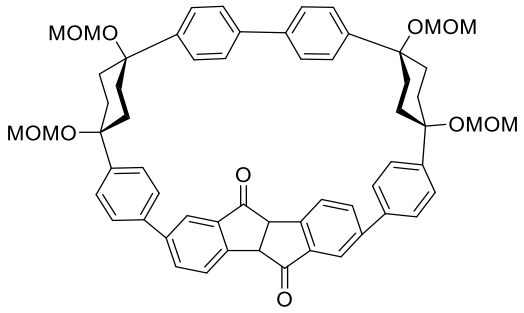

Acyclic precursor **7a** (100 mg, 91 µmol, 1.00 eq.), bis(1,5-cyclooctadiene)nickel(0) (75 mg, 272 µmol, 3.00 eq.) and 2,2'-bipyridine (57 mg, 363 µmol, 4.00 eq.) were dissolved in anhydrous THF (50 mL) and stirred at room temperature for 30 min and then at 65 °C for 22 h under an argon atmosphere. The mixture was cooled to room temperature and passed through a pad of Celite® (washed with mixture of CH_2Cl_2 and EtOAc). The solvents were removed under reduced pressure, and the crude product was purified by column chromatography (silica gel, cyclohexane/EtOAc, 10/1 to 1/1). The title compound (34 mg, 31.5 µmol, 40%) was obtained as a white solid.

***R*$_f$** 0.50 (cyclohexane/EtOAc: 1/1); ^{1}**H NMR** (400 MHz, $CDCl_3$): δ 7.85–7.83 (m, 4H), 7.77–7.76 (m, 2H), 7.48–7.45 (m, 4H), 7.42–7.39 (m, 4H), 7.36–7.32 (m, 4H), 7.30–7.27 (m, 4H), 4.57 (s, 2H), 4.57 (s, 2H), 4.55 (s, 2H), 4.55 (s, 2H), 4.50 (s, 2H), 3.42 (s, 6H), 3.41 (s, 6H), 2.31–2.21 (m, 8H), 2.15–1.69 (m, 8H); ^{13}**C NMR** (101 MHz, $CDCl_3$): δ 202.3, 148.9, 141.6, 139.4, 137.7, 134.4, 133.9, 128.0, 127.2, 127.0, 126.9, 126.7, 122.9, 92.6, 92.6, 77.9, 77.7, 56.1, 56.0, 53.1, 34.0, 33.4, 33.3, 33.0.; **HRMS** (pos. ESI): *m/z* calcd for $C_{60}H_{60}NaO_{10}$ 963.4079 $[M+Na]^+$, found 963.4088.

2,7-Bis((1's,4's)-4''-bromo-1',4'-dimethoxy-1',4'-dihydro-[1,1':4',1''-terphenyl]-4-yl)-4b,9b-dihydroindeno[2,1-*a*]indene-5,10-dione (7a)

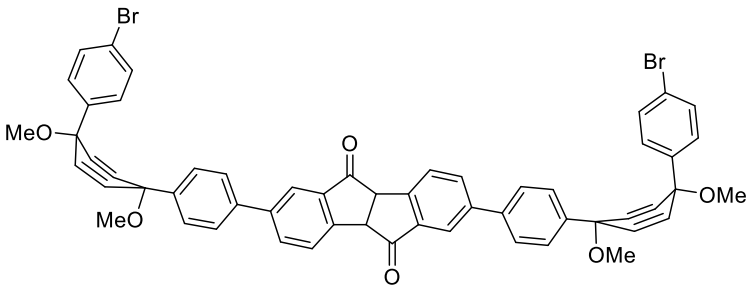

Borylated diketone **5** (0.090 g, 0.18 mmol, 1.00 eq.), **6b** (0.35 g, 0.79 mmol, 4.50 eq.), K_2CO_3 (0.24 g, 1.75 mmol, 10.0 eq.) and Pd(dppf)Cl_2 (9 mg, 0.01 mmol, 7 mol%) were added to a mixture of toluene (8 mL), dioxane (8 mL) and water (1 mL). The mixture was purged with argon for 1 h and then refluxed for 20 h under an argon atmosphere. Water was added, and the mixture was extracted with CH_2Cl_2. The combined organic layers were washed with brine and dried over Na_2SO_4. The solvents were removed under reduced pressure, and the crude product was purified by column chromatography (silica gel, cyclohexane/EtOAc, 1/0 to 4/1). The title compound (0.10 g, 59%) was obtained as a white solid.

***R*$_f$** 0.19 (cyclohexane/EtOAc: 4/1); [1]**H NMR** (300 MHz, $CDCl_3$): δ 8.00–7.97 (m, 2H), 7.91–7.88 (m, 4H), 7.53–7.47 (m, 4H), 7.46–7.42 (m, 8H), 7.34–7.29 (m, 4H), 6.17–6.12 (m, 4H), 6.10–6.05 (m, 4H), 4.48 (s, 2H), 3.41 (s, 6H), 3.40 (s, 6H); **^{13}C NMR** -[1]; **HRMS** (pos. ESI): *m/z* calcd for $C_{56}H_{44}Br_2NaO_6$ 993.1397 $[M+Na]^+$, found 993.1385.

[1] Due to relatively fast decomposition no clean ^{13}C NMR spectrum could be measured.

8b

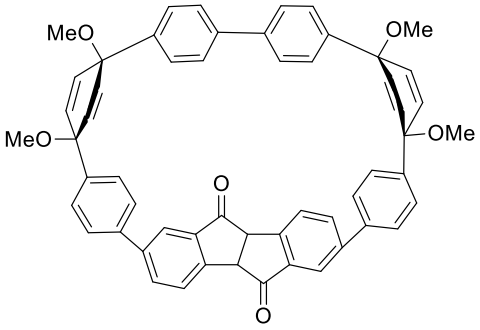

Acyclic precursor **7b** (220 mg, 0.23 mmol, 1.00 eq.), bis(1,5-cyclooctadiene)nickel(0) (187 mg, 0.68 mmol, 3.00 eq.) and 2,2'-bipyridine (141 mg, 0.91 mmol, 4.00 eq.) were dissolved in anhydrous THF (150 mL) and stirred at room temperature for 40 min and then at 65 °C for 44 h under an argon atmosphere. The mixture was cooled down to room temperature and passed through a pad of Celite® (washed with mixture of CH_2Cl_2 and EtOAc). The solvents were removed under reduced pressure, and the crude product was purified by column chromatography (silica gel, cyclohexane/EtOAc, 1/0 to 4/1). The title compound (70 mg, 38%) was obtained as a white solid.

***R*$_f$** 0.67 (cyclohexane/EtOAc: 1/1); ^{1}**H NMR** (500 MHz, $CDCl_3$): δ 7.88–7.85 (m, 2H)[2], 7.76–7.73 (m, 4H), 7.50–7.46 (m, 4H), 7.41–7.37 (m, 4H), 7.33–7.30 (m, 4H), 7.21–7.18 (m, 4H), 6.24–6.20 (m, 4H), 6.07–6.03 (m, 4H), 4.57 (s, 2H), 3.44 (s, 6H), 3.43 (s, 6H).; ^{13}**C NMR** (126 MHz, $CDCl_3$): δ 202.4, 148.8, 143.1, 142.9, 142.0, 134.9, 134.3, 134.1, 134.0, 133.0, 132.7, 127.7, 126.8, 126.8, 126.7, 126.1, 123.9, 75.0, 74.6, 53.1, 52.2, 51.9; **HRMS** (neg. ESI): *m/z* calcd for $C_{53}H_{35}O_4$ 735.2541 $[M\text{-}2OMe\text{-}Me]^-$, found 735.2541.

[2] For the two multiplets (7.88–7.85 and 7.76–7.73) one would expect three separate *dd* signals. Two of them are overlapping and one is only resolved as a *doublet*, which makes the assignment of coupling constants difficult.

Diketon-based hoop 3

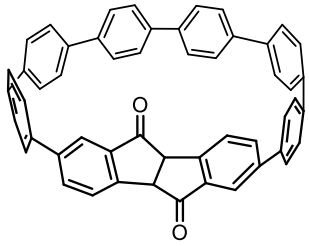

Synthesis from **8a:** Cyclic **8a** (108 mg, 115 µmol, 1.00 eq.), $NaHSO_4 \cdot H_2O$ (530 mg, 3.44 mmol, 30.0 eq.) and 2,3-dichloro-5,6-dicyano-1,4-benzoquinone (130 mg, 574 mmol, 5.00 eq.) were dissolved in a mixture of mesitylene (10 mL) and DMSO (1 mL) and stirred at 155 °C on air for 19 h. The mixture was passed through a pad of Celite® (washed with mixture of CH_2Cl_2 and EtOAc). The solvent was removed under reduced pressure and the crude product was purified by column chromatography (silica gel, cyclohexane/EtOAc, 20/1 to 10/1). The title compound was obtained as a yellowish solid (12 mg, 15%[3]).

Synthesis from **8b:** In a 250 mL round bottom flask $SnCl_2 \cdot 2\ H_2O$ (1.05 g, 4.64 mmol, 65.0 eq.) was dissolved in freshly distilled[4] THF (60 mL). Concentrated aqueous HCl (12 M, 0.77 mL, 9.28 mmol, 130 eq.) was added, and the resulting solution was stirred at room temperature for 1 h. **8b** (58 mg, 71 µmol, 1.00 eq.) was dissolved in freshly distilled THF (25 mL) and then slowly added to the reaction mixture. After stirring at room temperature for 3 hours the reaction was quenched through addition of aqueous saturated $NaHCO_3$ solution. The mixture was extracted with CH_2Cl_2, washed with brine and dried over Na_2SO_4. The solvent was removed under reduced pressure, and the crude product was purified by column chromatography (silica gel, cyclohexane/EtOAc: 1/0 to 9/1). The title compound (37 mg, 75%) was obtained as a yellowish solid.

R_f 0.45 (cyclohexane/EtOAc: 2/1); **^{1}H NMR** (500 MHz, $CDCl_3$, 333 K): δ 7.89 (dd, *J* = 8.3, 1.9 Hz, 2H), 7.81 (dd, *J* = 8.2, 0.6 Hz, 2H), 7.70 (dd, *J* = 1.9, 0.6 Hz, 2H), 7.54 (s, 8H), 7.50–7.48 (m, 4H), 7.48–7.46 (m, 4H), 7.39–7.36 (m, 4H), 7.36–7.34 (m, 4H), 4.48 (s, 2H); **^{13}C NMR** (126 MHz, $CDCl_3$, 333 K): δ 202.4, 148.6, 141.7, 140.2, 138.7, 138.2, 138.0, 137.6, 136.8, 134.5, 133.7, 127.9, 127.9, 127.8, 127.8, 127.7, 127.3, 127.1, 122.9, 53.0; **HRMS** (pos. ESI): *m/z* calcd for $C_{52}H_{32}O_2$ 688.2397 $[M]^+$, found 688.2408; **UV/Vis** (CH_2Cl_2): λ (ε in $M^{-1}cm^{-1}$) = 325 (6.4×10^4), 367 (shoulder, 1.7×10^4), 390 (shoulder, 1.3×10^4), **Fluorescence** (CH_2Cl_2): λ_{max} = 481 nm.

[3] The reaction from **8a** was not well reproducible regarding its yield, and the subsequent Grignard-addition with products obtained from this reaction led to very poor or no yields.

[4] To remove the dibutylhydroxytoluene (BHT, 200 ppm) as stabilizer

S2

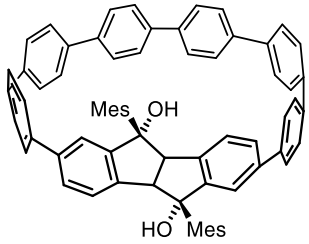

In a Schlenk tube anhydrous $CeCl_3$ (65 mg, 261 µmol, 4.00 eq.) was dried at 130 °C *in vacuo* (10^{-3} mbar) for 5 h. After cooling to room temperature and introducing argon, anhydrous THF (3.5 mL) was added. The mixture was stirred at room temperature for 19 h. In a separate Schlenk[5] tube **3** (45 mg, 65 µmol, 1.00 eq.) was dissolved in anhydrous THF (3.5 mL), added to the reaction mixture and then stirred at room temperature for 4.5 h. A solution[6] of mesityl magnesium bromide in THF (0.92 M, 0.28 mL, 255 µmol, 3.90 eq.), was added to the $CeCl_3$ suspension at 0 °C. The resulting mixture was stirred at 0 °C for 1 h. The solution was allowed to warm up to room temperature and was stirred for another 2 h. Aq. AcOH (10%, 10 mL) was added, and the mixture was extracted with CH_2Cl_2, washed with brine and dried over Na_2SO_4. The solvent was removed under reduced pressure, and the crude product was purified by column chromatography (silica gel, cyclohexane/EtOAc: 1/0 to 5/1). The title compound **S2** (60 mg, 99%) was obtained as a yellow solid.

***R*$_f$** 0.70 (cyclohexane/EtOAc: 2/1); **^{1}H NMR** (300 MHz, $CDCl_3$, 300 K): δ 7.95–7.89 (m, 2H), 7.72–7.70 (m, 2H), 7.60–7.44 (m, 18H), 7.39–7.27 (m, 8H), 6.85–6.73 (m, 4H), 4.34 (s, 2H), 2.20 (s, 6H), 2.19 (s, 6H), 1.40 (s, 6H); **HRMS** (neg. ESI): *m/z* calcd for $C_{70}H_{55}O_2$ 927.4208 $[M-H]^-$, found 927.4193; The compound was used in the next step without further characterization.

[5] Following our standard procedure for $CeCl_3$-mediated Grignard additions one would add the carbonyl compound as a solid. Due to the small amount of starting material it was dissolved beforehand to ensure complete addition.
[6] A stock solution of the Grignard reagent which was titrated few hours before applying it to the reaction.

DBP[6]CPP hoop 1

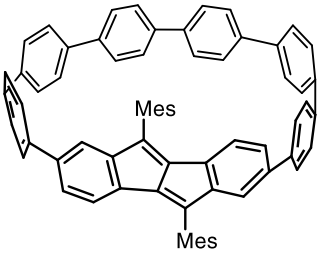

In a Schlenk tube **S2** (60 mg, 65 µmol, 1.00 eq.) and Burgess's reagent (123 mg, 0.52 mmol, 8.00 eq.) were dissolved in dry degassed 1,4-dioxane (12 mL) and stirred at 80 °C for 20 h[7]. After cooling to room temperature saturated aqueous $NaHCO_3$ solution was added to the reaction mixture. The aqueous phase was extracted with CH_2Cl_2, the combined organic phases were washed with saturated aqueous $NaHCO_3$ solution, water and saturated aqueous NaCl solution. After drying over Na_2SO_4 the solvent was removed under reduced pressure. The crude product was purified by column chromatography (silica gel, cyclohexane/EtOAc, 1/0 to 10/1). The title compound (42 mg, 73%) was obtained as a red to brown solid.

***R*f** 0.82 (cyclohexane/EtOAc: 2/1); **^{1}H NMR** (500 MHz, $CDCl_3$, 300 K): δ 7.56–7.53 (m, 4H), 7.51–7.49 (m, 8H), 7.46–7.39 (m, 12H), 7.02 (dd, *J* = 8.2, 1.8 Hz, 2H), 6.99 (bs, 2H), 6.77 (bs, 2H), 6.59 (d, *J* = 1.7 Hz, 2H), 6.39 (d, *J* = 8.2 Hz, 2H), 2.43 (s, 6H), 2.35 (s, 6H), 1.23 (s, 6H); **^{13}C NMR** (126 MHz, $CDCl_3$, 300 K): δ 151.2, 143.6, 140.8, 139.2, 138.2, 138.1, 138.0, 137.9, 137.8, 137.6, 137.4, 137.1, 135.5, 133.1, 129.8, 128.3, 128.3, 127.7, 127.6, 127.6, 127.6, 127.5, 126.8, 125.6, 123.1, 120.4, 21.3, 20.5, 19.4; **HRMS** (pos. APCI): *m/z* calcd for $C_{70}H_{53}$ 893.4142 $[M+H]^+$, found 893.4136; **UV/Vis** (CH_2Cl_2): λ (ε in M^{-1} cm^{-1}) = 345 (8.5×10^4), 447 (0.3×10^4), 510 (800).

[7] The yellow, fluorescent solution quickly turned dark red after a few minutes at 80 °C.

2.2 Synthesis of DBP[7]CPP hoop 2

S4, **S5 and 9** were synthesized according to previously reported procedures[7].

C-shaped precursor-diol (S5)

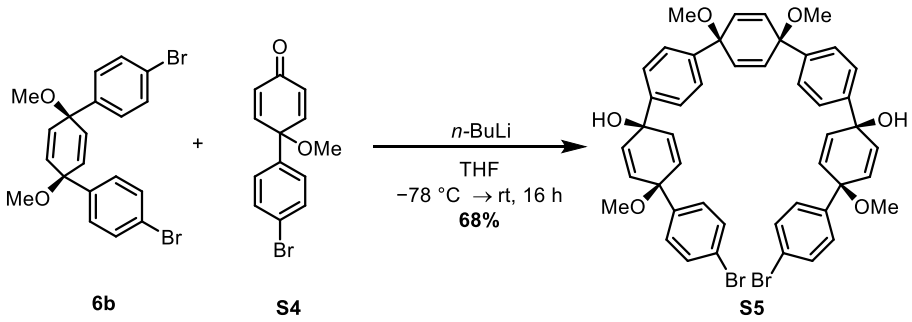

A solution of corner unit **6b** (4.35 g, 9.67 mmol, 1.00 eq) in anhydrous THF (200 mL) was cooled to −78 °C under argon before *n*-BuLi (2.7 M solution in toluene, 7.88 mL, 1.36 g, 21.3 mmol, 2.20 eq) was added dropwise. After stirring for 5 min 4-(4-bromophenyl)-4-methoxycyclohexadien-1-one (**S4**, 6.48 g, 23.2 mmol, 2.40 eq.) was added in one portion. The mixture was stirred at −78 °C and was allowed to warm to room temperature overnight. The reaction was quenched with H_2O (250 mL). THF was removed under reduced pressure and the residue was extracted with ethyl acetate (3 × 100 mL). The organic extracts were washed with brine (400 mL), dried over $MgSO_4$, filtered, and the solvent was removed under reduced pressure. Column chromatography (silica gel, cyclohexane/ethyl acetate: 9/1 to 1/1) yielded the title compound as a white-yellow solid (5.61 g, 6.60 mmol, 68%).

R_f = 0.28 (cyclohexane/ethyl acetate: 2/1); **^{1}H NMR** (500 MHz, C_6D_6): δ 7.64–7.59 (m, 4H), 7.54–7.48 (m, 4H), 7.34–7.29 (m, 4H), 7.26–7.22 (m, 4H), 5.99–5.90 (m, 8H), 5.57–5.47 (m, 4H), 3.28 (s, 6H), 3.13 (s, 6H), 1.74 (s, 2H); **^{13}C NMR** (126 MHz, C_6D_6): δ 144.1, 143.7, 143.4, 135.6, 133.8, 131.7, 129.8, 128.4, 126.8, 126.0, 121.9, 75.0, 74.7, 69.3, 51.9, 51.4; **HRMS** (neg. ESI): *m/z* calcd for $C_{46}H_{41}O_6Br_2^-$ 847.1275 $[M-H]^-$, found 847.1275.

C-shaped precursor (9)

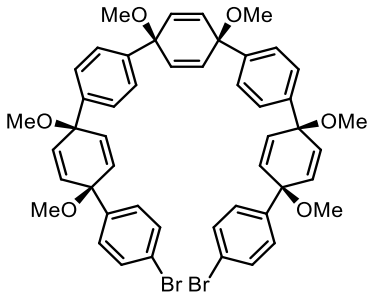

C-shaped precursor-alcohol **S5** (3.92 g, 4.61 mmol, 1.00 eq) was dissolved in THF (100 mL). Powdered KOH (1.09 g, 19.4 mmol, 4.21 eq) and MeI (2.87 mL, 6.54 g, 46.1 mmol, 10.0 eq) were added. The reaction mixture was stirred at room temperature for 17 h. The reaction mixture was quenched with H_2O (200 mL) and extracted with CH_2Cl_2 (3 × 100 mL). The organic extracts were washed with brine (200 mL), dried over $MgSO_4$, filtered, and the solvent was removed under reduced pressure. The title compound was afforded as a colorless solid (3.74 g, 4.25 mmol, 92%).

***R*$_f$** = 0.38 (cyclohexane/ethyl acetate: 4/1); **^{1}H NMR** (500 MHz, $CDCl_3$): δ 7.45–7.41 (m, 4H), 7.38–7.31 (m, 8H), 7.28–7.21 (m, 4H), 6.13–6.10 (m, 4H), 6.08 (s, 4H), 6.06–6.02 (m, 4H), 3.42 (s, 6H), 3.42 (s, 6H), 3.41 (s, 6H); **^{13}C NMR** (126 MHz, $CDCl_3$): δ 143.1, 142.7, 142.7, 133.9, 133.5, 133.1, 131.6, 128.0, 126.2, 126.1, 121.7, 74.7, 74.7, 74.6, 68.1, 52.2, 52.2, 52.1; **HRMS** (neg. ESI): *m/z* calcd for $C_{48}H_{46}O_6Br_2Cl^-$ 911.1355 $[M+Cl]^-$, found 911.1359.

10

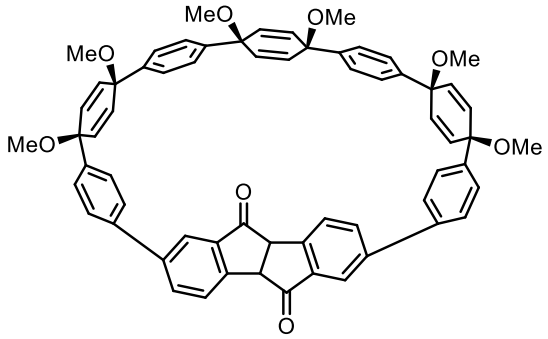

A flame-dried flask was charged with boronic ester **5** (390 mg, 802 µmol, 1.00 eq.), C-shaped precursor **9** (705 mg, 802 µmol, 1.00 eq.), K_3PO_4 (1.70 g, 8.02 mmol, 10.0 eq.), $Pd(OAc)_2$ (72.0 mg, 321 µmol, 40 mol%) and SPhos (263 mg, 642 µmol, 80 mol%). The flask was evacuated and backfilled with argon and a mixture of degassed 1,4-dioxane (400 mL) and H_2O (20 mL) was added. The reaction was stirred at 90 °C for 4 d under an argon atmosphere. After cooling to room temperature, the reaction mixture was diluted with water (500 mL). The mixture was extracted with ethyl acetate (3 × 200 mL). The organic extracts were washed with brine (200 mL), dried over $MgSO_4$, filtered, and the solvent was removed under reduced pressure. Column chromatography (silica gel, CH_2Cl_2/EtOAc: 1/0 to 10/1) afforded the title compound (209 mg, 27%) as a colorless solid.

***R*$_f$** = 0.19 (cyclohexane/EtOAc: 4/1); **^{1}H NMR** (500 MHz, $CDCl_3$): δ = 7.90–7.85 (m, 4H), 7.83 (dd, *J* = 1.6, 0.9 Hz, 2H), 7.48–7.39 (m, 8H), 7.36–7.28 (m, 8H), 6.25–6.15 (m, 4H), 6.14–6.02 (m, 4H), 6.00–5.91 (m, 4H), 4.55 (s, 2H), 3.45 (s, 6H), 3.38 (s, 6H), 3.37 (s, 6H); **^{13}C NMR** (126 MHz, $CDCl_3$): δ = 202.7, 149.0, 143.6, 143.4, 142.9, 142.0, 137.8, 134.4, 134.2, 134.2, 133.9, 133.2, 133.1, 133.1, 132.6, 127.0, 126.7, 126.6, 126.5, 126.4, 123.1, 75.2, 74.6, 73.4, 53.2, 52.3, 52.0, 51.8; **HRMS** (neg. APCI): *m*/*z* calcd for $C_{64}H_{54}O_8Cl^-$ 985.3513 $[M+Cl]^-$, found 985.3514.

Diketone-based hoop 4

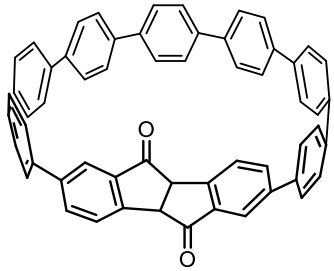

$SnCl_2 \cdot 2H_2O$ (1.39 g, 6.15 mmol, 40.0 eq.) was dissolved in freshly distilled THF (200 mL). Concentrated aq. HCl (37% w/w, 12 M, 1.04 mL, 457 mg, 12.5 mmol, 80.0 eq.) was added dropwise, and the resulting solution was stirred at room temperature for 30 min. In a separate flask **10** (149 mg, 157 µmol, 1.00 eq.) was dissolved in freshly distilled THF (40 mL) and the resulting solution was added dropwise to the H_2SnCl_4 solution. The fluorescent solution was stirred at room temperature for 6 d. The reaction was quenched by addition of aq. KOH (2 M, 400 mL). The mixture was extracted with ethyl acetate (4 × 150 mL). The organic extracts were washed with brine (300 mL), dried over $MgSO_4$, filtered, and the solvent was removed under reduced pressure. Column chromatography (silica gel, *n*-pentane/CH_2Cl_2: 1/0 to 1/2) afforded the title compound (41.7 mg, 35%) as a fluorescent yellow solid.

R_f = 0.57 (CH_2Cl_2); **^{1}H NMR** (500 MHz, $CDCl_3$) δ 7.89 (dd, *J* = 8.3, 1.9 Hz, 2H), 7.83 (dd, *J* = 8.3, 0.6 Hz, 2H), 7.75 (dd, *J* = 1.8, 0.6 Hz, 2H), 7.57–7.50 (m, 20H), 7.45–7.41 (m, 8H), 4.51 (s, 2H); **^{13}C NMR** (126 MHz, $CDCl_3$): δ 202.4, 148.6, 141.6, 140.3, 138.6, 138.4, 138.3, 138.0, 137.7, 136.9, 134.4, 133.8, 127.9, 127.8, 127.7, 127.7, 127.5, 127.3, 127.2, 127.0, 122.8, 52.9; **HRMS** (pos. ESI): *m*/*z* calcd for $C_{58}H_{36}O_2^+$ 764.2710 $[M]^+$, found 764.2700. **UV/Vis** (CH_2Cl_2): λ (ε in $M^{-1}\,cm^{-1}$) = 329 (8.5×10^4), 368 (shoulder, 2.6×10^4), 388 (shoulder, 1.8×10^4), **Fluorescence** (CH_2Cl_2): λ_{max} = 470 nm.

S3

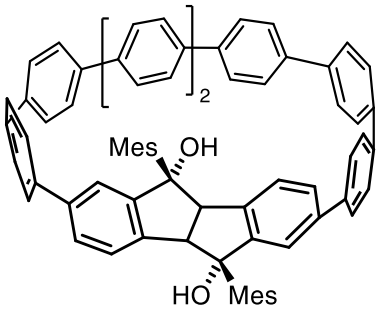

$CeCl_3$ (145 mg, 589 µmol, 15.0 eq) was dried *in vacuo* at 200 °C for 1.5 h. After cooling down under vacuum, anhydrous THF (50 mL) was added, and the resulting suspension was stirred at room temperature for 18 h under argon. **4** (30.0 mg, 39.3 µmol, 1.00 eq) was added to the $CeCl_3$-suspension and the mixture was cooled to 0 °C. 2-Mesitylmagnesium bromide solution (1.0 M in diethyl ether, 0.24 mL, 52.6 mg, 236 µmol, 6.00 eq) was added dropwise. The resulting suspension was stirred at 0 °C for 1 h before it was allowed to warm to room temperature while stirring for another 22 h. The reaction was quenched by addition of aq. AcOH (5%, 200 mL). The mixture was extracted with ethyl acetate (3 × 100 mL). The organic extracts were washed with brine (100 mL), dried over $MgSO_4$, filtered, and the solvent was removed *in vacuo*. Column chromatography (silica gel, cyclohexane/CH_2Cl_2: 1/0 to 1/1) afforded **S3** (33.0 mg, 84%) as a fluorescent colorless solid.

R_f = 0.47 (cyclohexane/CH_2Cl_2: 1/1); **^{1}H NMR** (400 MHz, $CDCl_3$) δ 7.94 (d, *J* = 8.1 Hz, 2H), 7.76 (d, *J* = 1.8 Hz, 2H), 7.61 (dd, *J* = 8.2, 1.9 Hz, 2H), 7.59–7.49 (m, 23H), 7.49–7.40 (m, 8H), 6.89–6.71 (m, 5H), 4.36 (s, 2H), 2.22–2.19 (m, 6H)[8]; **HRMS** (neg. ESI): *m*/*z* calcd for $C_{76}H_{60}O_2Cl^-$ 1039.4287 $[M+Cl]^-$, found 1039.4282; The compound was used in the next step without further characterization.

[8] Not all hydrogen atoms could be assigned in the ^{1}H NMR spectrum.

DBP[7]CPP hoop 2

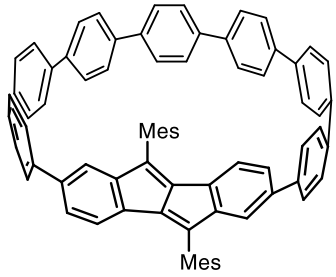

A flame-dried flask was charged with **S3** (18.0 mg, 179 µmol, 1.00 eq.) and Burgess's reagent (51.2 mg, 215 µmol, 12.0 eq.). The flask was evacuated, and backfilled with argon and anhydrous 1,4-dioxane (10 mL) was added. The reaction mixture was stirred at 100 °C in a sealed flask for 20 h. After cooling to room temperature, the reaction was quenched by addition of saturated aqueous $NaHCO_3$ (100 mL). The aqueous mixture was extracted with CH_2Cl_2 (3 × 50 mL). The organic extracts were washed with brine (100 mL), dried over $MgSO_4$, filtered, and the solvent was removed under reduced pressure. Column chromatography (silica gel, *n*-pentane/CH_2Cl_2: 1/0 to 7/3) afforded the title compound (14.3 mg, 82%) as a red-brown solid.

R_f = 0.32 (*n*-pentane/CH_2Cl_2 7/3); **^{1}H NMR** (400 MHz, $CDCl_3$) δ 7.59–7.56 (m, 4H), 7.55–7.50 (m, 12H), 7.49–7.48 (m, 4H), 7.47–7.40 (m, 8H), 7.07 (dd, *J* = 8.1, 1.8 Hz, 2H), 7.03–6.99 (m, 2H), 6.81–6.77 (m, 2H), 6.66–6.59 (m, 2H), 6.44 (dd, *J* = 8.1, 0.4 Hz, 2H), 2.42 (s, 6H), 2.34 (s, 6H), 1.33 (s, 6H); **^{13}C NMR** (100 MHz, $CDCl_3$): δ = 151.0, 143.6, 140.3, 139.3, 138.5, 138.5, 138.2, 138.0, 137.4, 137.0, 135.5, 133.5, 129.8, 128.3, 128.2, 127.7, 127.6, 127.5, 127.4, 126.9, 125.6, 122.9, 120.1, 21.4, 20.5, 19.2[9]; **HRMS** (pos. ESI): *m*/*z* calcd for $C_{76}H_{56}^+$ 968.4377 $[M]^+$, found 968.4370; **UV/Vis** (CH_2Cl_2): λ (ε in M^{-1} cm^{-1}) = 345 (1.1×10^5), 393 (shoulder, 1.8×10^4), 445 (0.5×10^4), 507 (659); **Fluorescence** (CH_2Cl_2): λ_{max} = 479 nm.

[9] Three aromatic carbon signals are overlapping

2.3 Chiral Resolution of 3 and Synthetic Transformation to (*M*)-1 and (*P*)-1

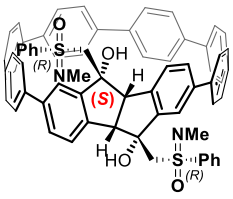

12

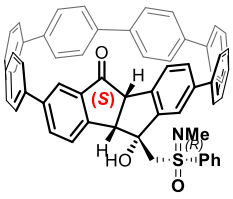

13

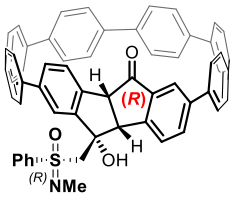

14

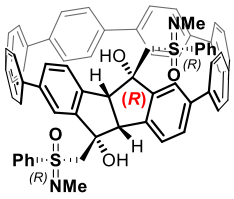

15

This procedure was done in analogy to a previously reported one.[4] Anhydrous $CeCl_3$ (43.7 mg, 177 µmol, 3.6 eq.) was placed in a dry Schlenk tube and was further dried under vacuum (10^{-3} mbar) at 135 °C for 4 h. The tube was backfilled with argon while hot and cooled to rt. Racemic **3** (33.8 mg, 49.1 µmol) was added and the tube was evacuated and backfilled with argon before anhydrous THF (3.0 mL) was added at 0 °C. The mixture was stirred vigorously at room temperature overnight. In another dry Schlenk tube, a solution of sulfoximine **11** (0.20 M in anhydrous THF, 0.88 mL, 176 µmol, 3.6 eq., 98% *ee*) was cooled to 0 °C, EtMgBr (0.87 M in THF, 0.19 mL, 165 µmol, 3.4 eq.) was added dropwise, and the resulting yellow solution was stirred for 1 h at 0 °C. This sulfoximine-MgBr solution was added dropwise to the $CeCl_3$/**3** slurry at 0 °C, upon which it turned yellow. The reaction mixture was stirred at 0 °C for 4 h. The reaction was quenched with 10% aq. HOAc (4 mL) at 0 °C and warmed to room temperature. CH_2Cl_2 (15 mL) was added to the mixture, and the aq. layer was extracted with CH_2Cl_2 (2 × 10 mL). The combined organic layers were washed with sat. aq. $NaHCO_3$ (10 mL), brine (10 mL), dried over Na_2SO_4 and concentrated under reduced pressure. Flash column chromatography (SiO_2, CH_2Cl_2/cyclohexane/EtOAc: 3/1/0 to 1/0/1) yielded **14** (9.2 mg, 11 µmol, 22%), **15** (2.4 mg, 2 µmol, 5%), **13** (14 mg, 16 µmol, 33%) and **12** (8 mg, 8 µmol, 16%) as green fluorescent solids.

Analytical data for **14**: R_f 0.48 (CH_2Cl_2/EtOAc: 50/1); **^{1}H NMR** (500 MHz, $CDCl_3$): δ 8.14 (s, 1H), 7.99–7.95 (m, 2H), 7.87 (d, *J* = 1.3 Hz, 2H), 7.73–7.71 (m, 1H), 7.70–7.59 (m, 3H), 7.59–7.52 (m, 8H), 7.52–7.47 (m, 7H), 7.45 (dd, *J* = 8.2, 1.9 Hz, 1H), 7.43–7.39 (m, 2H), 7.39–7.29 (m, 7H), 7.26–7.23 (m, 2H), 5.29 (d, *J* = 5.4 Hz, 1H), 4.36 (dd, *J* = 5.4, 1.1 Hz, 1H), 3.62 (d, *J* = 14.0 Hz, 1H), 3.19 (d, *J* = 14.0 Hz, 1H), 2.86 (s, 3H); **^{13}C NMR** (126 MHz, $CDCl_3$): δ 204.1, 150.7, 145.7, 140.8, 139.8, 139.6, 139.6, 138.5, 138.4, 138.2, 138.2, 137.7, 137.6, 137.3, 137.2, 137.0, 136.2, 136.0, 133.8, 132.4, 130.4, 130.0, 129.2, 128.1, 127.8, 127.8, 127.8, 127.6, 127.6, 127.5, 127.5, 127.2, 127.2, 126.1, 121.5, 120.9, 83.2, 64.4, 56.5, 48.4, 29.2; **HRMS** (pos. ESI): *m/z* calcd for $C_{60}H_{44}O_3NS$ 858.3036 $[M+H]^+$, found 358.3045.

Analytical data for **15**: R_f 0.38 (CH_2Cl_2/EtOAc: 50/1); **^{1}H NMR** (400 MHz, $CDCl_3$) δ 7.99–7.94 (m, 6H), 7.66 (d, *J* = 8.1 Hz, 2H), 7.64–7.58 (m, 6H), 7.57–7.52 (m, 8H), 7.51–7.47 (m, 4H), 7.47–7.43 (m, 4H), 7.42 (dd, *J* = 8.1, 1.7 Hz, 2H), 7.40 (d, *J* = 1.7 Hz, 2H), 7.35–7.31 (m, 4H), 7.27–7.23 (m, 4H), 5.05 (s, 2H), 3.50 (d, *J* = 13.9 Hz, 2H), 3.15 (d, *J* = 13.9 Hz, 2H), 2.81 (s, 6H); **^{13}C NMR** (101 MHz, $CDCl_3$)[10]: δ 146.9, 139.1, 138.9, 138.7, 138.5, 138.0, 137.9, 137.6, 137.3, 137.1, 133.5, 129.7, 129.5, 129.4, 129.2, 128.8, 127.7, 127.6, 127.4, 127.3, 127.1, 126.9, 119.4, 83.5, 63.8, 52.2, 29.1; **^{1}H NMR** (300 MHz, $CDCl_3$): δ 8.00–7.93 (m, 6H),

[10] Assignment of carbon signals is difficult due to thermal decomposition of the sample during measurement. Similarity of the carbon atoms of the cycloparaphenylene chain further hinders assignment.

7.66 (d, *J* = 8.1 Hz, 2H), 7.63–7.57 (m, 6H), 7.56–7.52 (m, 8H), 7.51–7.39 (m, 12H), 7.36–7.31 (m, 4H), 7.27–7.23 (m, 4H), 5.04 (s, 2H), 3.50 (d, *J* = 13.9 Hz, 2H), 3.16 (d, *J* = 13.9 Hz, 2H), 2.81 (s, 6H); **HRMS** (pos. ESI): *m/z* calcd for $C_{68}H_{55}O_4N_2S_2$ 1027.3598 $[M+H]^+$, found 1027.3604.

Analytical data for **13**: R_f 0.66 (CH_2Cl_2/EtOAc: 10/1); **^{1}H NMR** (400 MHz, $CDCl_3$): δ 7.98–7.93 (m, 2H), 7.88–7.87 (m, 1H), 7.86 (d, *J* = 1.8 Hz, 1H), 7.72–7.69 (m, 1H), 7.68–7.59 (m, 5H), 7.58–7.52 (m, 8H), 7.51–7.43 (m, 10H), 7.38–7.31 (m, 6H), 7.29–7.25 (m, 2H), 4.16 (d, *J* = 5.4 Hz, 1H), 4.11 (d, *J* = 5.4 Hz, 1H), 3.73 (d, *J* = 14.1 Hz, 1H), 3.47 (d, *J* = 14.1 Hz, 1H), 2.82 (s, 3H); **^{13}C NMR** (101 MHz, $CDCl_3$)[11]: δ 203.6, 149.1, 144.5, 140.4, 140.1, 139.6, 139.3, 138.8, 138.4, 138.2, 138.0, 138.0, 137.8, 137.6, 137.5, 137.1, 136.7, 136.3, 135.3, 133.7, 132.9, 132.3, 130.1, 129.9, 129.5, 129.1, 128.8, 128.2, 127.7, 127.7, 127.6, 127.5, 127.4, 127.3, 127.2, 127.1, 126.9, 125.7, 122.6, 121.0, 82.3, 65.5, 55.4, 50.9, 29.2; **^{1}H NMR** (300 MHz, $CDCl_3$): δ 7.98–7.92 (m, 2H), 7.87 (s, 1H), 7.86 (d, *J* = 1.8 Hz, 1H), 7.71–7.69 (m, 1H), 7.71–7.55 (m, 5H), 7.55 (s, 8H), 7.51–7.43 (m, 10H), 7.38–7.30 (m, 6H), 7.28 (s, 2H), 4.16 (d, *J* = 5.3 Hz, 1H), 4.10 (d, *J* = 5.3 Hz, 1H), 3.74 (d, *J* = 14.0 Hz, 1H), 3.47 (d, *J* = 14.0 Hz, 1H), 2.82 (s, 3H); **HRMS** (pos. ESI): *m/z* calcd for $C_{60}H_{44}O_3NS$ 858.3036 $[M+H]^+$, found 358.3028.

Analytical data for **12**: R_f 0.13 (CH_2Cl_2/EtOAc: 10/1); **^{1}H NMR** (400 MHz, $CDCl_3$): δ 7.89–7.85 (m, 4H), 7.65 (d, *J* = 8.1 Hz, 2H), 7.63–7.52 (m, 16H), 7.52–7.42 (m, 12H), 7.36–7.33 (m, 4H), 7.29–7.25 (m, 4H), 3.83 (s, 2H), 3.46 (d, *J* = 14.0 Hz, 2H), 3.25 (d, *J* = 14.0 Hz, 2H), 2.75 (s, 6H); **^{13}C NMR** (101 MHz, $CDCl_3$): δ 145.9, 139.1, 139.1, 139.0, 138.5, 138.1, 137.9, 137.6, 137.1, 135.7, 133.4, 132.9, 129.9, 129.7, 129.5, 129.1, 129.1, 128.8, 127.7, 127.6, 127.6, 127.5, 127.4, 127.4, 127.3, 127.2, 127.2, 127.1, 120.7, 82.3, 77.3, 64.8, 53.7, 29.2; **^{1}H NMR** (300 MHz, $CDCl_3$): δ 7.90–7.85 (m, 4H), 7.65 (d, *J* = 8.1 Hz, 2H), 7.63–7.52 (m, 16H), 7.52–7.41 (m, 12H), 7.38–7.33 (m, 4H), 7.29–7.25 (m, 4H), 3.85 (s, 2H), 3.46 (d, *J* = 14.0 Hz, 2H), 3.25 (d, *J* = 14.0 Hz, 2H), 2.75 (s, 6H); **HRMS** (pos. ESI): *m/z* calcd for $C_{68}H_{55}O_4N_2S_2$ 1027.3598 $[M+H]^+$, found 1027.3588.

[11] In the range of 128 to 127 ppm several signals from nanohoop **3** appear due to thermal decomposition. These can be assigned by stacking both ^{13}C NMR spectra.

(*R*,*R*)-3

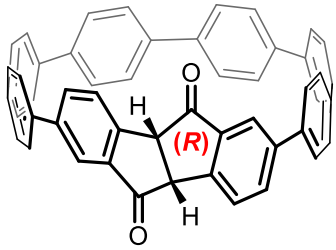

15 (10 mg, 12 µmol) was dissolved in toluene (2 mL) and stirred at 90 °C for 3 h. The solvent was removed under reduced pressure, and the residue was purified by column chromatography (SiO_2, CH_2Cl_2/cyclohexane 1/1 to CH_2Cl_2) to yield enantiopure diketone-based hoop **(*R*,*R*)-3** as yellow fluorescent solid (3.8 mg, 5.5 µmol, 47%).

14 (9.2 mg, 11 µmol) was dissolved in toluene (1.5 mL) and stirred at 90 °C for 3 h. The solvent was removed under reduced pressure, and the residue was purified by column chromatography (SiO_2, CH_2Cl_2/cyclohexane 1/1 to CH_2Cl_2) to yield enantiopure diketone-based hoop **(*R*,*R*)-3** as yellow fluorescent solid (4.6 mg, 6.7 µmol, 62%).

The spectroscopic data is in accordance with the racemic molecule.

HPLC (Chiralpak IA, λ = 280 nm, *n*-heptane/CH_2Cl_2 = 30/70, 0.5 mL min^{-1}, 22 °C): t_R = 9.3 min (major), 11.5 min (minor), > 99% *ee*.

(*S*,*S*)-3

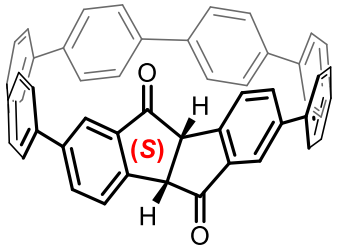

12 (8.0 mg, 7.8 µmol) was dissolved in toluene (2 mL) and stirred at 90 °C for 3 h. The solvent was removed under reduced pressure, and the residue was purified by column chromatography (SiO_2, CH_2Cl_2/cyclohexane 1/1 to CH_2Cl_2) to yield enantiopure diketone-based hoop **(*S*,*S*)-3** as yellow fluorescent solid (4.4 mg, 6.4 µmol, 82%).

13 (14.0 mg, 16.3 µmol) was dissolved in toluene (2 mL) and stirred at 90 °C for 3 h. The solvent was removed under reduced pressure, and the residue was purified by column chromatography (SiO_2, CH_2Cl_2/cyclohexane 1/1 to CH_2Cl_2) to yield enantiopure diketone-based hoop **(*S*,*S*)-3** as yellow fluorescent solid (8.4 mg, 12 µmol, 75%).

The spectroscopic data is in accordance with the racemic molecule.

Crystals (yellow fluorescent plates) that were suitable for single crystal X-ray diffraction were obtained by vapor diffusion of MeOH into a PhCl solution of **(*S*,*S*)-3** and unambiguously confirmed the absolute configuration.

HPLC (Chiralpak IA, λ = 312 nm, *n*-heptane/CH_2Cl_2 = 30/70, 0.5 mL min^{-1}, 22 °C): t_R = 11.8 min (major), 9.3 min (minor), > 98% *ee*.

(*R*,*R*)-S2

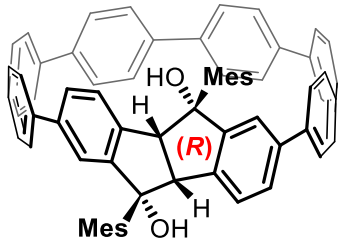

Anhydrous $CeCl_3$ (20.7 mg, 84.0 µmol, 5.7 eq.) was placed in a dry Schlenk tube and was further dried under vacuum ($1 \cdot 10^{-3}$ mbar) at 135 °C for 4 h. The tube was backfilled with argon while hot and cooled to room temperature. Anhydrous THF (1.6 mL) was added at 0 °C, the tube was sealed, and the mixture was stirred vigorously at room temperature overnight. The mixture was cooled to 0 °C, MesMgBr (0.92 M in THF, 0.07 mL, 64 µmol, 4.4 eq.) was added, and the mixture was stirred at 0 °C for 1 h. **(*R*,*R*)-3** (10.2 mg, 14.8 µmol) was added in one portion, and the orange mixture was stirred at 0 °C for 5 h, warmed to room temperature and stirred for further 1.5 h. The reaction was quenched with 10% aq. HOAc (0.5 mL) and H_2O (5 mL) and CH_2Cl_2 (10 mL) were added. The aq. layer was extracted with CH_2Cl_2 (2 × 5 mL). The combined organic layer was washed with sat. aq. $NaHCO_3$ (5 mL), dried over Na_2SO_4, and the solvent was removed under reduced pressure. Flash column chromatography (SiO_2, cyclohexane to cyclohexane/EtOAc 6/1) yielded diol **(*R*,*R*)-S2** as a green-yellow fluorescent solid (9.4 mg, 10 µmol, 68%).

(*S*,*S*)-S2

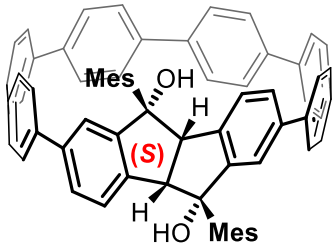

(*S*,*S*)-S2 was synthesized in the same way as **(*R*,*R*)-S2** using diketone **(*S*,*S*)-3** (13.6 mg, 19.7 µmol), $CeCl_3$ (29.0 mg, 118 µmol, 6.0 eq.), MesMgBr (0.92 M in THF, 0.10 mL, 92 µmol, 4.7 eq.) and anh. THF (2.2 mL) to yield **(*S*,*S*)-S2** as a green-yellow fluorescent solid (14.0 mg, 15.1 µmol, 76%).

(*P*)-1

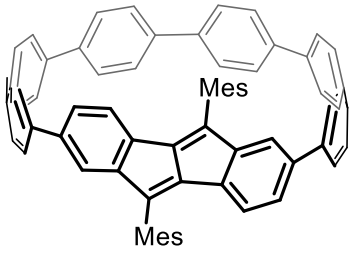

(*R*,*R*)-S2 (9.4 mg, 10 µmol) and Burgess' reagent (25.5 mg, 107 µmol, 10.6 eq.) were placed in a dry Schlenk tube. The tube was evacuated and back filled with argon (3 times). Anh. 1,4-dioxane (2 mL) was added, the tube was sealed, and heated at 80 °C for 4 h. The red solution was quenched with sat. aq. $NaHCO_3$ (2 mL). H_2O (5 mL), CH_2Cl_2 (15 mL) and brine (10 mL) were added, the aq. layer was extracted with CH_2Cl_2 (2 × 10 mL). The combined organic layer was dried over Na_2SO_4 and the solvent was removed under reduced pressure. Flash column chromatography (SiO_2, cyclohexane to cyclohexane/EtOAc: 50/1) yielded **(*P*)-1** as a red solid (1.2 mg, 0.33 µmol, 3%).

The spectroscopic data is in accordance with the racemic molecule.

(*M*)-1

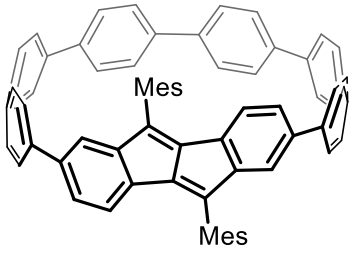

(*M*)-1 was synthesized in the same way as **(*P*)-1** using diol **(*S*,*S*)-S2** (14.0 mg, 15.1 µmol), Burgess' reagent (36.9 mg, 155 µmol, 10.3 eq.) and anh. 1,4-dioxane (3.0 mL) to yield the title compound as a red solid (3.3 mg, 0.90 µmol, 6%).

The spectroscopic data is in accordance with the racemic molecule.

2.3.1 Assignment of Stereodescriptors in Enantiopure Nanohoops 1

For the nomenclature of the enantiomeric nanohoops – according to the IUPAC Goldbook[8] – we assumed a helical motive in the structure with the two annealed benzene rings (and the connecting C-C-bonds to the CPP moiety) as the fiducial groups. The exemplary depiction of the helix is shown with the blue dotted lines. A right-handed helix is described as *P* (or plus), a left-handed one is described as *M* (or minus).

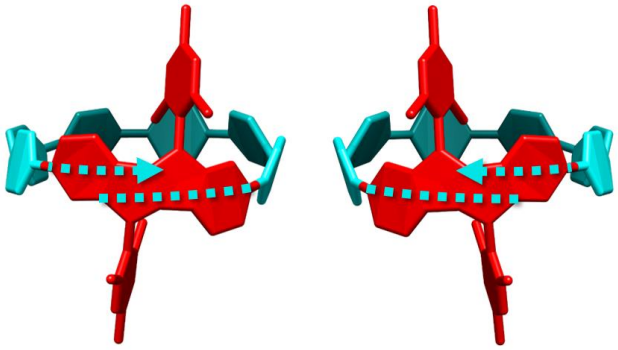

(*P*)-1 (*M*)-1

Figure S1. Graphical description of the helical motive.

2.3.2 HPLC Elugrams

Method: CHIRALPAK IA, nHeptan/DCM 30:70, 0,5ml/min, 22°C

Vial: 193 Injection Volume (µl): 5

Run Time: 09.11.2020 13:41:39 Analysis Time: 11.11.2020 13:30:51

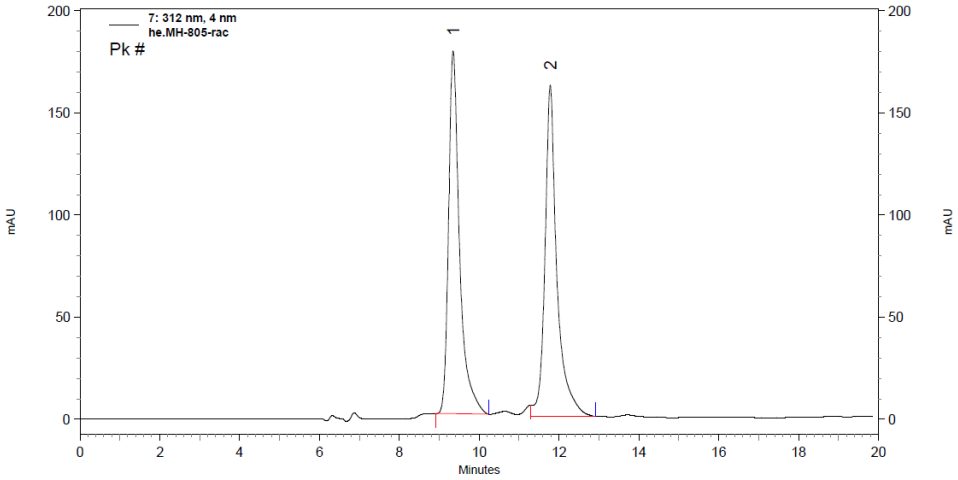

7: 312 nm, 4 nm Results

Pk #	Retention Time	Area Percent	Lambda Max
1	9,347	50,242	324
2	11,780	49,758	324

Figure S2. HPLC elugrams of racemic **3** (Chiralpak IA, λ = 312 nm, *n*-heptane/CH_2Cl_2 = 30/70, 0.5 mL min^{-1}, 22 °C): t_R = 9.3 min, 11.8 min.

Method: CHIRALPAK IA, nHeptan/DCM 30:70, 0,5ml/min, 22°C

Vial: 185 Injection Volume (µl): 5

Run Time: 10.11.2020 10:57:14 Analysis Time: 11.11.2020 13:49:44

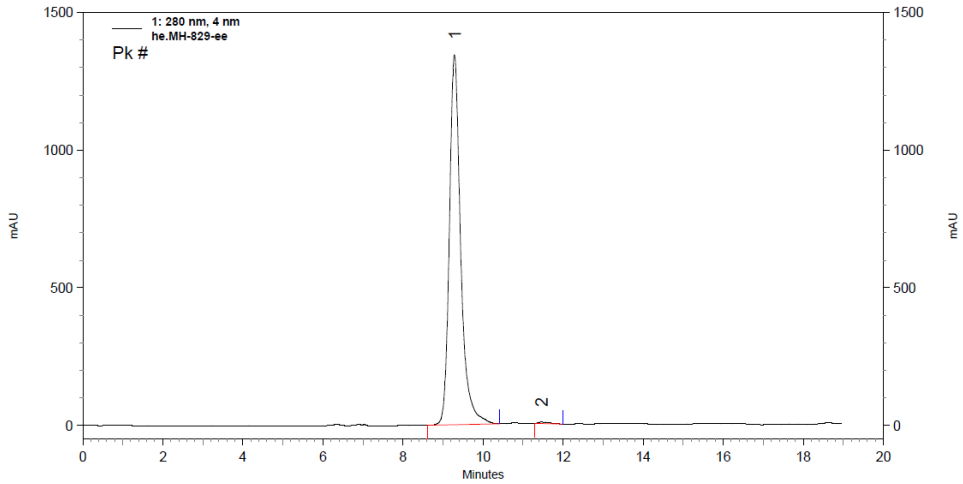

1: 280 nm, 4 nm Results

Pk #	Retention Time	Area Percent	Lambda Max
1	9,287	99,584	339
2	11,460	0,416	234

Figure S3. HPLC elugrams of **(*R,R*)-3** (Chiralpak IA, λ = 280 nm, *n*-heptane/CH_2Cl_2 = 30/70, 0.5 mL min^{-1}, 22 °C): t_R = 9.3 min (major), 11.5 min (minor), 99% *ee*.

Method: CHIRALPAK IA, nHeptan/DCM 30:70, 0,5ml/min, 22°C

Vial: 186 Injection Volume (µl): 5

Run Time: 10.11.2020 11:17:34 Analysis Time: 11.11.2020 13:51:39

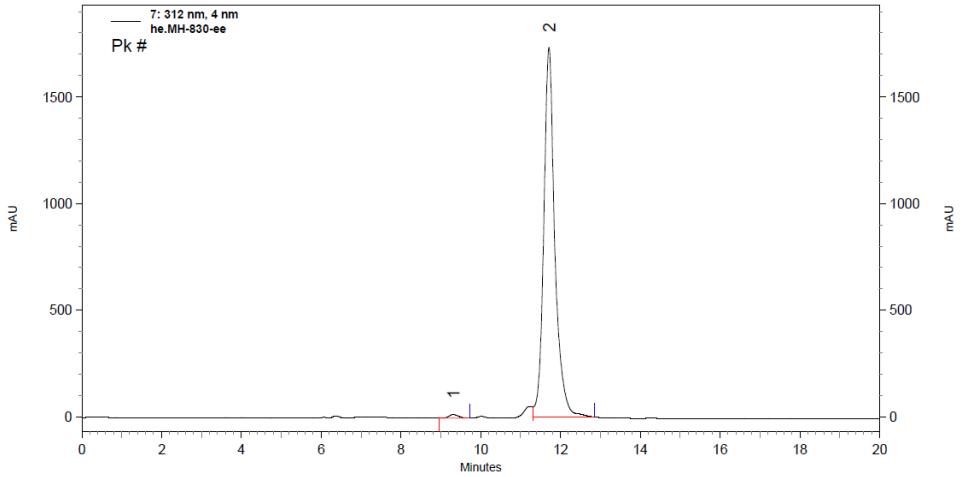

7: 312 nm, 4 nm Results

Pk #	Retention Time	Area Percent	Lambda Max
1	9,313	0,834	328
2	11,713	99,166	322

Figure S4. HPLC elugrams of **(*S,S*)-3** (Chiralpak IA, λ = 312 nm, *n*-heptane/CH_2Cl_2 = 30/70, 0.5 mL min^{-1}, 22 °C): t_R = 11.8 min (major), 9.3 min (minor). 98% *ee*.

3 NMR Spectra

3.1 NMR Spectra of Synthesized Title Compounds

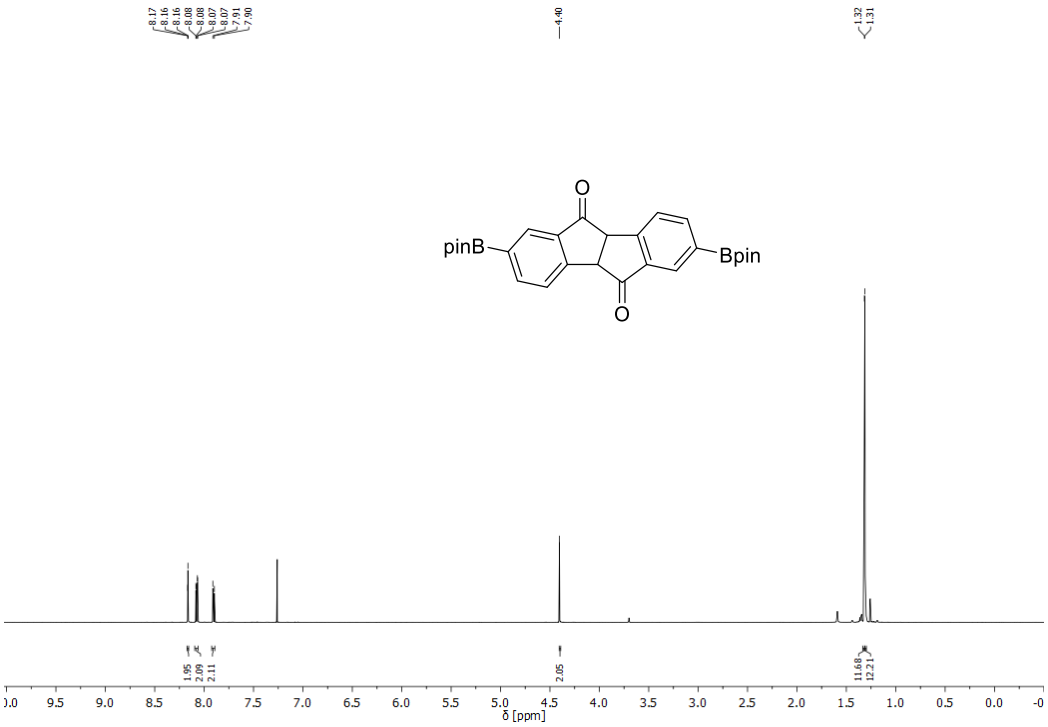

Figure S5. ^{1}H NMR spectrum (400 MHz, $CDCl_3$) of **5**.

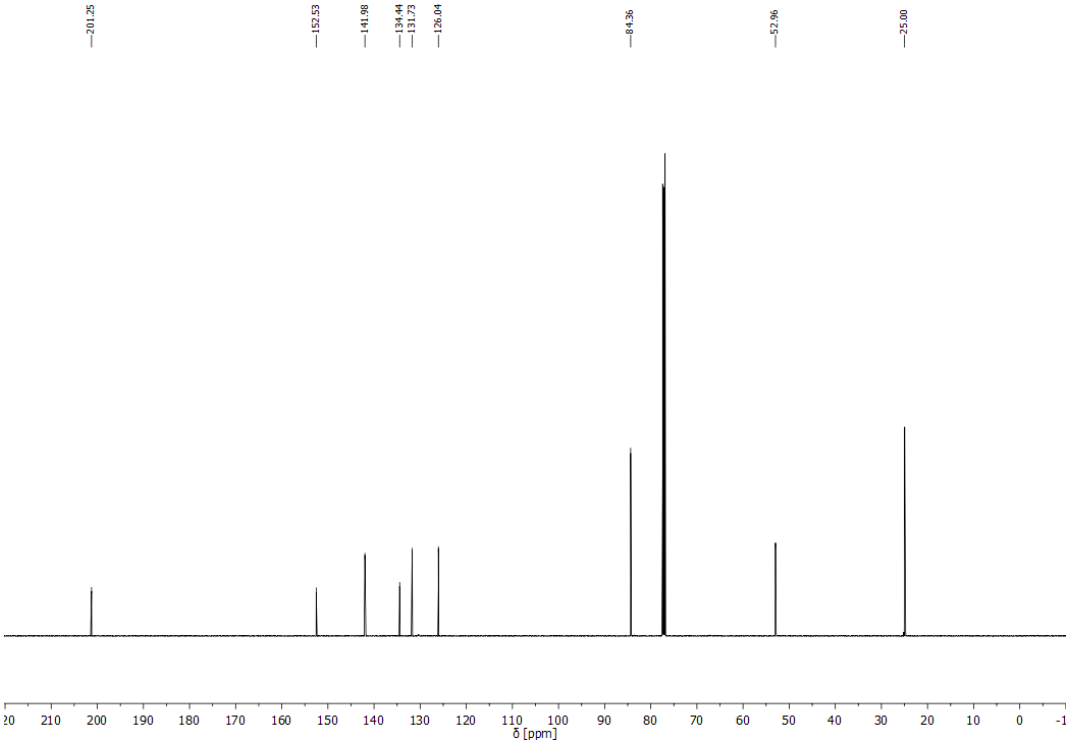

Figure S6. ^{13}C NMR spectrum (101 MHz, $CDCl_3$) of **5**.

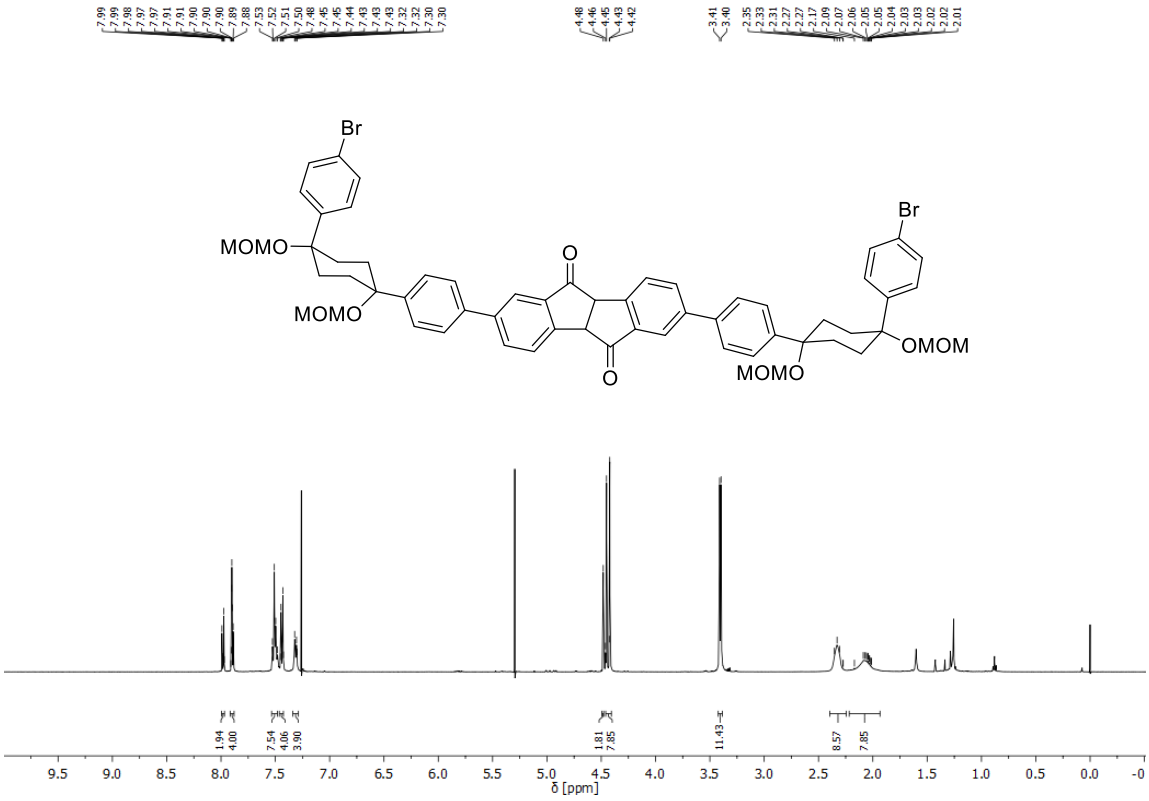

Figure S7. ^{1}H NMR spectrum (500 MHz, $CDCl_3$) of **7a**.

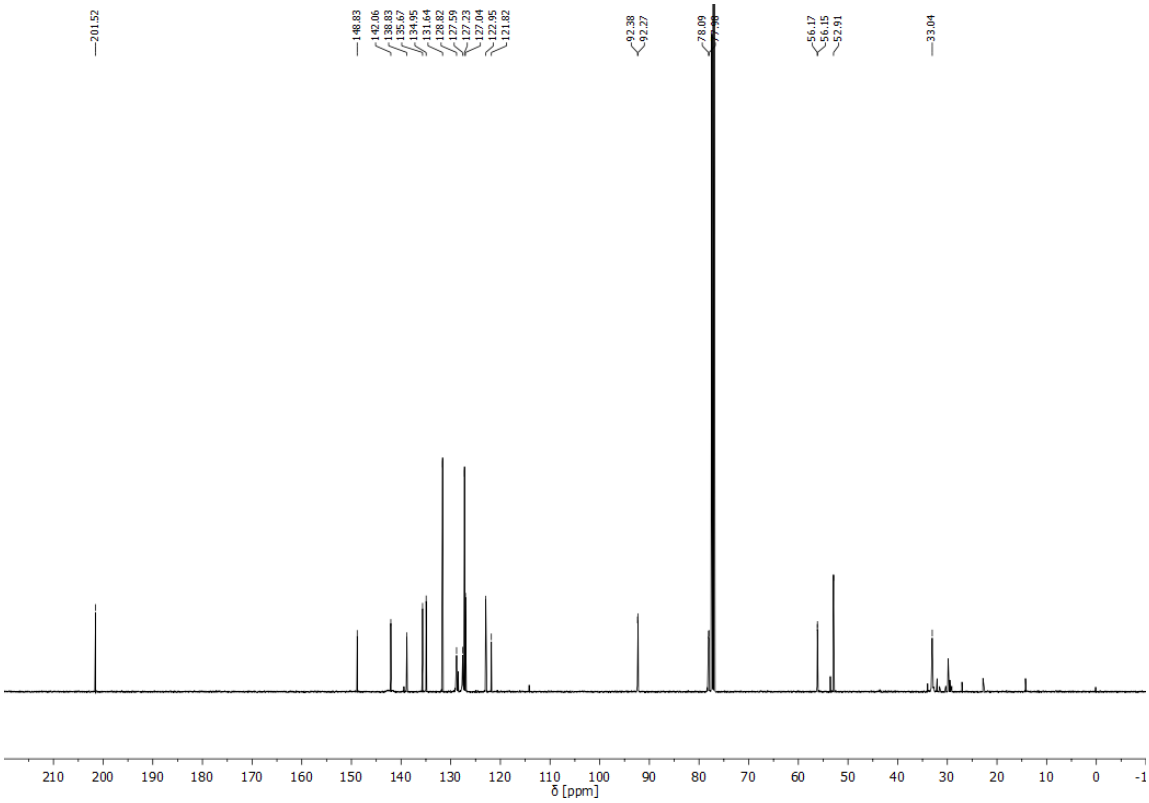

Figure S8. ^{13}C NMR spectrum (126 MHz, $CDCl_3$) of **7a**.

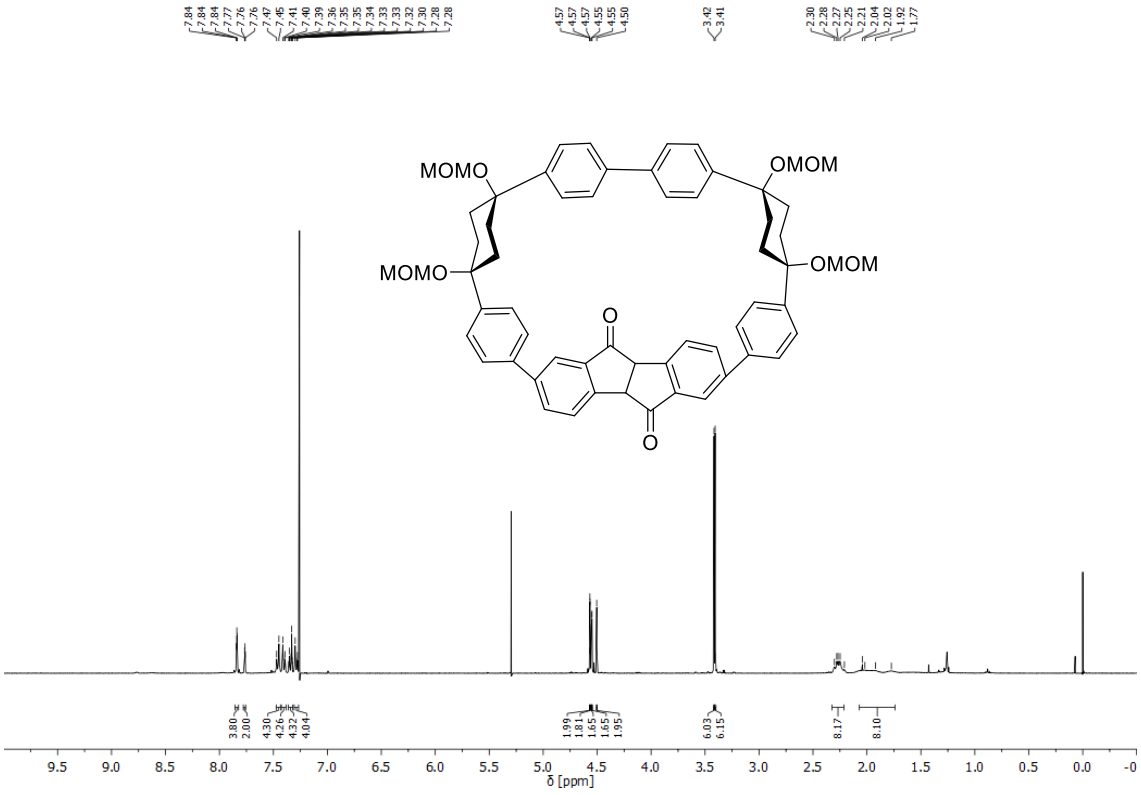

Figure S9. ^{1}H NMR spectrum (400 MHz, $CDCl_3$) of **8a**.

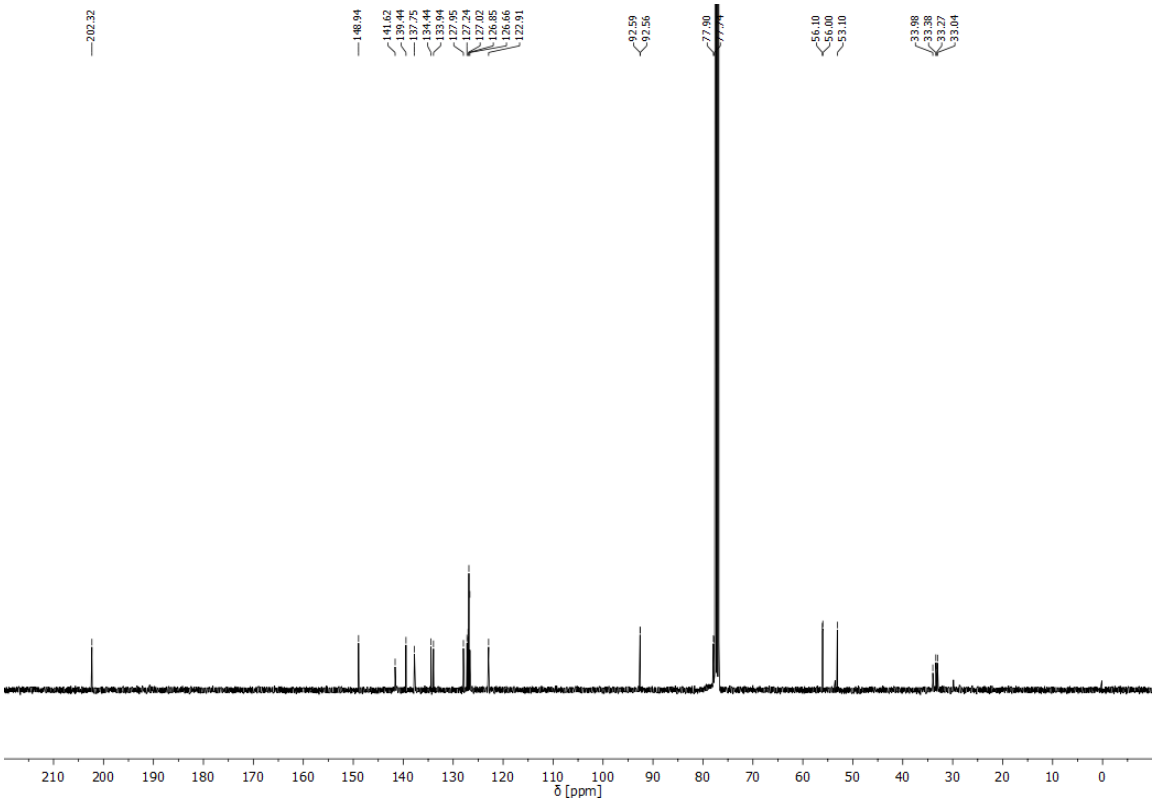

Figure S10. ^{13}C NMR spectrum (101 MHz, $CDCl_3$) of **8a**.

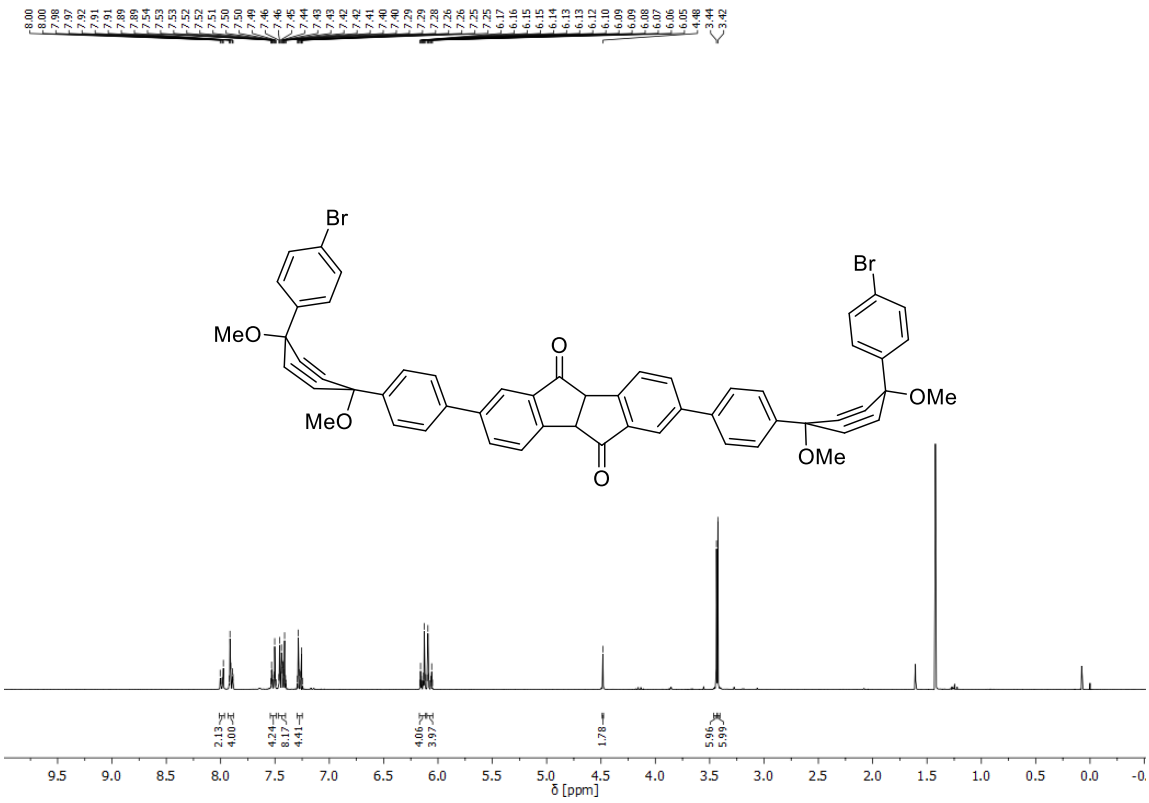

Figure S11. ^{1}H NMR spectrum (300 MHz, $CDCl_3$) of **7b**.

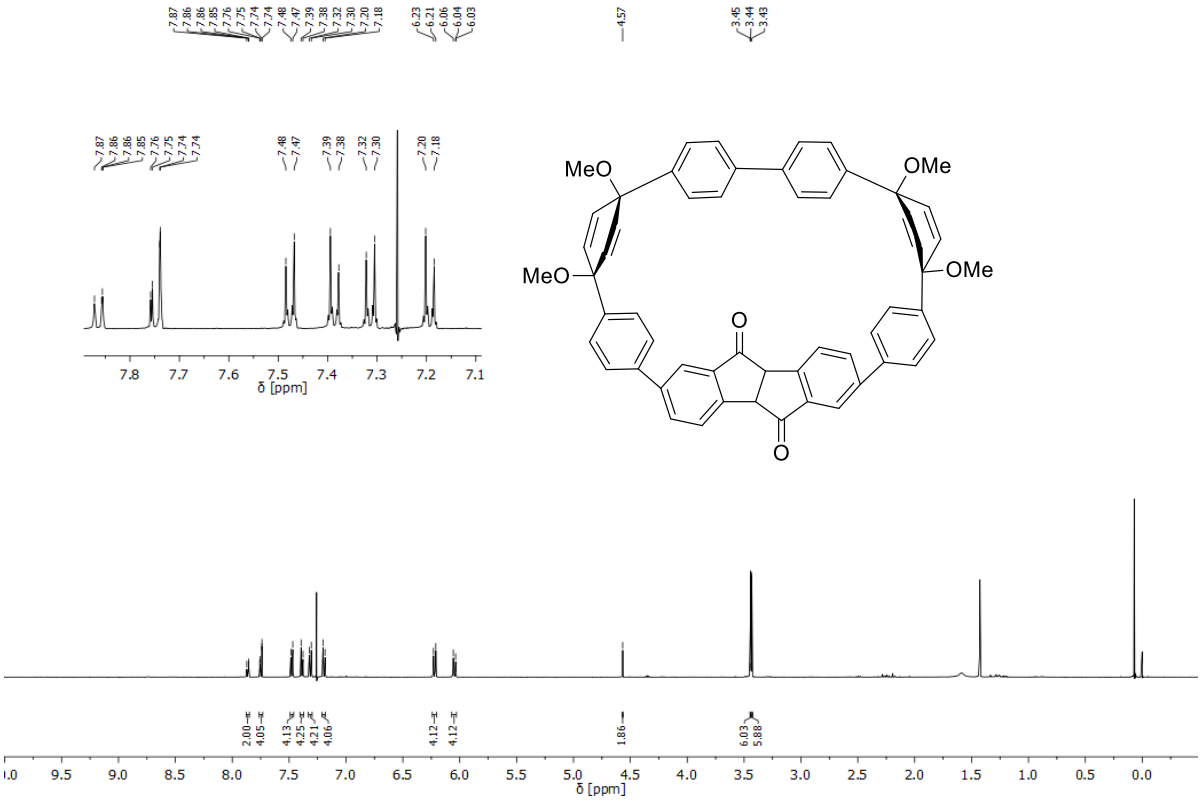

Figure S12. ^{1}H NMR spectrum (500 MHz, $CDCl_3$) of **8b**.

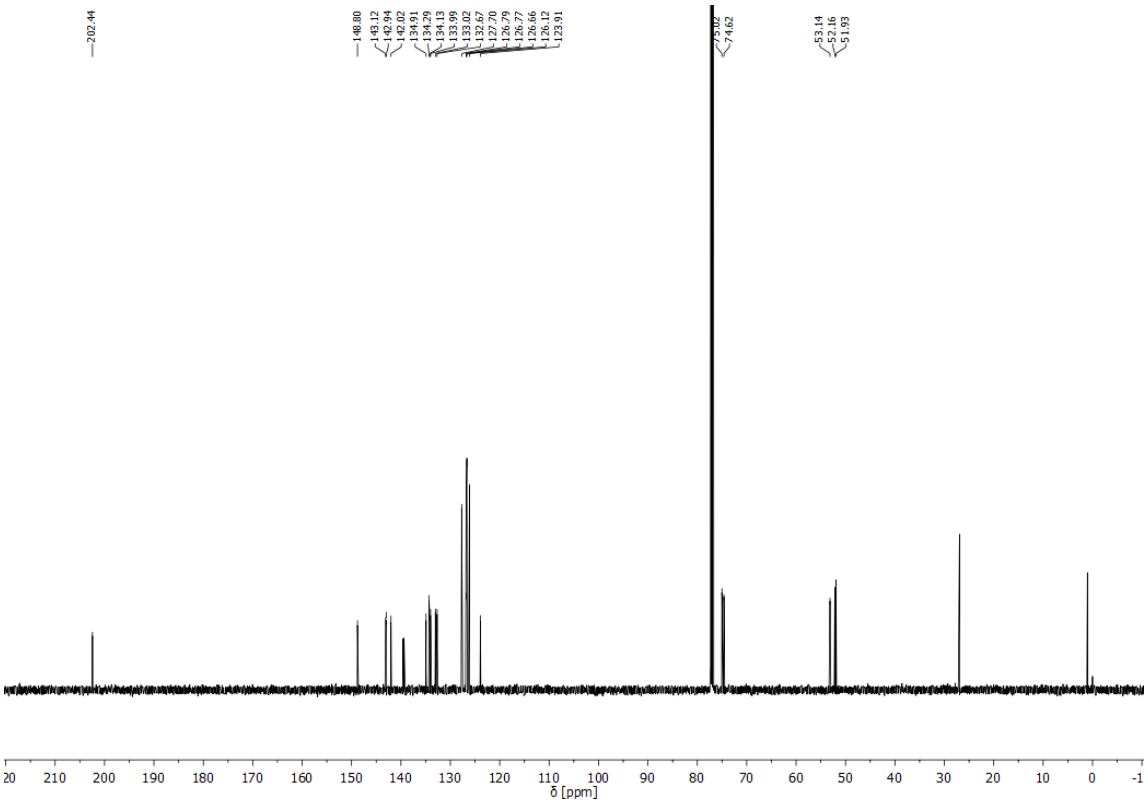

Figure S13. ^{13}C NMR spectrum (126 MHz, $CDCl_3$) of **8b**.

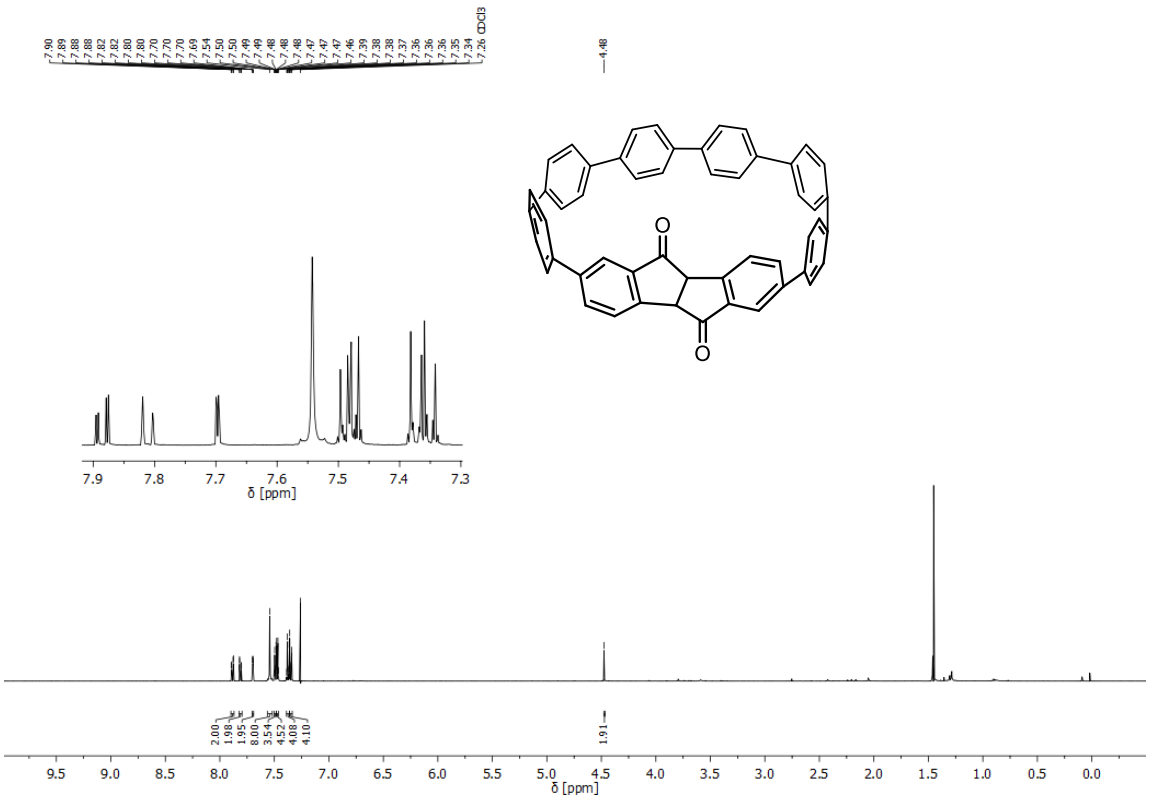

Figure S14. ^{1}H NMR spectrum (500 MHz, $CDCl_3$, 333 K) of **3**.

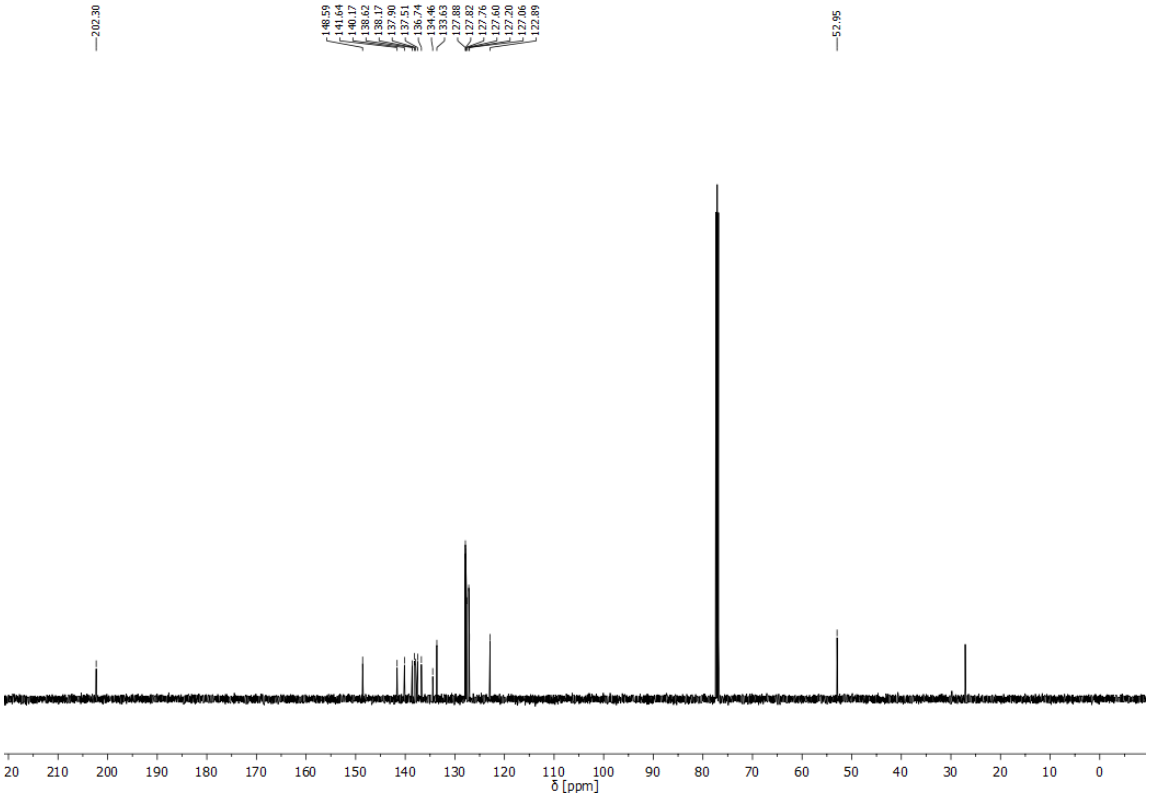

Figure S15. ^{13}C NMR spectrum (126 MHz, $CDCl_3$, 333 K) of **3**.

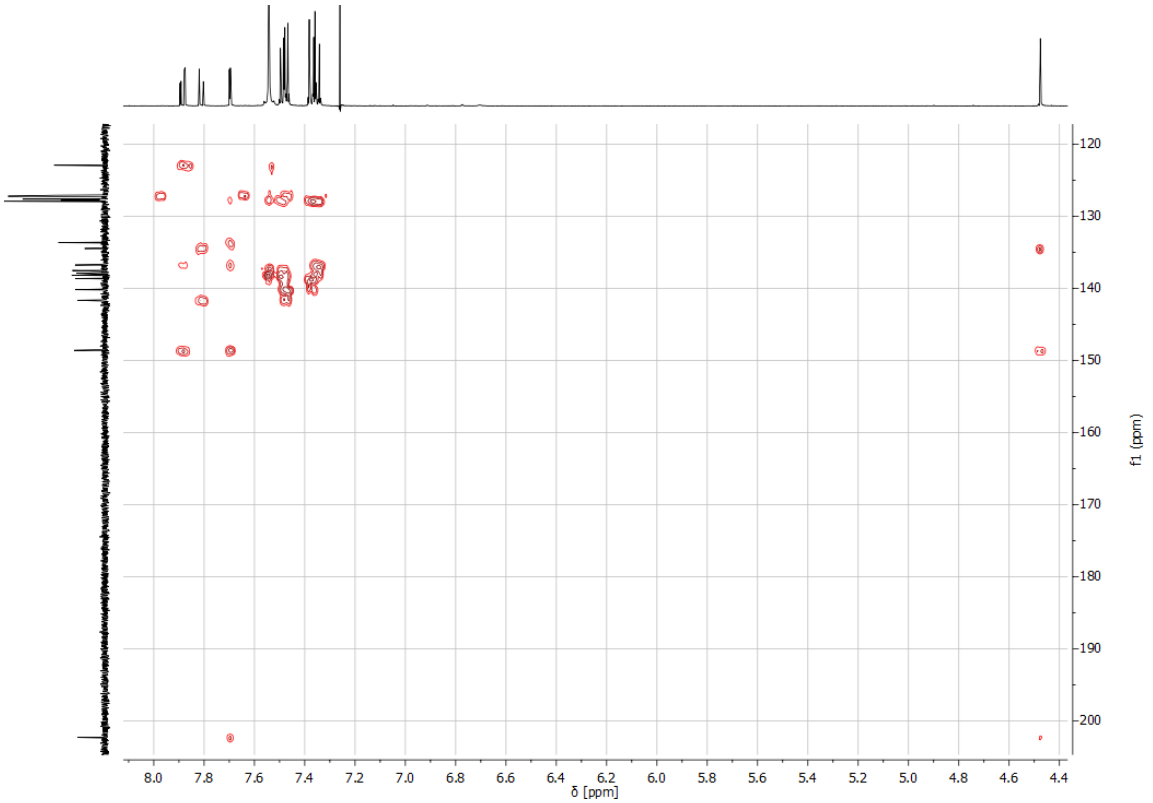

Figure S16. $^{1}H^{13}C$-HMBC NMR spectrum (500/126 MHz, $CDCl_3$, 333 K) of **3**.

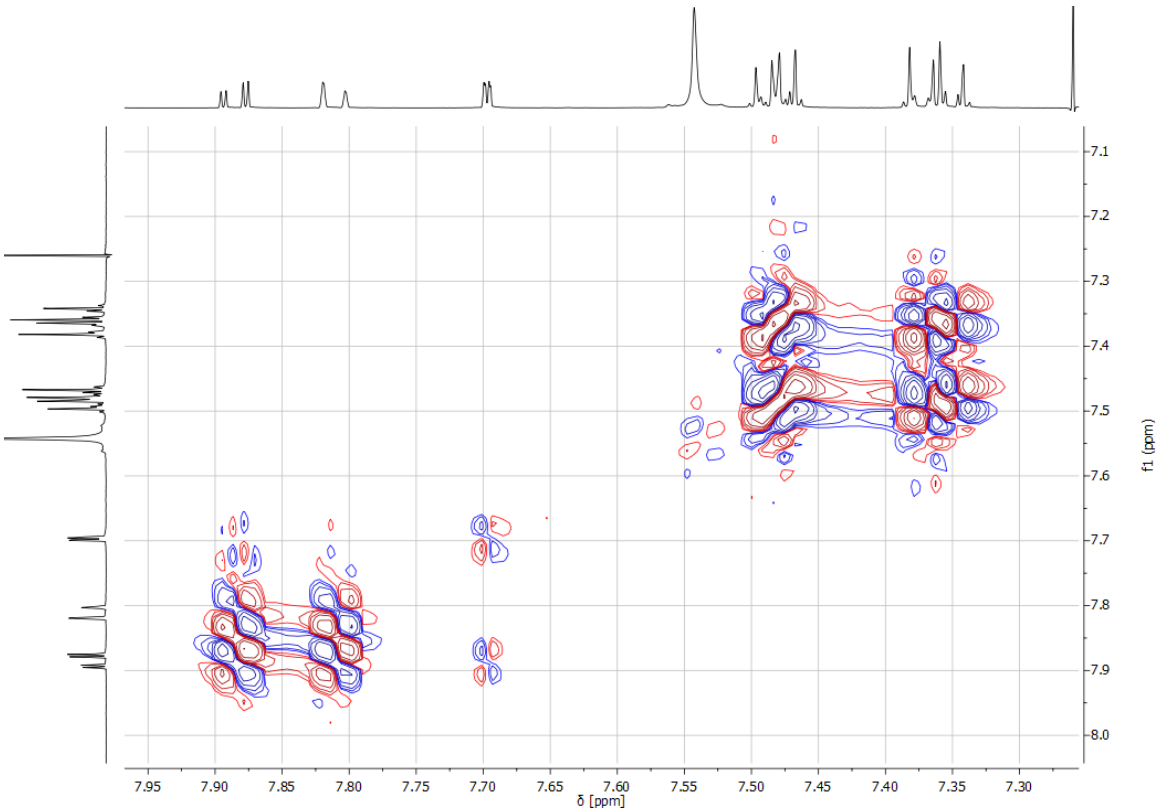

Figure S17. ^{1}H-^{1}H-COSY NMR spectrum (500 MHz, $CDCl_3$, 333 K) of **3**.

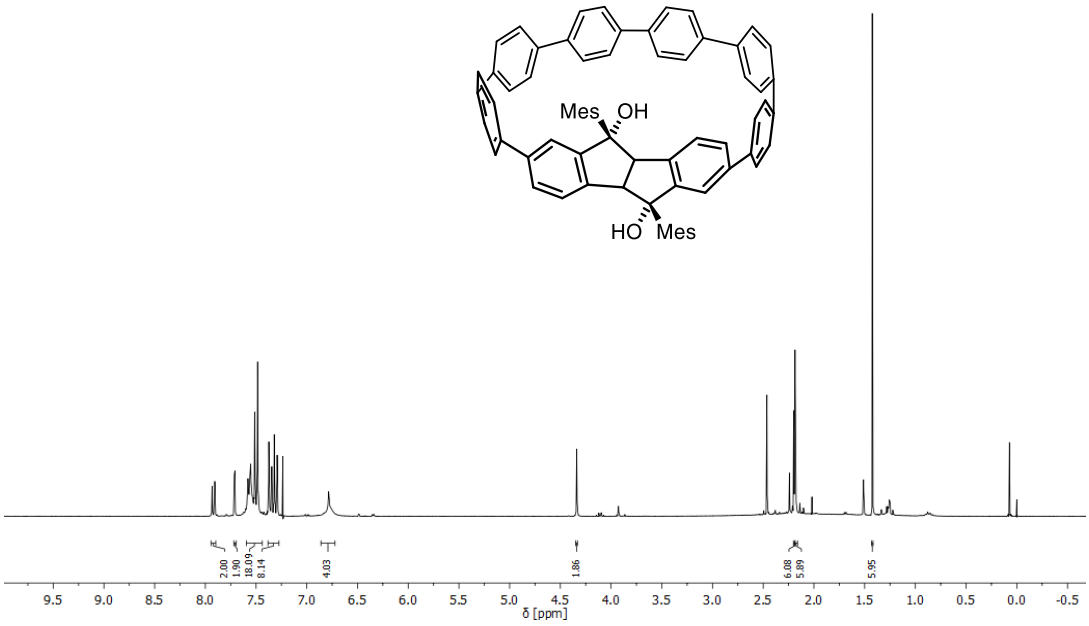

Figure S18. ^{1}H NMR spectrum (300 MHz, $CDCl_3$) of **S2**.

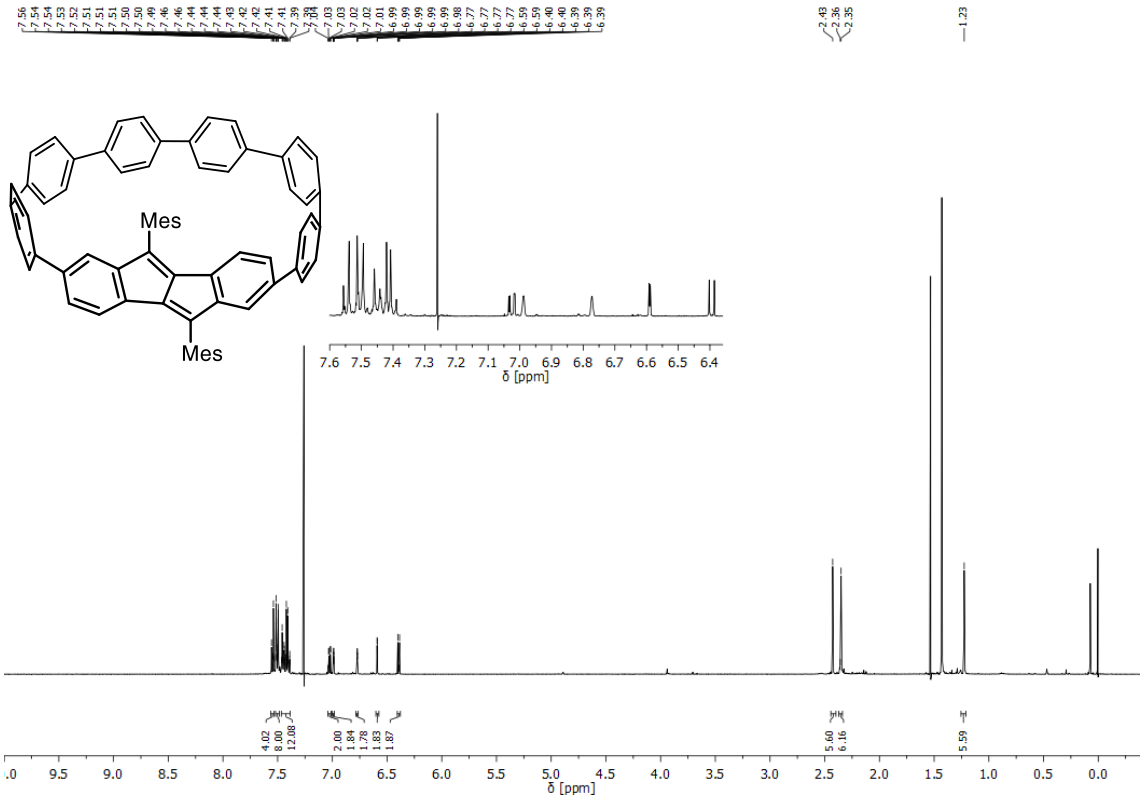

Figure S19. ^{1}H NMR spectrum (500 MHz, $CDCl_3$)of **1**.

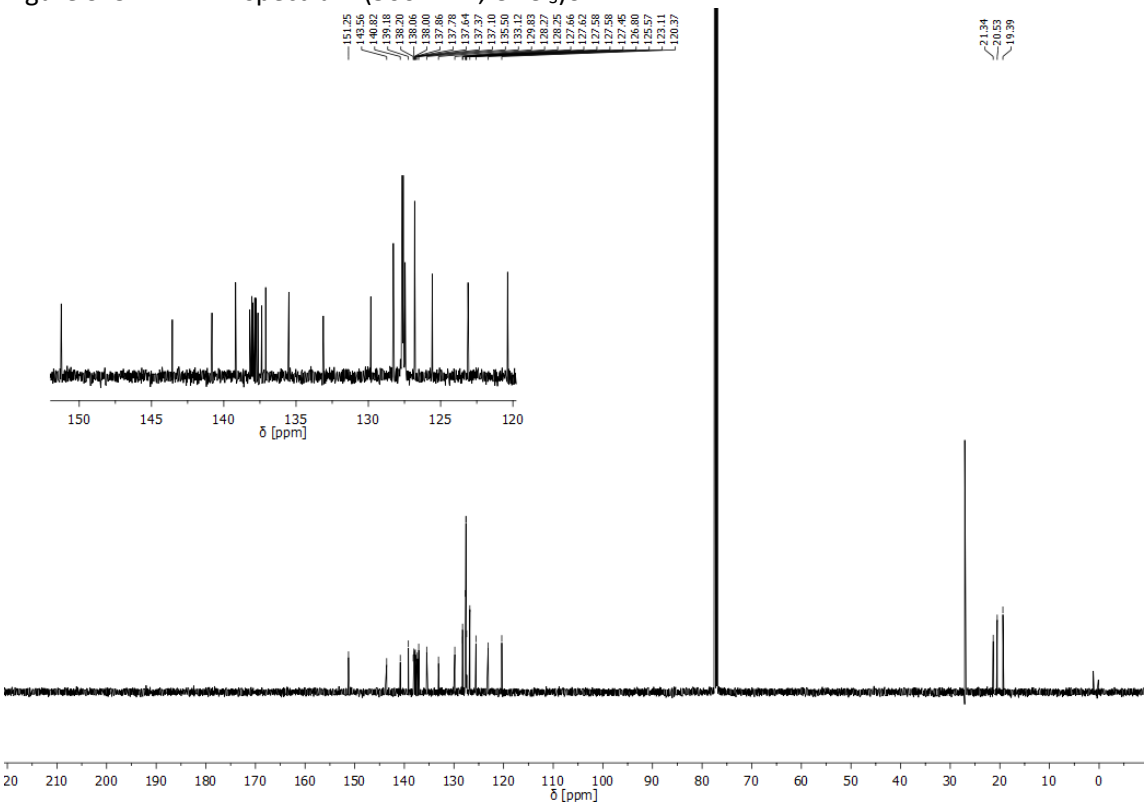

Figure S20. ^{13}C NMR spectrum (126 MHz, $CDCl_3$) of **1**.

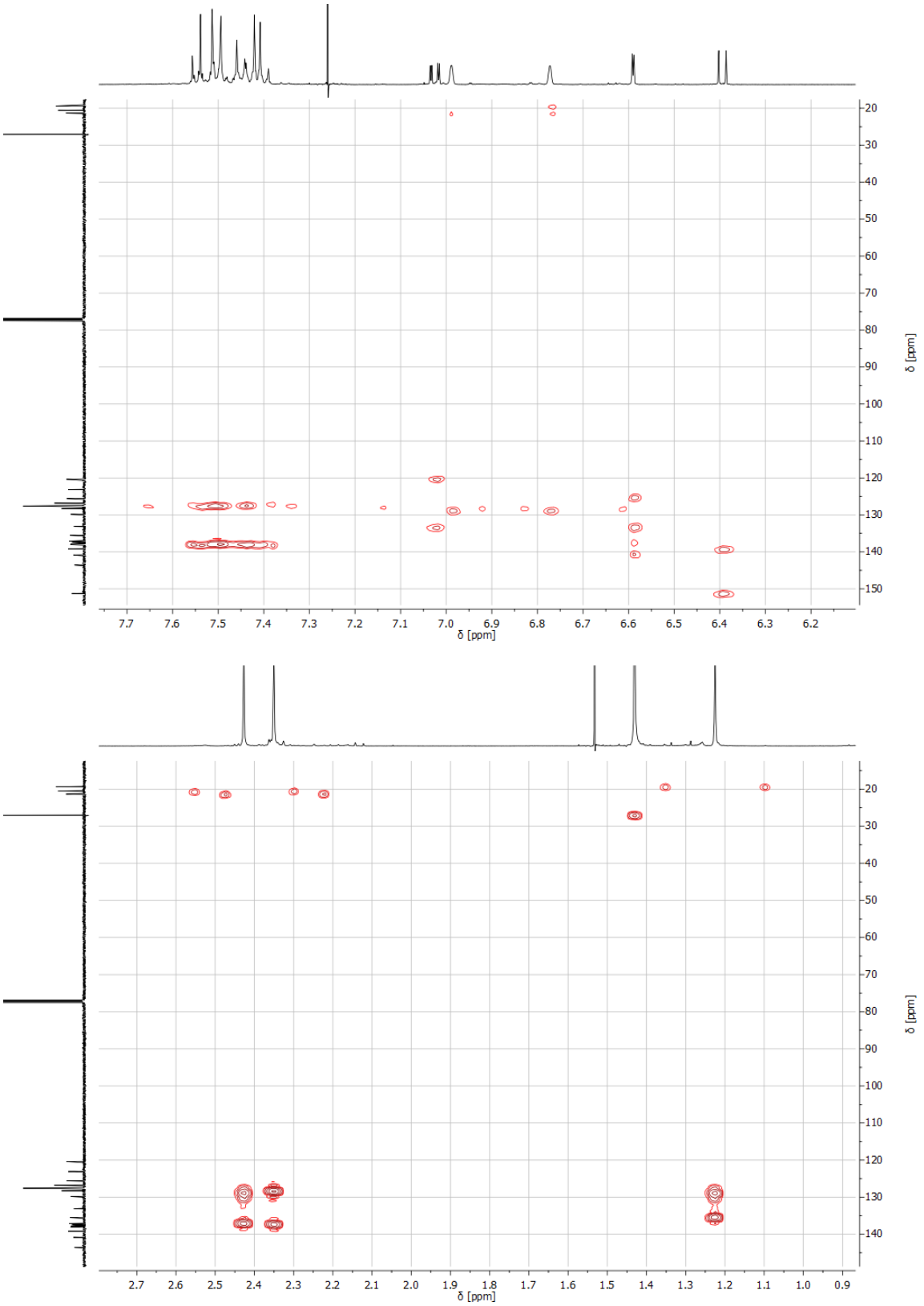

Figure S21. $^{1}H^{13}C$-HMBC NMR spectrum (500/126 MHz, $CDCl_3$) of **1**.

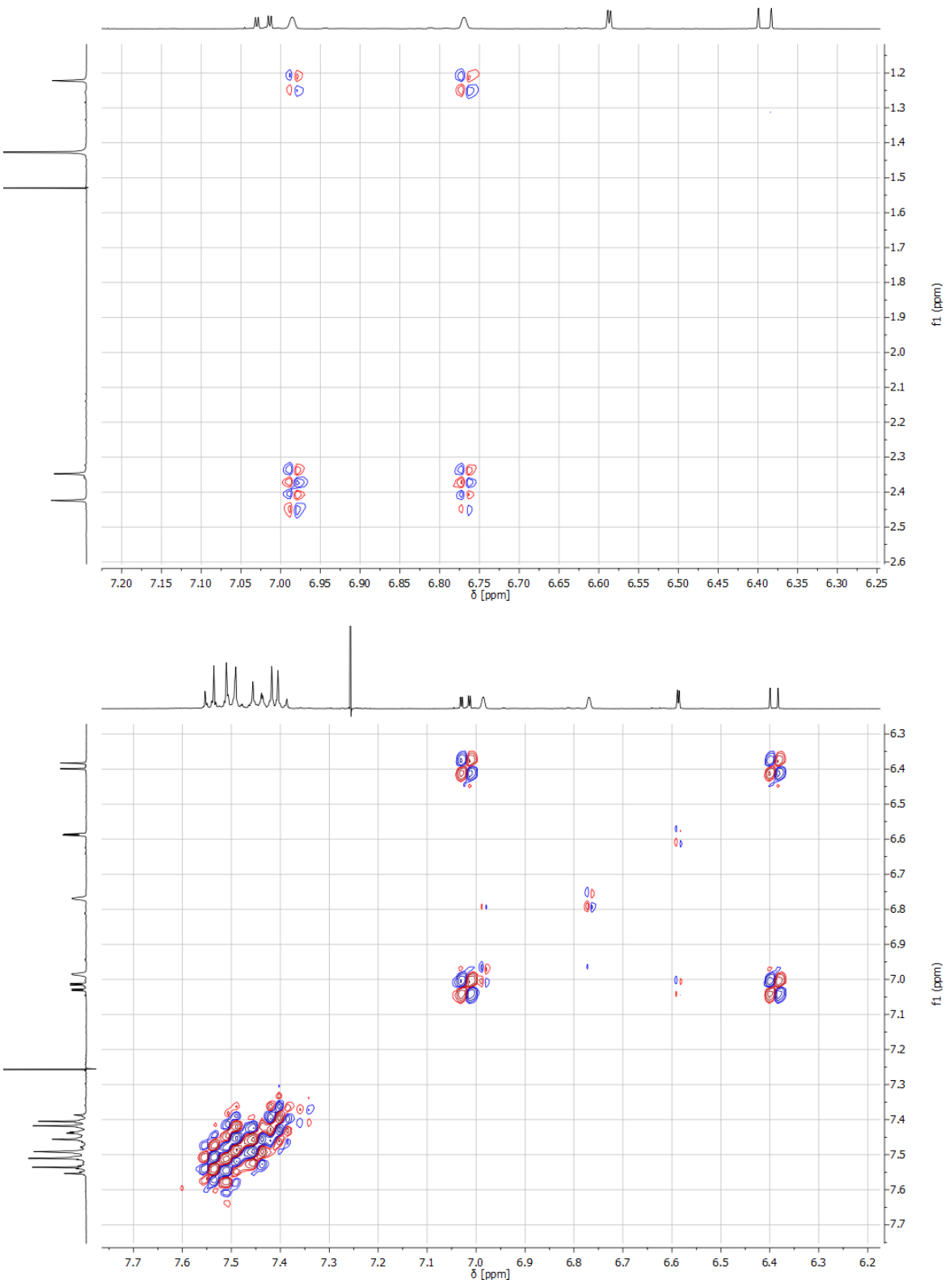

Figure S22. ^{1}H-^{1}H-COSY NMR spectrum (500 MHz, $CDCl_3$) of **1**.

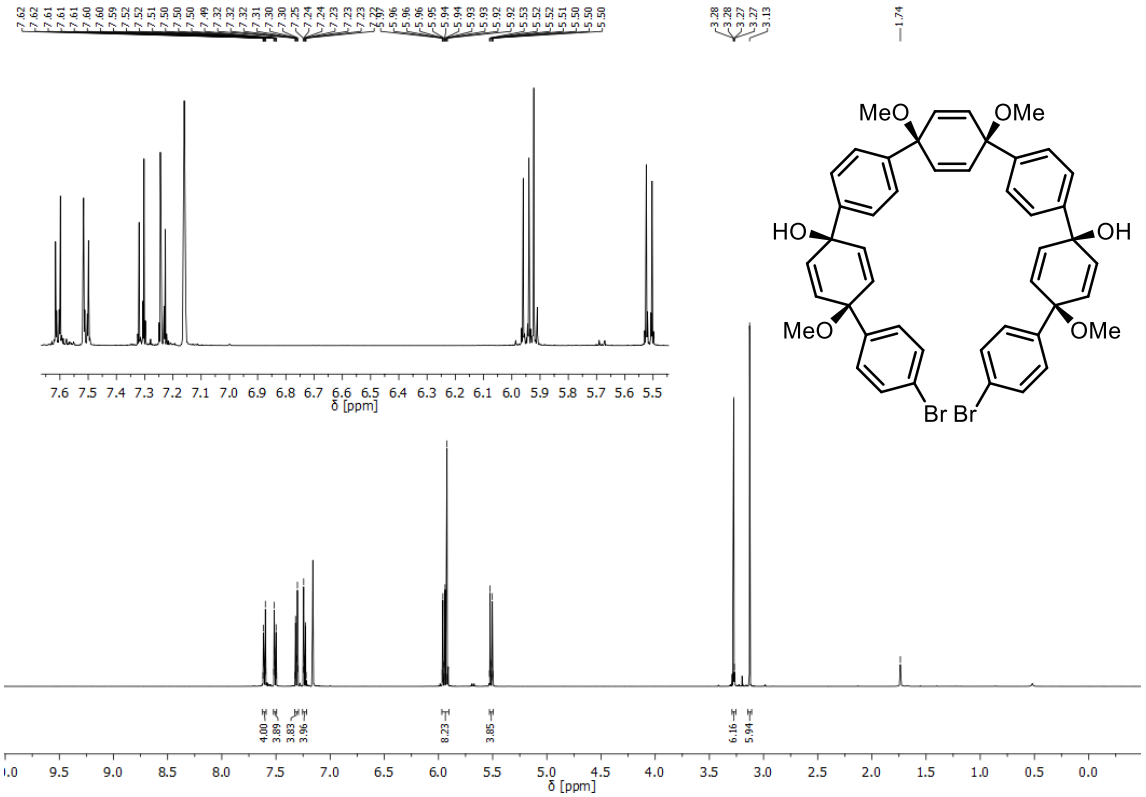

Figure S23. ^{1}H NMR spectrum (500 MHz, C_6D_6) of **S5**.

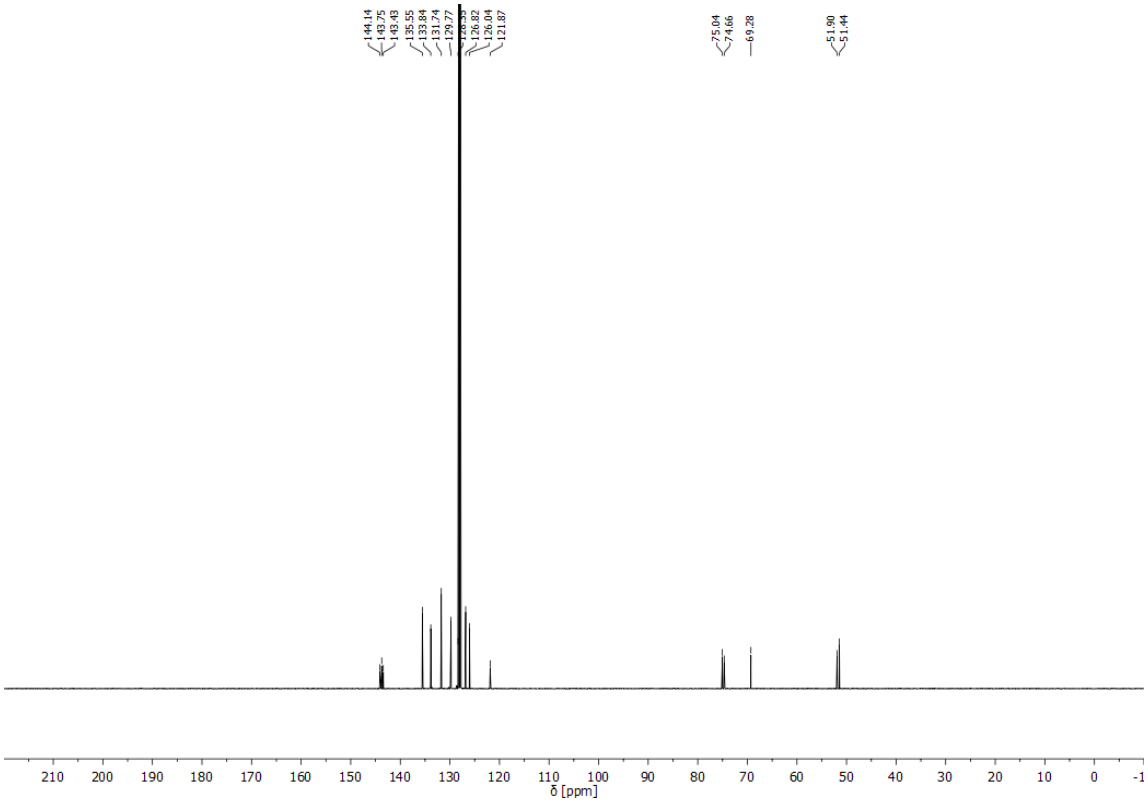

Figure S24. ^{13}C NMR spectrum (126 MHz, C_6D_6) of **S5**.

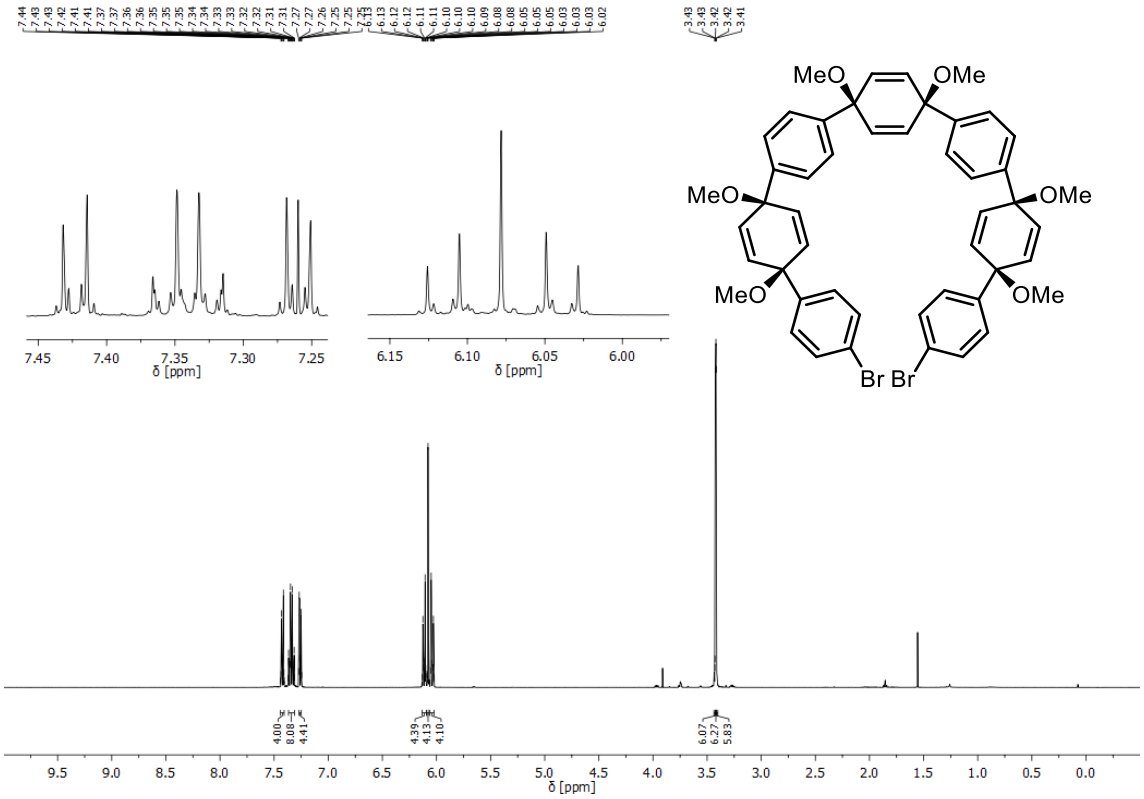

Figure S25. ^{1}H NMR spectrum (500 MHz, $CDCl_3$) of **9**.

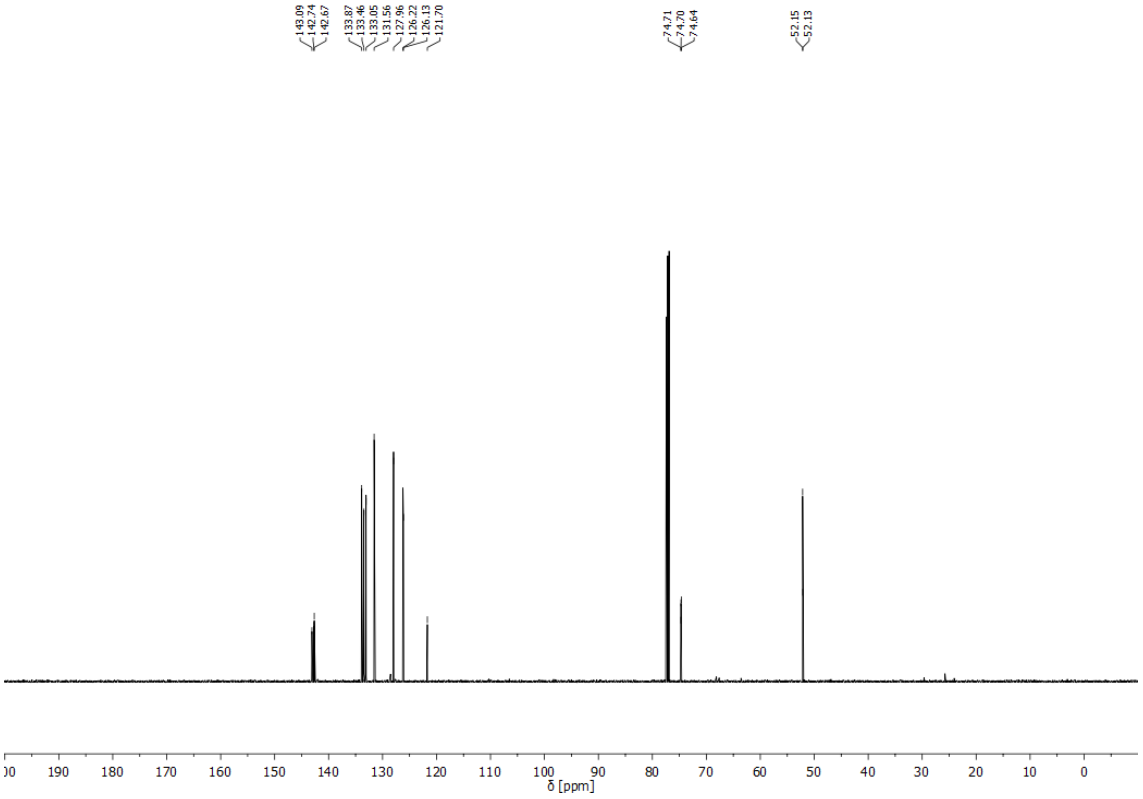

Figure S26. ^{13}C NMR (126 MHz, $CDCl_3$) spectrum of **9**.

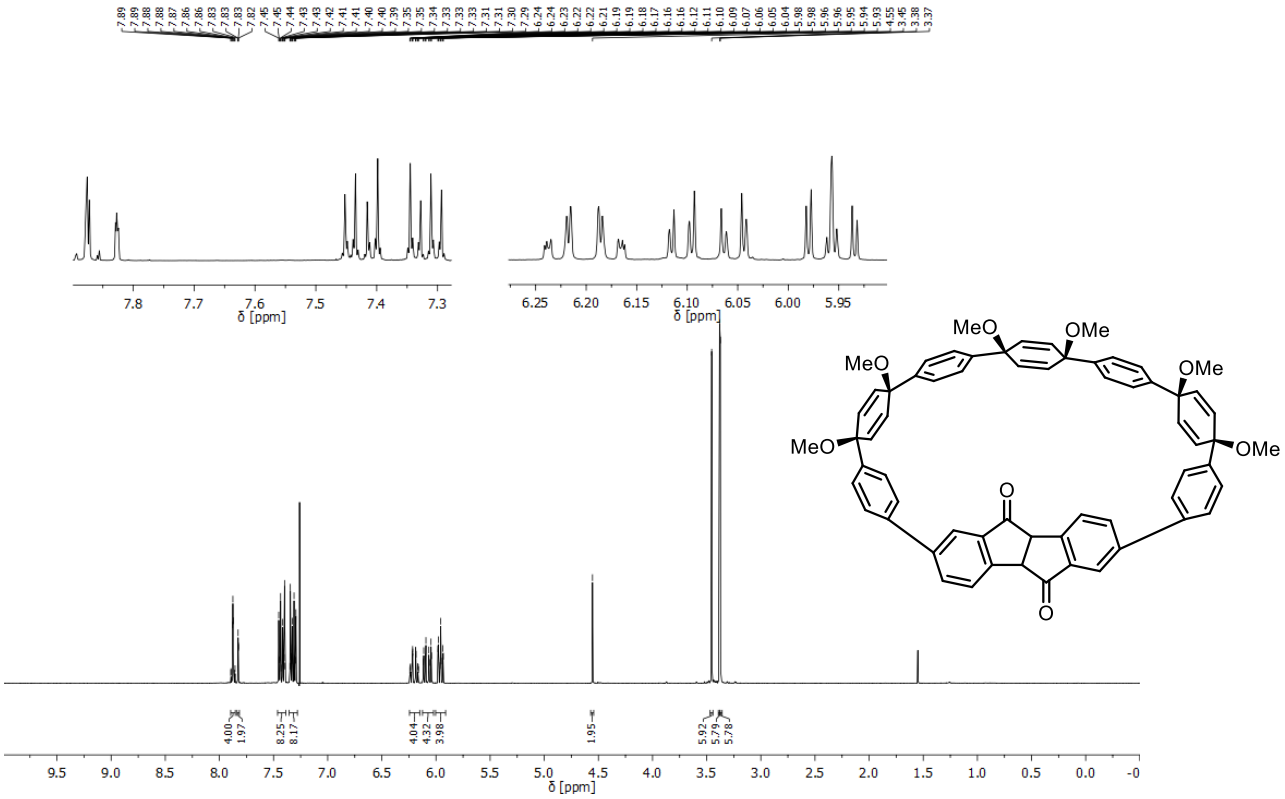

Figure S27. ^{1}H NMR spectrum (500 MHz, $CDCl_3$) of **10**.

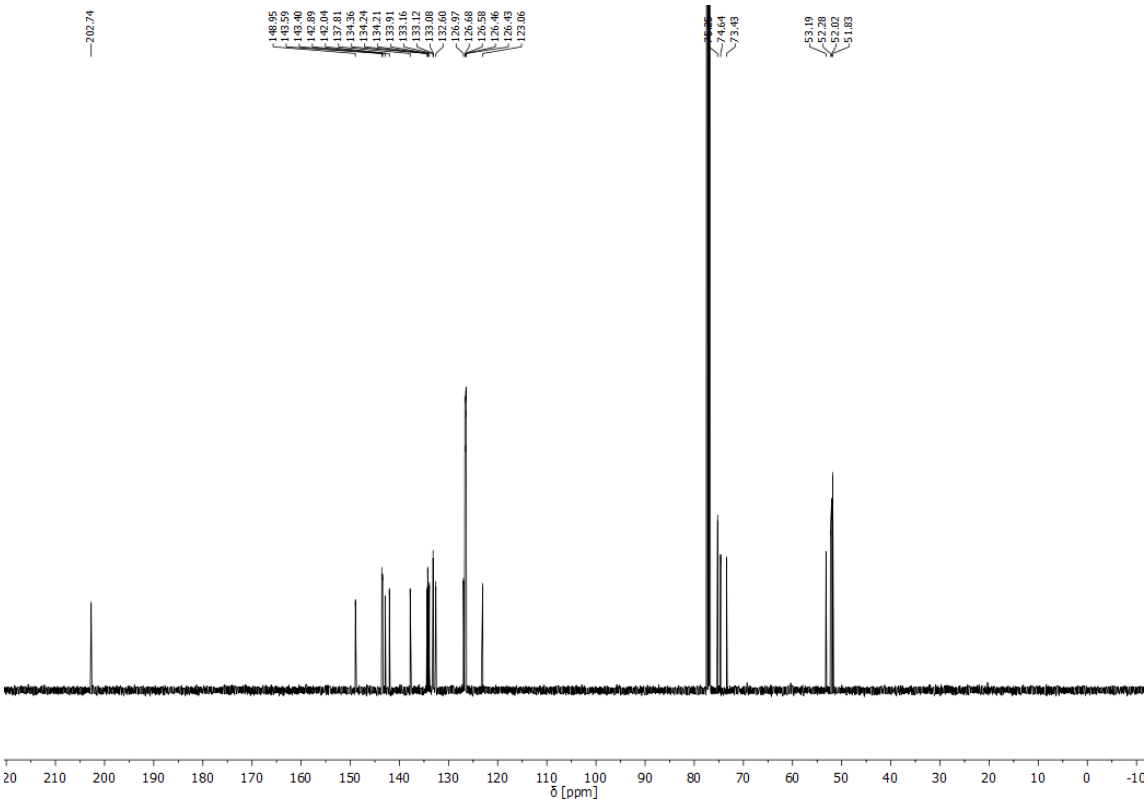

Figure S28. ^{13}C NMR spectrum (126 MHz, $CDCl_3$) of **10**.

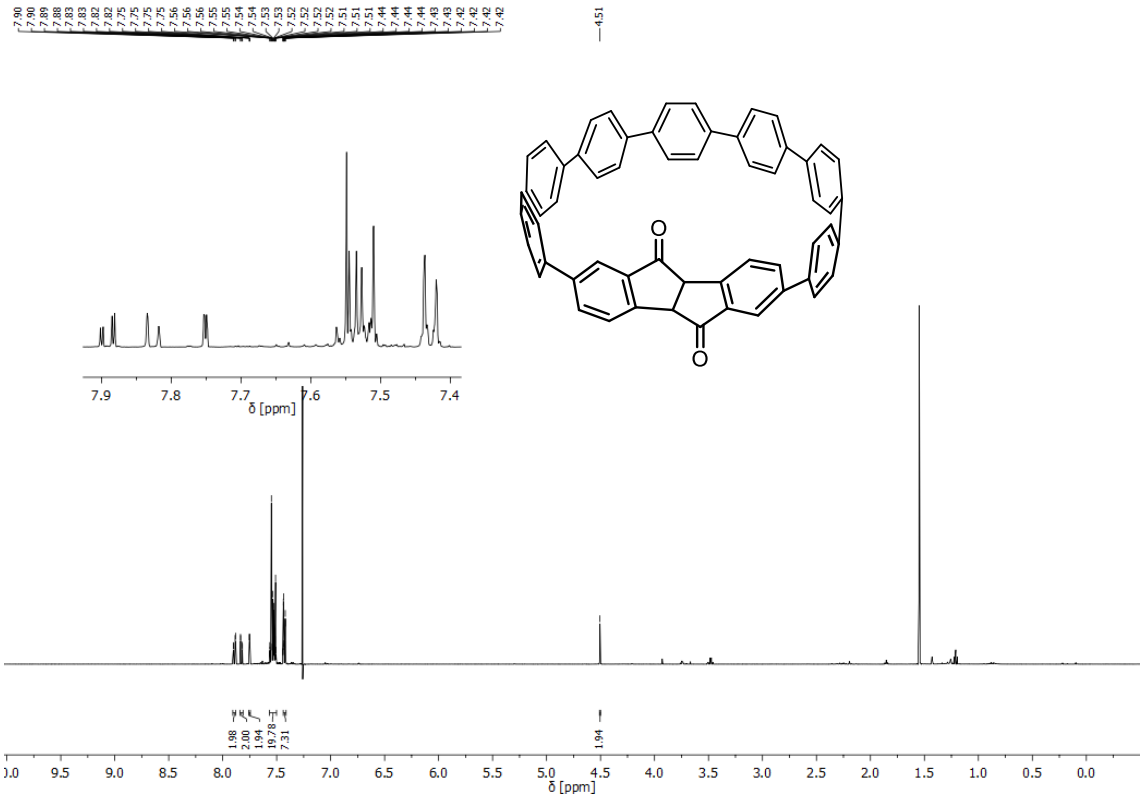

Figure S29. ^{1}H NMR spectrum (500 MHz, $CDCl_3$) of **4**.

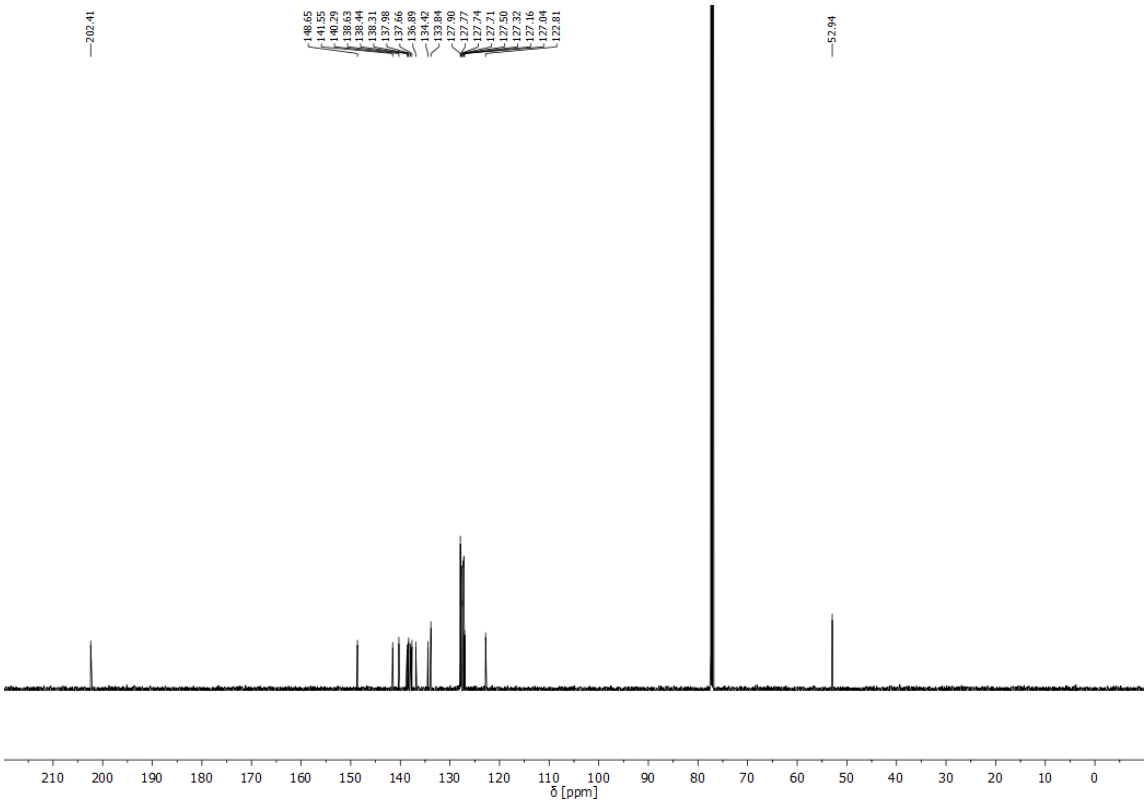

Figure S30. ^{1}H NMR spectrum (126 MHz, $CDCl_3$) of **4**.

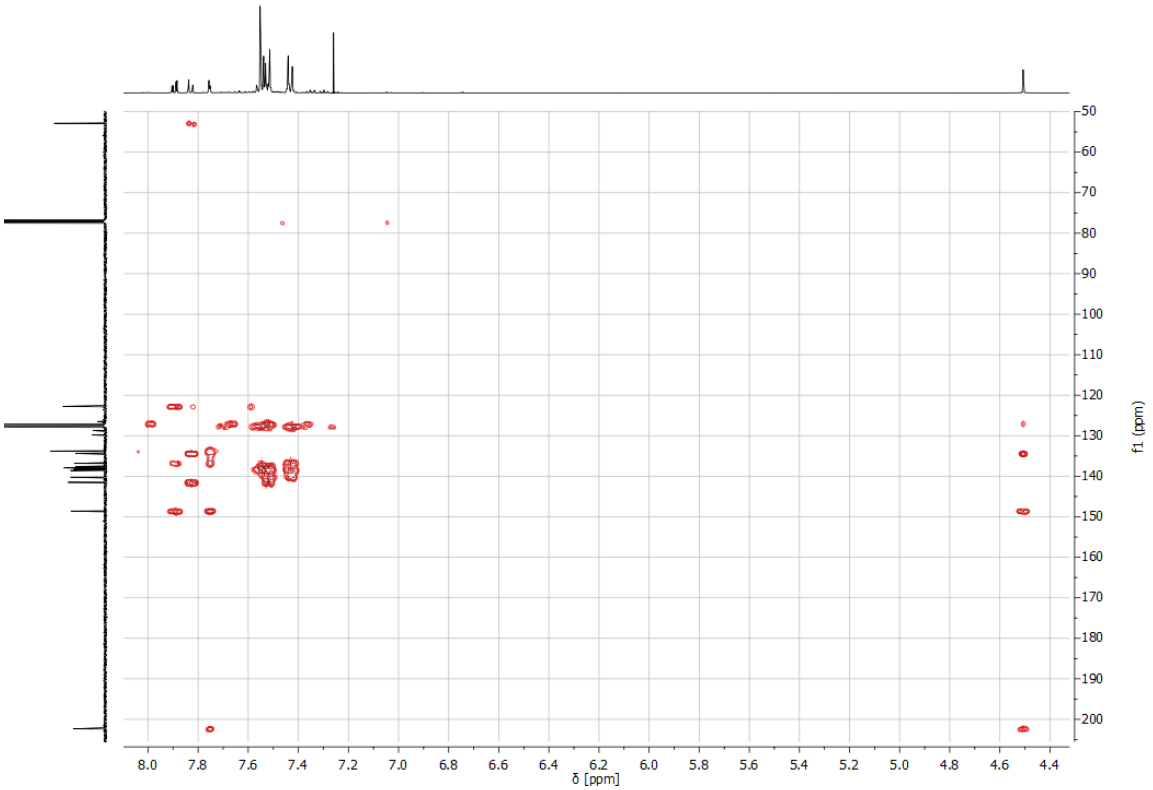

Figure S31. $^{1}H^{13}C$-HMBC spectrum (500/126 MHz, $CDCl_3$) of **4**.

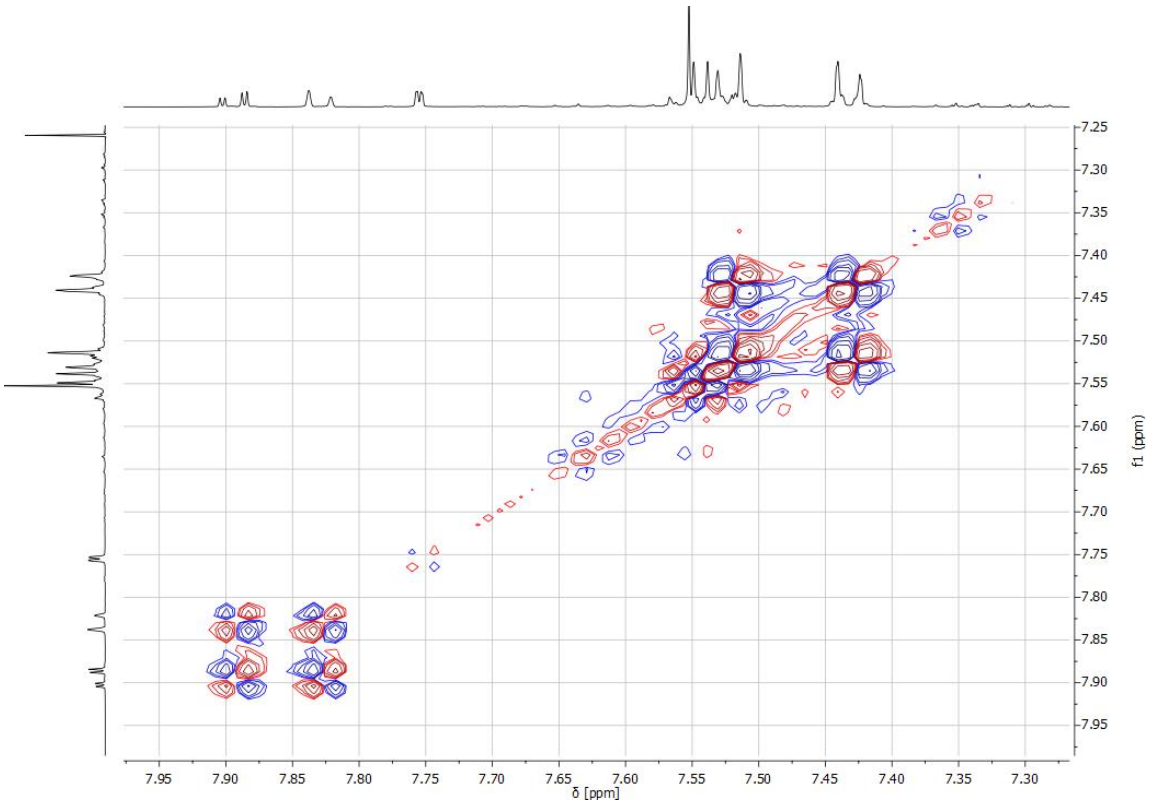

Figure S32. ^{1}H-^{1}H-COSY spectrum (500 MHz, $CDCl_3$) of **4**.

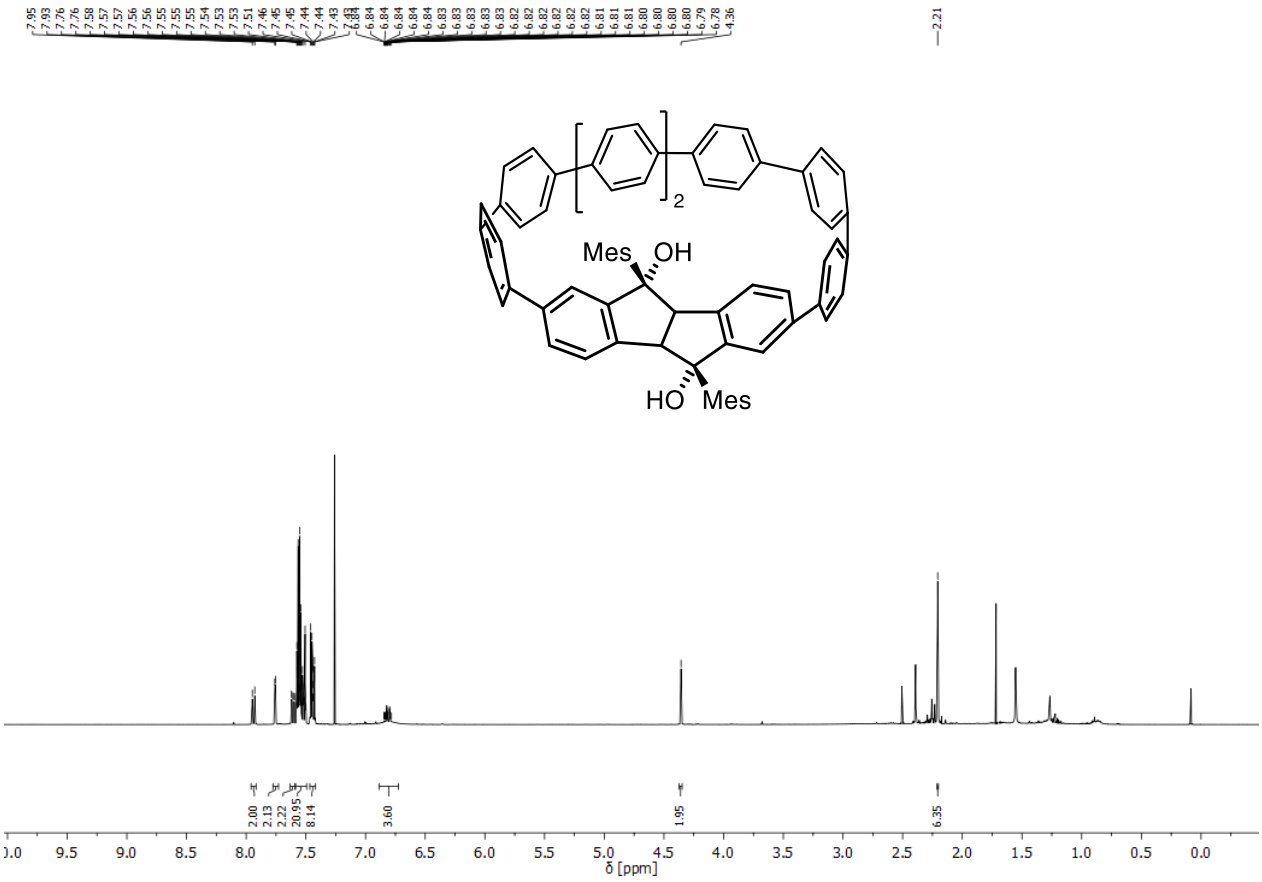

Figure S33. ^{1}H NMR spectrum (400 MHz, $CDCl_3$) of **S3**.

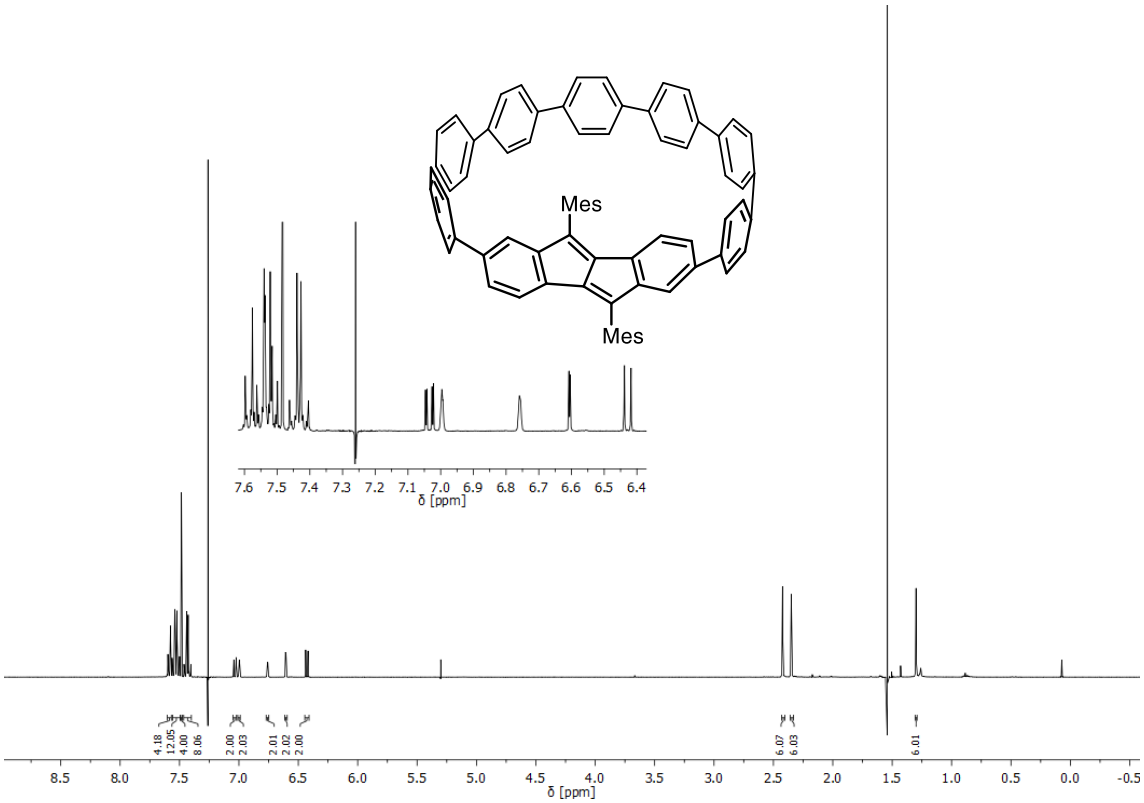

Figure S34. ^{1}H NMR spectrum (400 MHz, $CDCl_3$) of **2**.

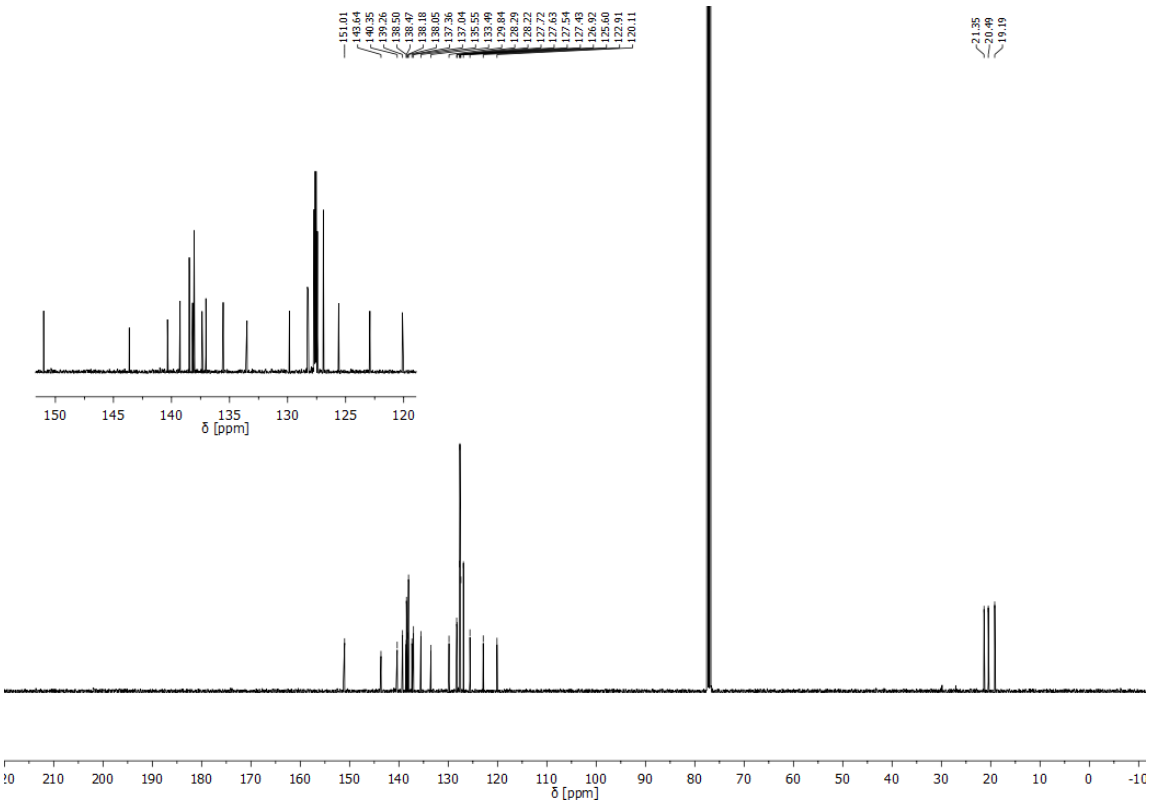

Figure S35. ^{13}C NMR spectrum (100 MHz, $CDCl_3$) of **2**.

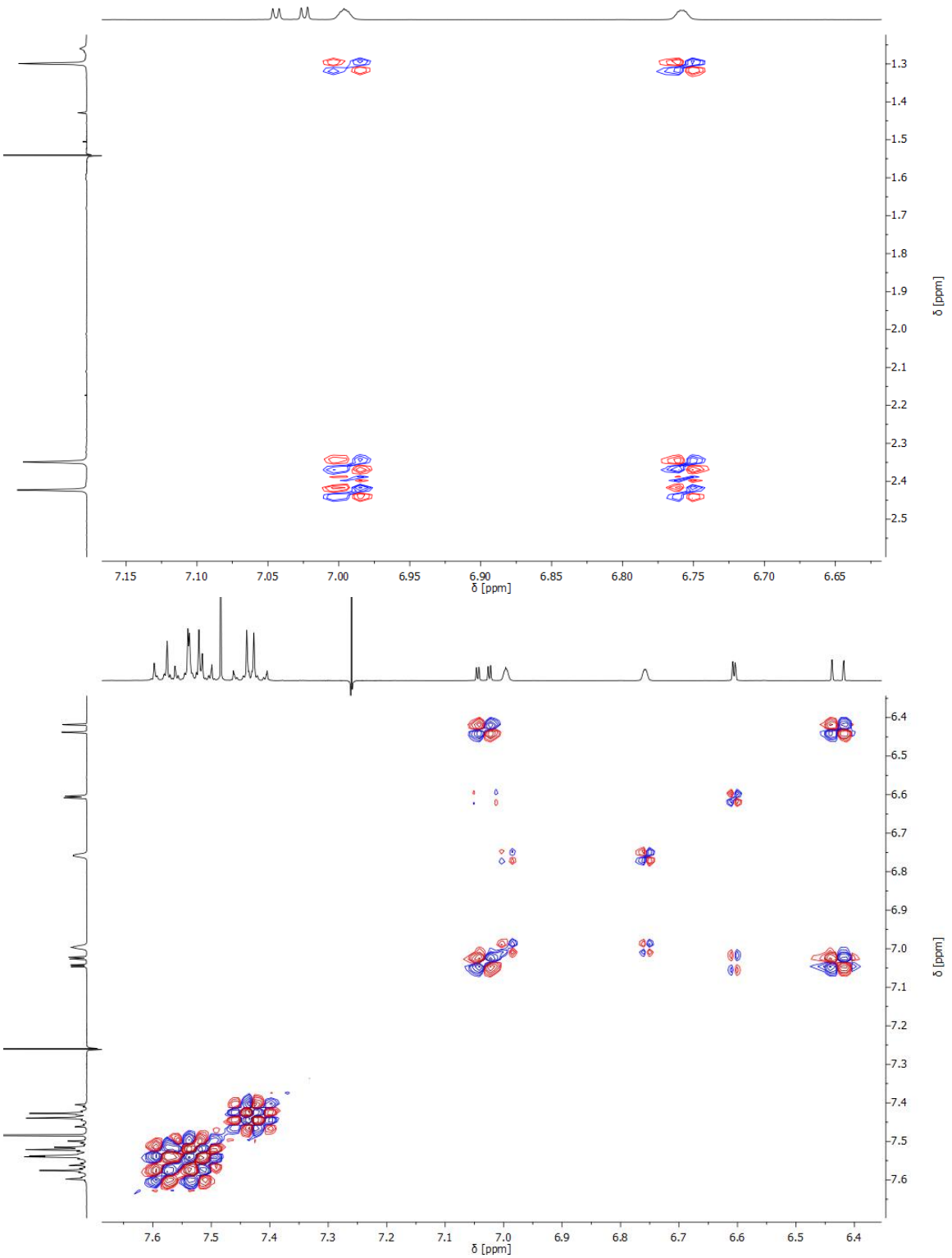

Figure S36. $^{1}H^{1}H$-COSY spectrum (400 MHz, $CDCl_3$) of **2**.

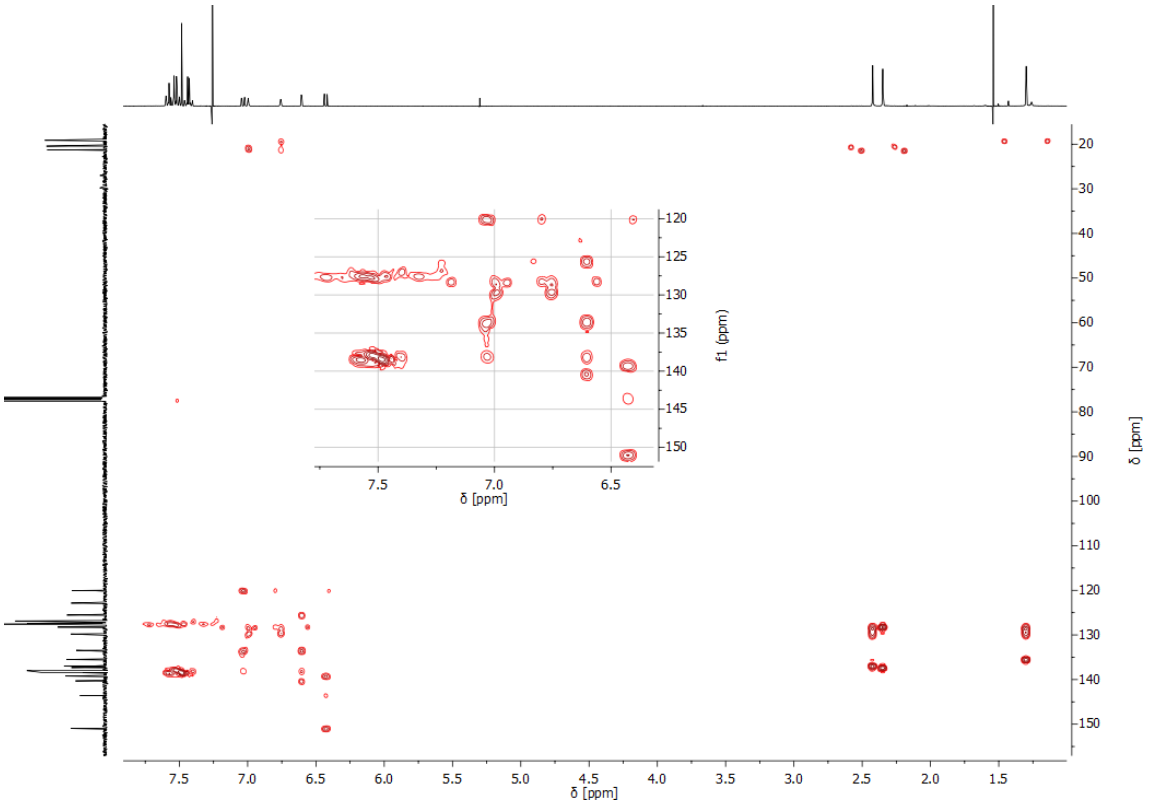

Figure S37. $^{1}H^{13}C$-HMBC spectrum (400/100 MHz, $CDCl_3$) of **2**.

3.2 NMR Spectra of Sulfoximine Adducts

The chiral resolution of hoop **3** by chiral derivatization is one of the key advancements of this publication. Therefore, we want to include as much data as possible to remove any doubts about the identity of the synthesized compounds. Due to the fast thermal decomposition of the products of the chiral sulfoximine derivatization to the diketone starting material we show the initial NMR spectra measured at 300 MHz (^{1}H NMR) as well as at 400 or 500 MHz (^{1}H, ^{13}C and 2D-NMR) where decomposition products are visible. The "decomposition pathways" (as can be seen in Scheme S1) are: **12** → **13** → **(*S*,*S*)-3** and **15** → **14** → **(*R*,*R*)-3**.

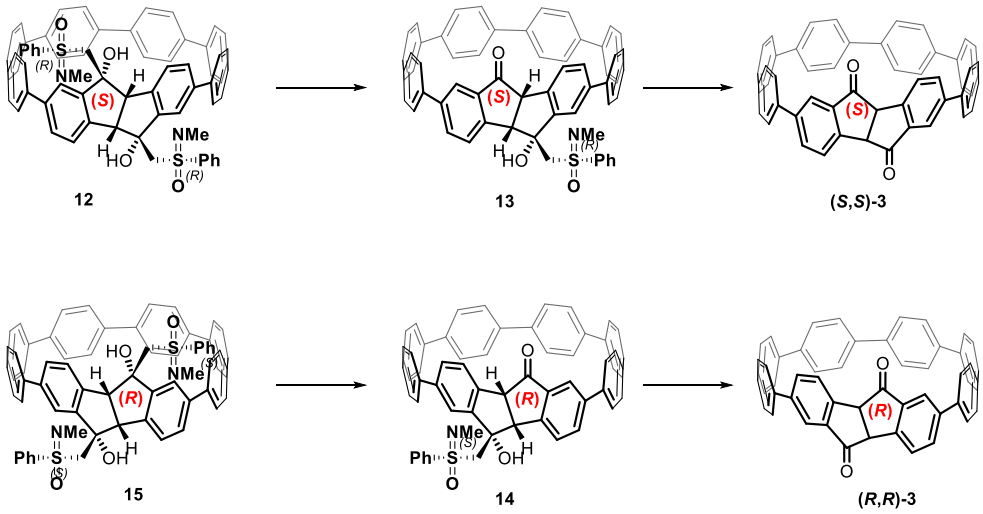

Scheme S1. Decomposition pathways for sulfoximine adducts.

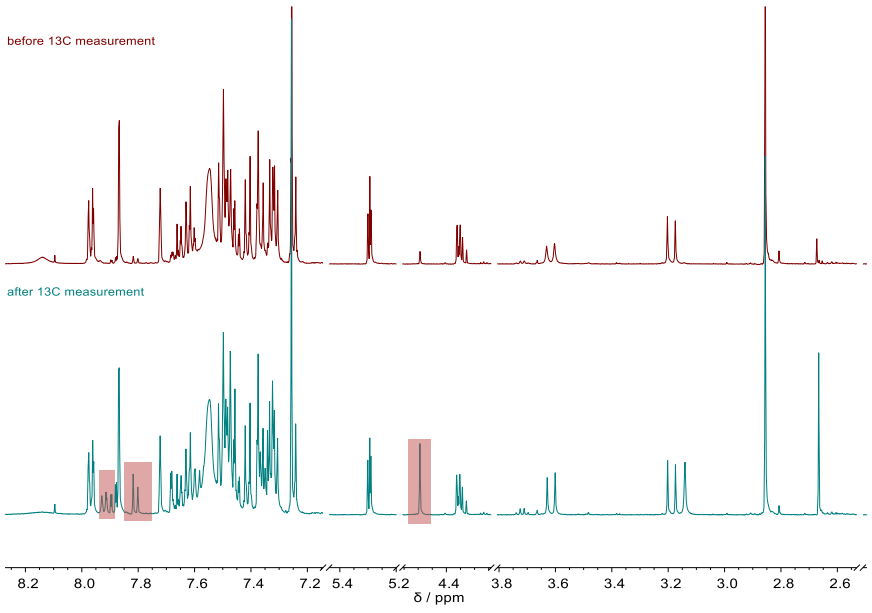

Figure S38. ^{1}H NMR spectra of **14** before and after the ^{13}C NMR measurement showing signals of decomposition products (in this case the decomposition of **14** yields **(*R*,*R*)-3**, marked red in the spectra above).

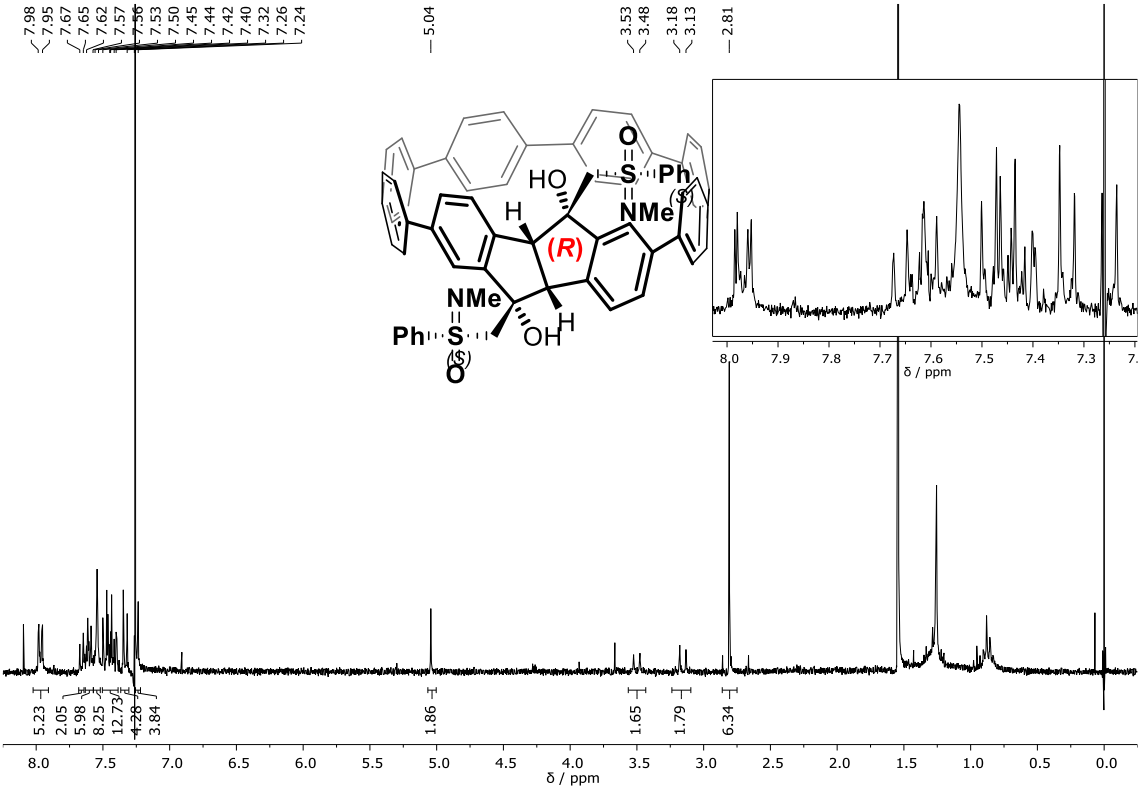

Figure S39. ^{1}H NMR spectrum (300 MHz) of **15**.

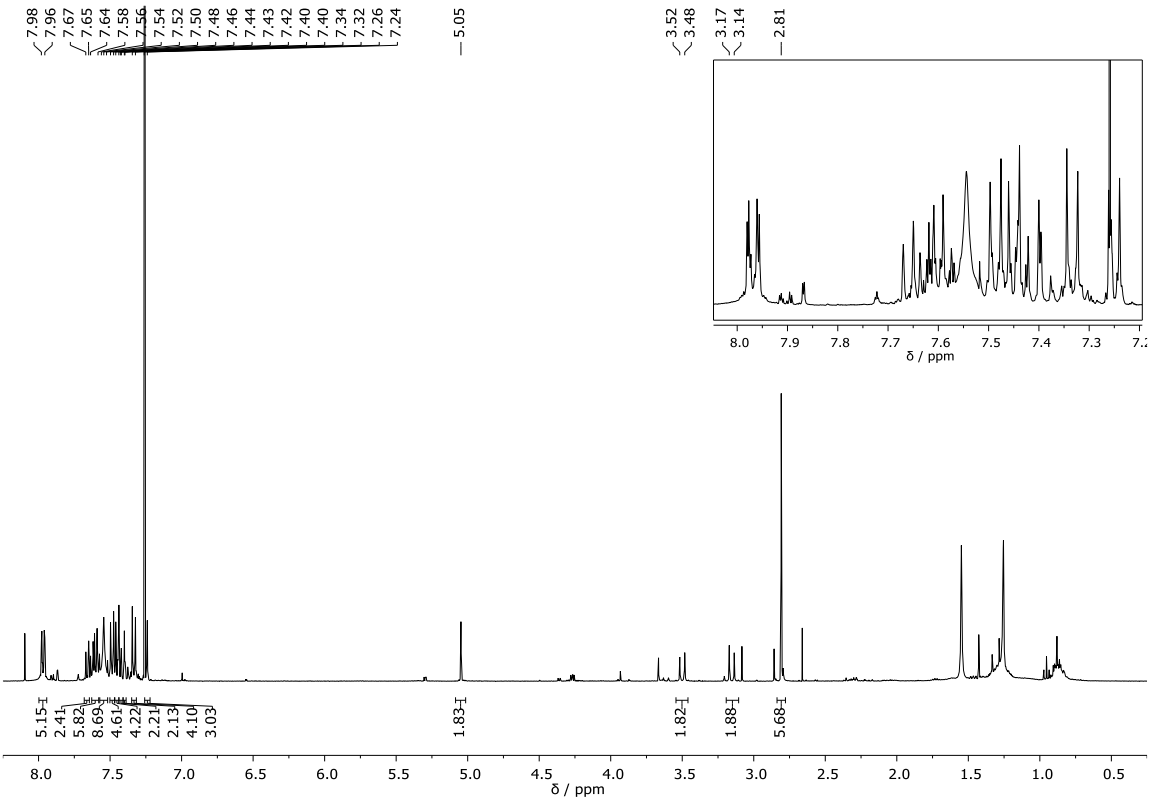

Figure S40. ^{1}H NMR spectrum (400 MHz) of **15**.

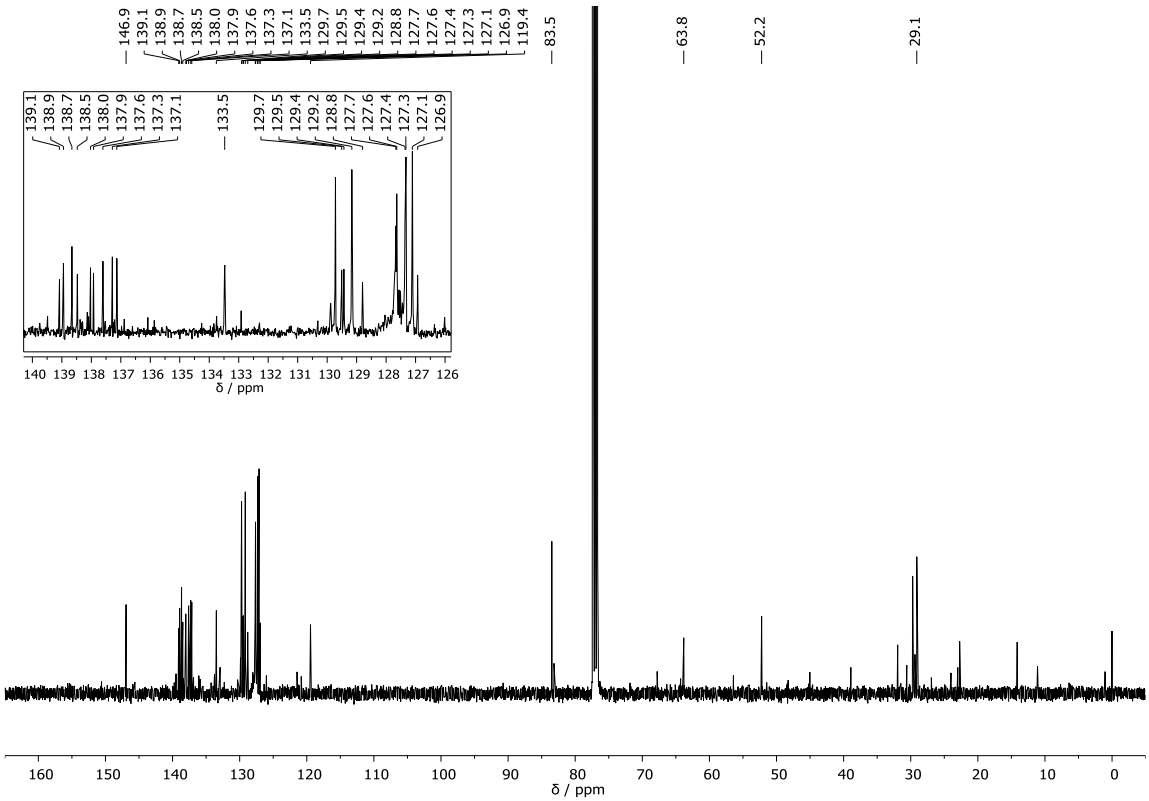

Figure S41. ^{13}C NMR spectrum (400 MHz) of **15**.

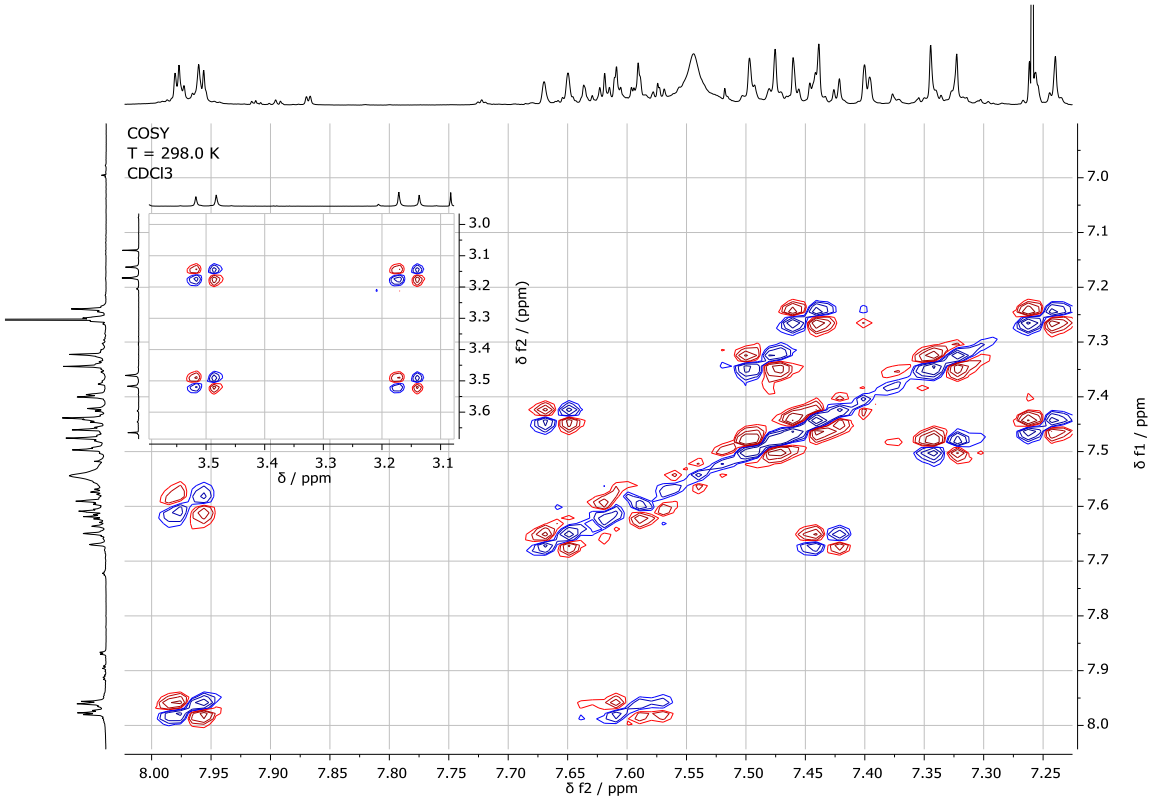

Figure S42. ^{1}H-^{1}H COSY NMR spectrum (400 MHz) of **15**.

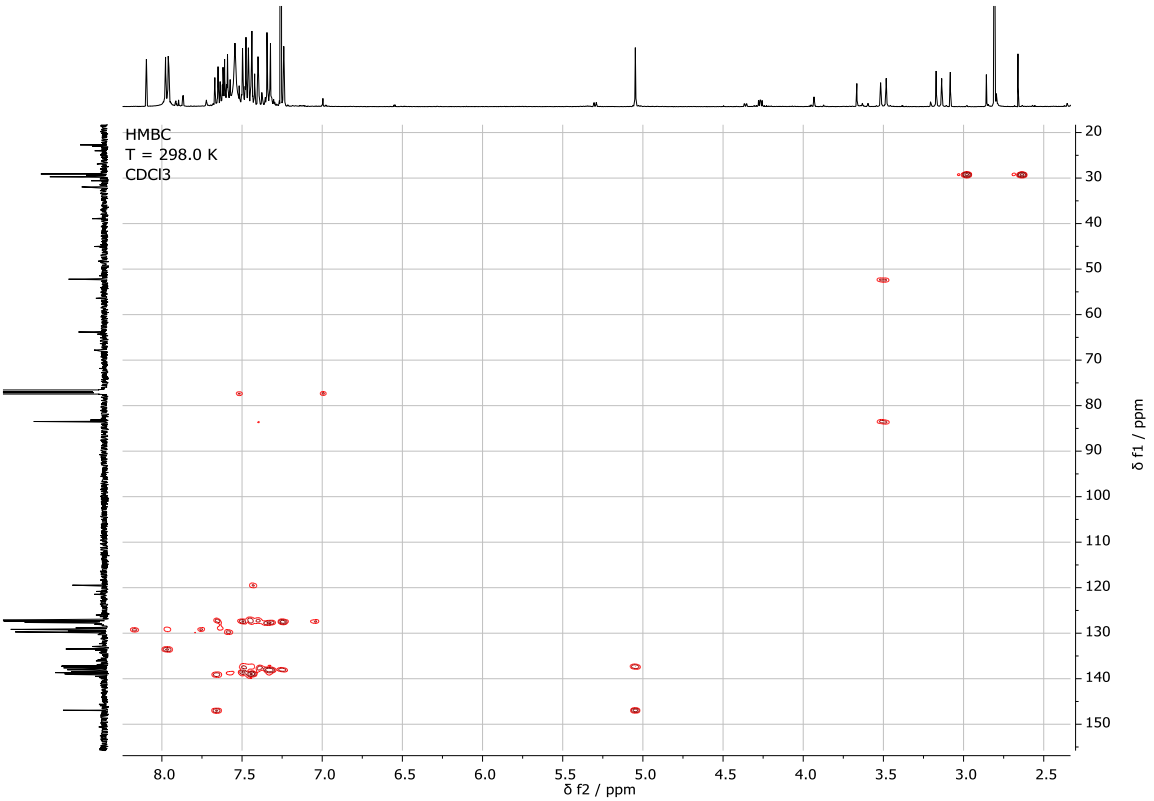

Figure S43. ^{1}H-^{13}C HMBC NMR spectrum (400 MHz) of **15**.

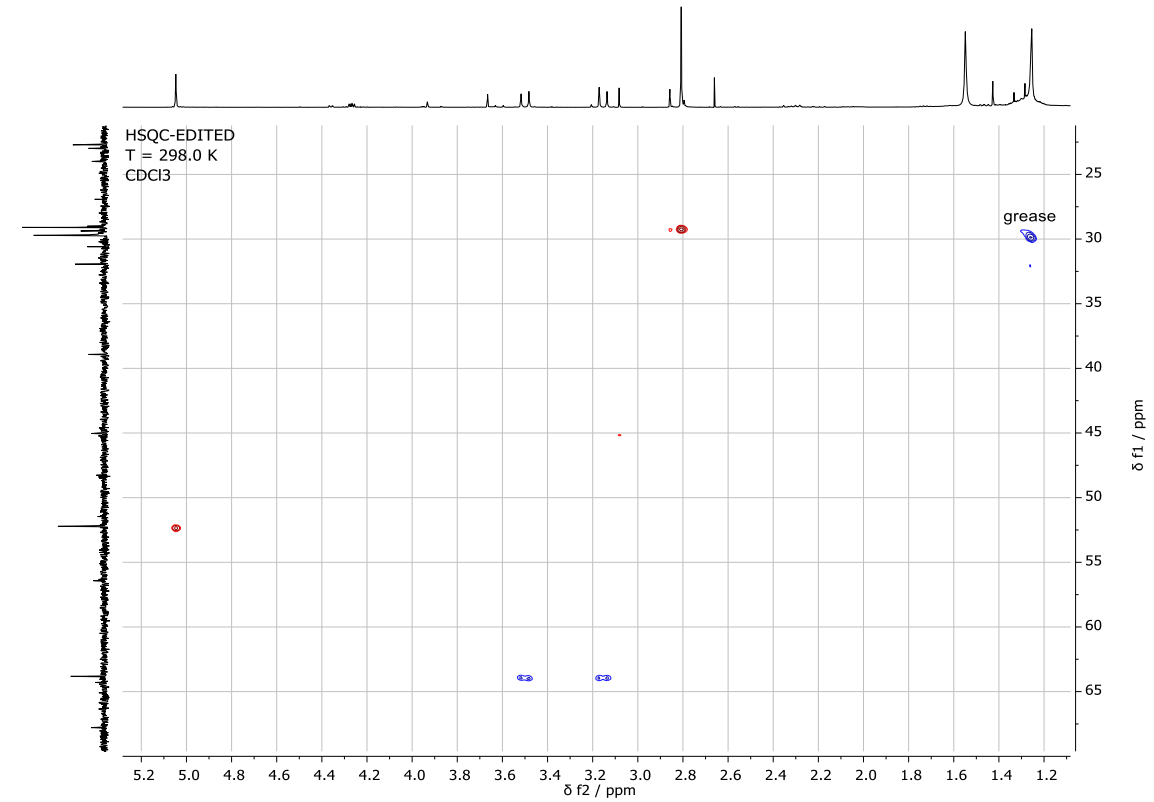

Figure S44. HSQC NMR spectrum (400 MHz) of **15**.

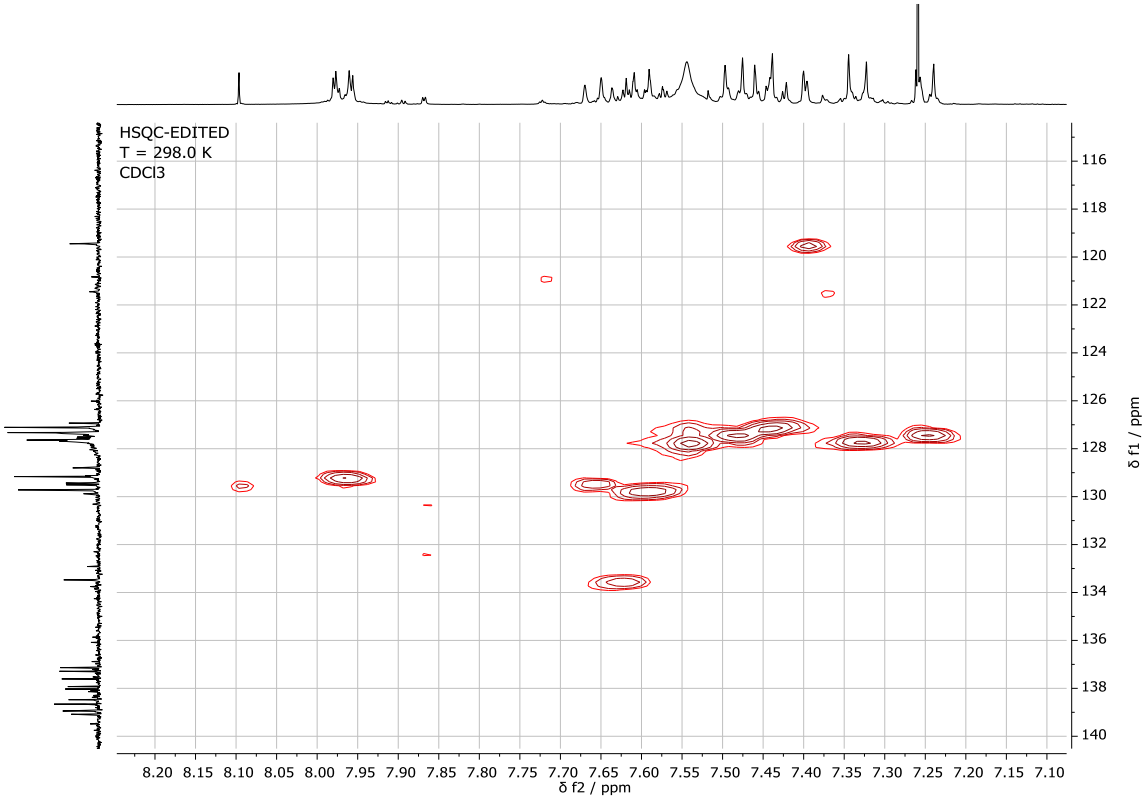

Figure S45. HSQC NMR spectrum (400 MHz) of **15**.

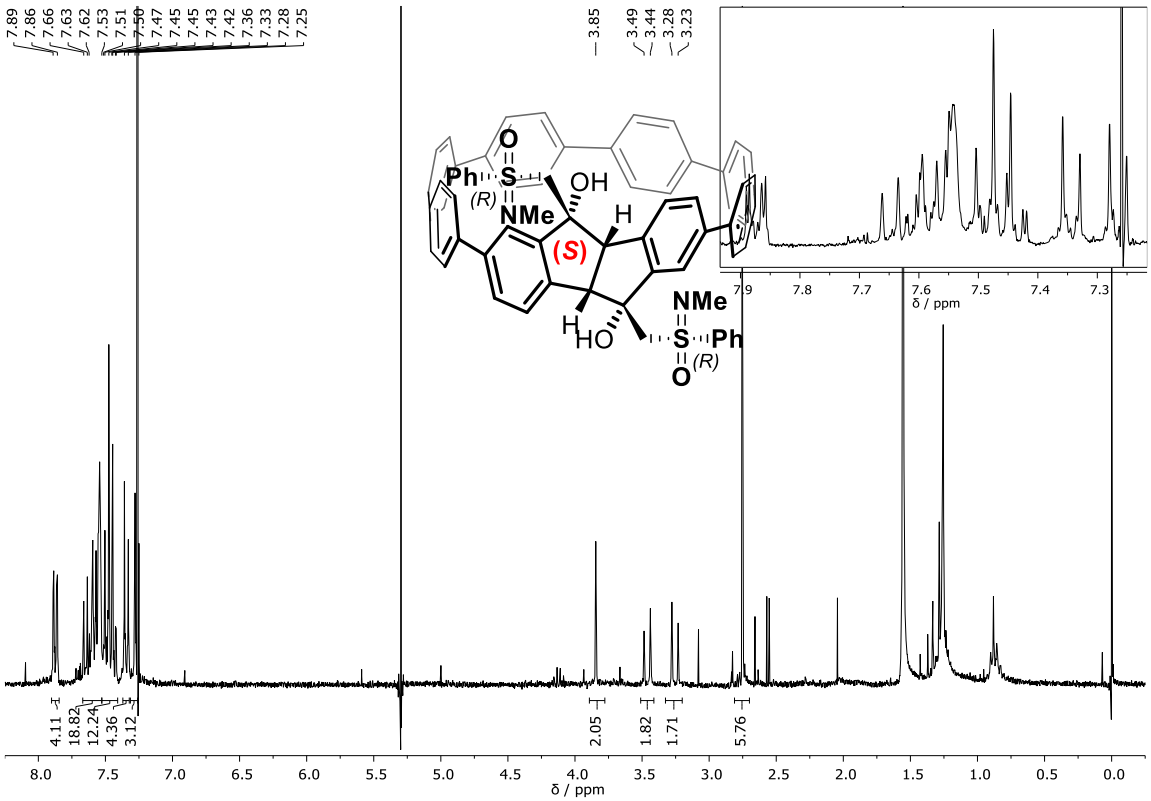

Figure S46. ^{1}H NMR spectrum (300 MHz) of **12**.

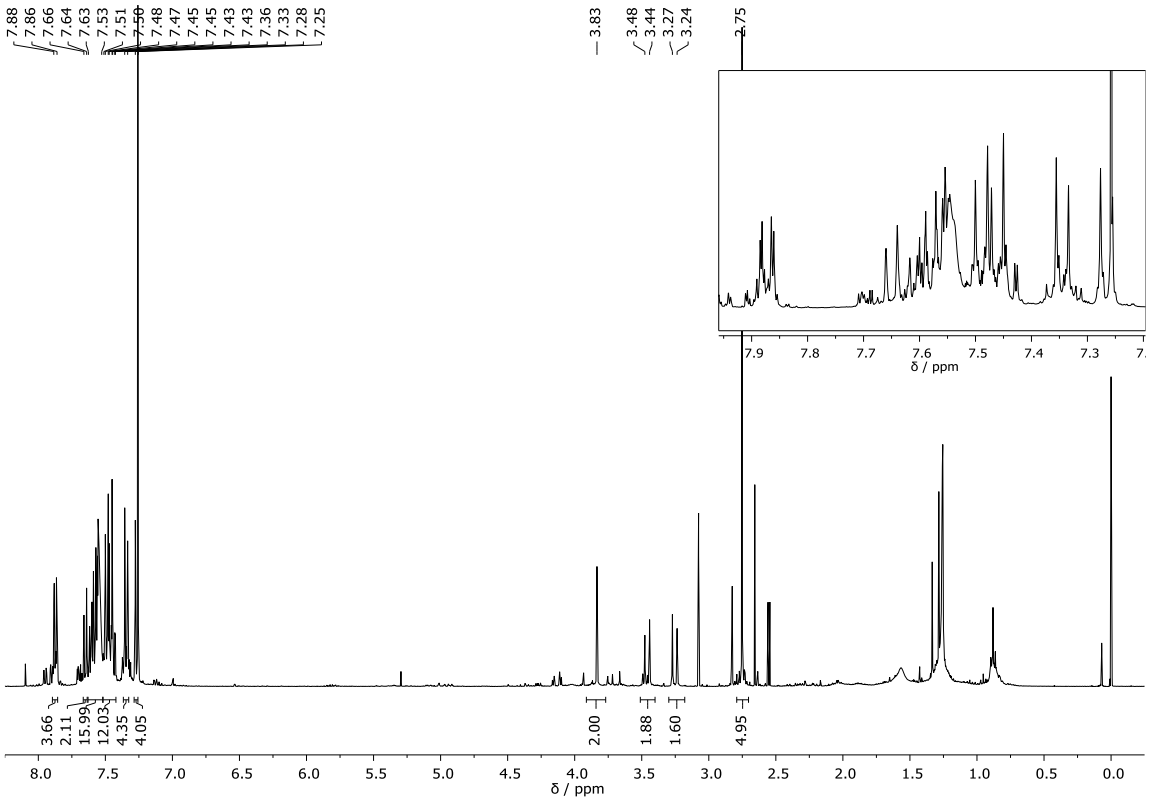

Figure S47. ^{1}H NMR spectrum (400 MHz) of **12**.

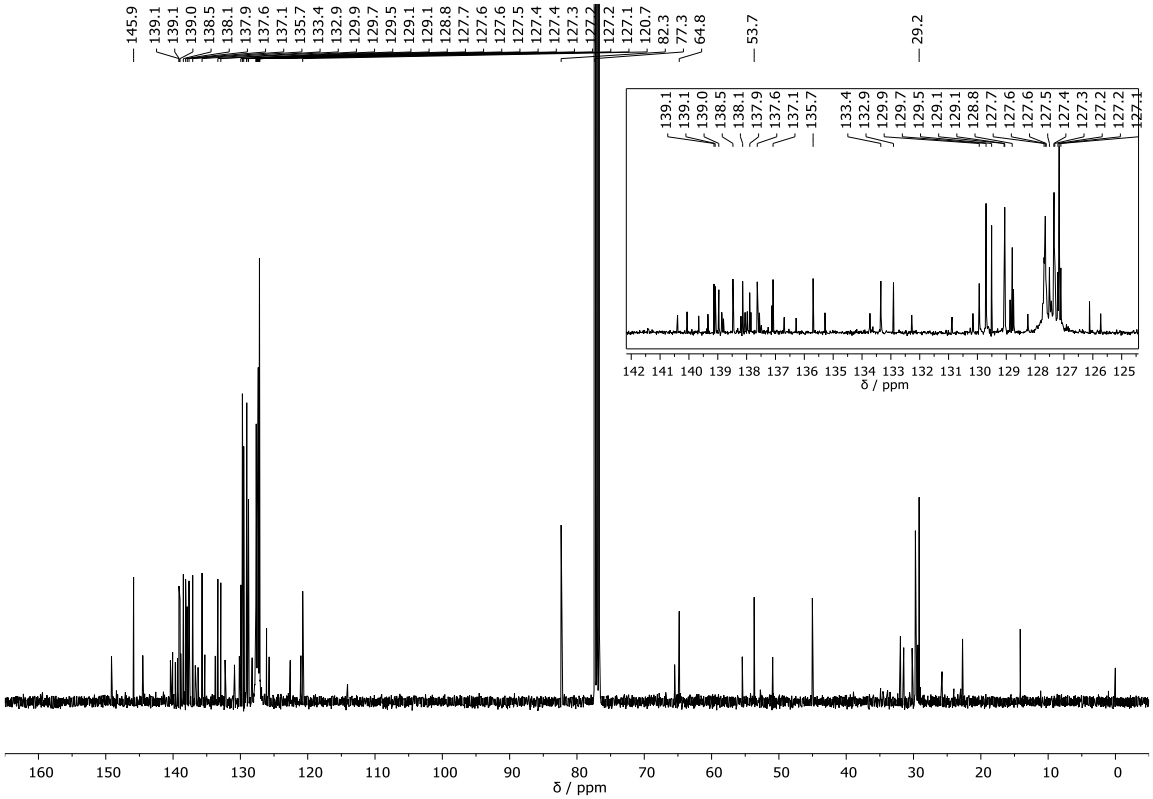

Figure S48. ^{13}C NMR spectrum (400 MHz) of **12**.

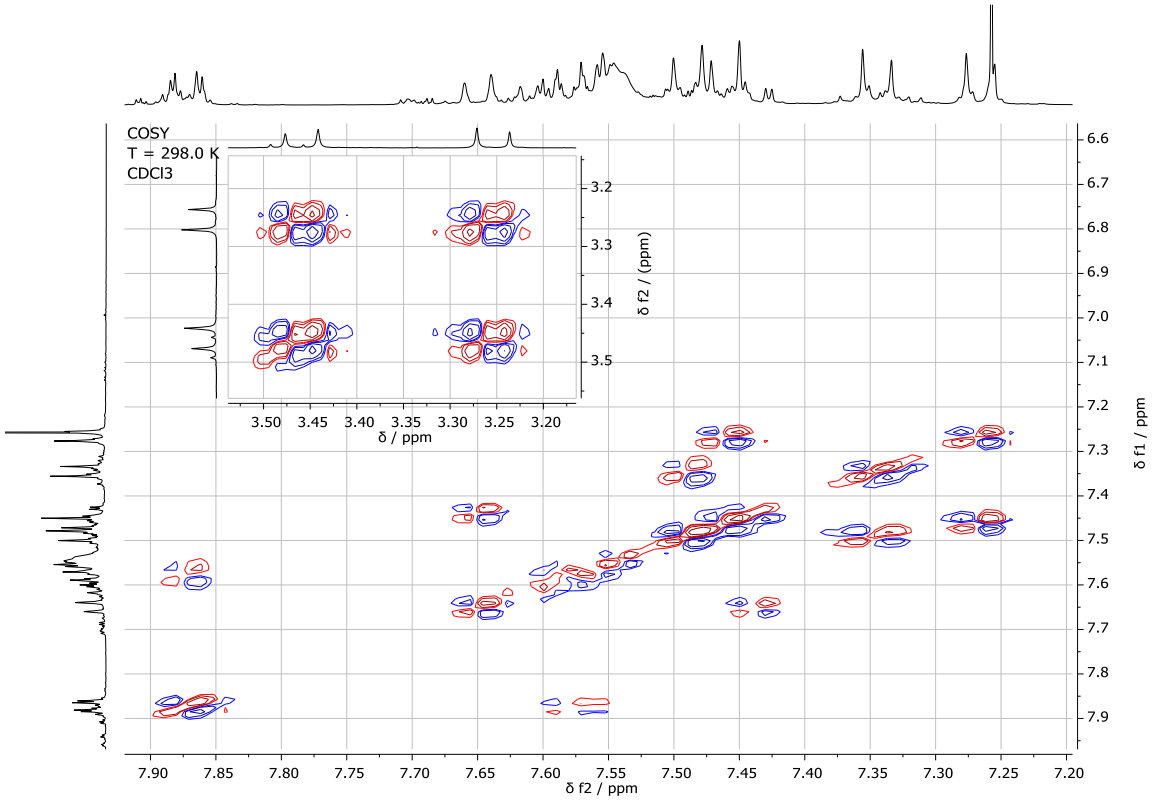

Figure S49. ^{1}H-^{1}H COSY NMR spectrum (400 MHz) of **12**.

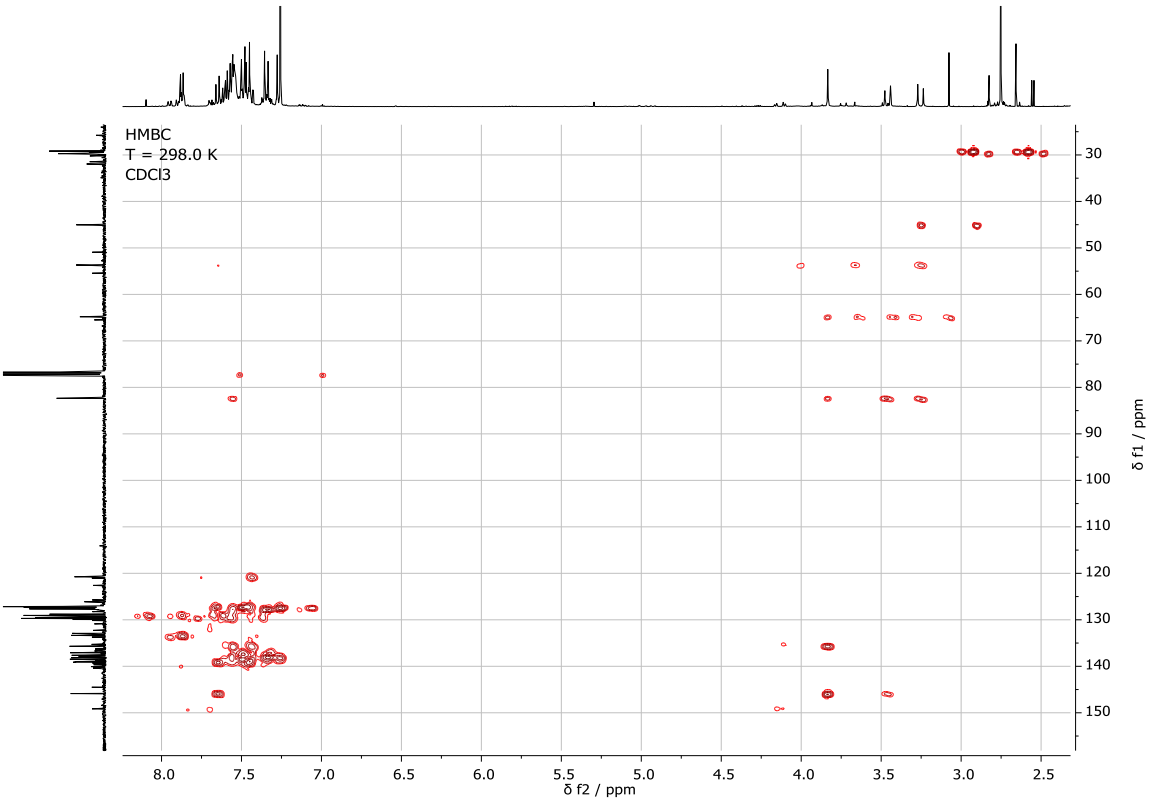

Figure S50. $^{1}H^{13}C$ HMBC NMR spectrum (400 MHz) of **12**.

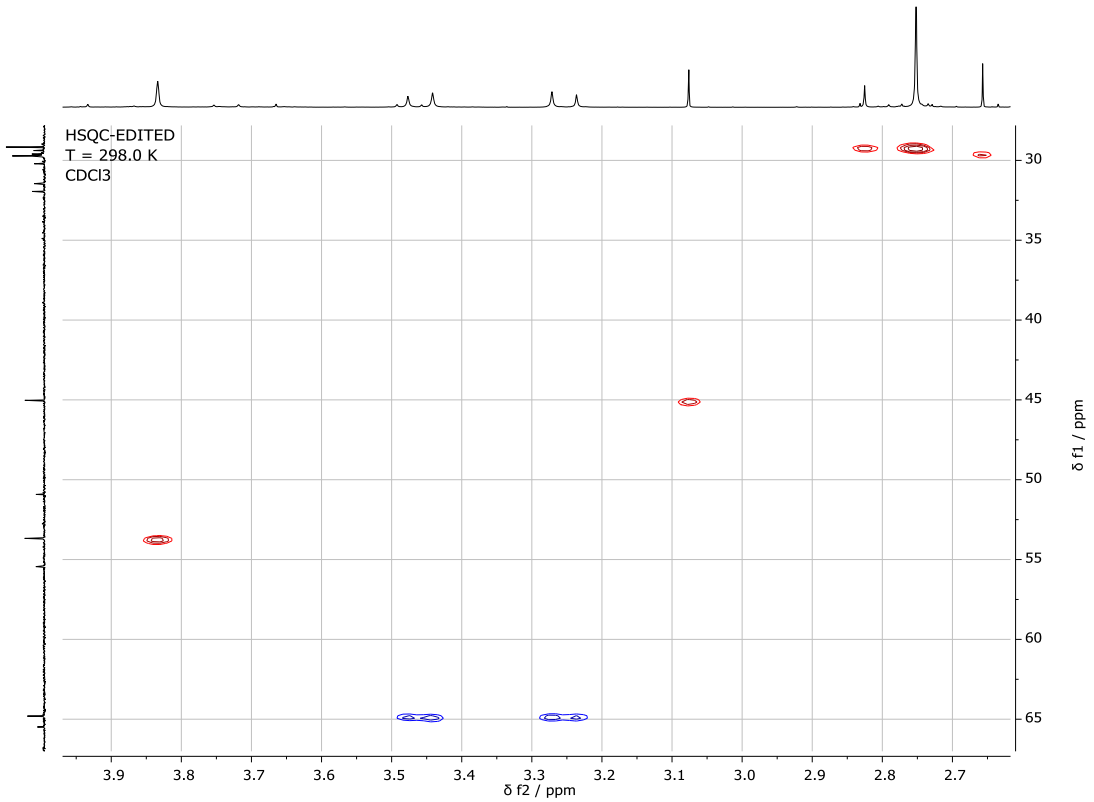

Figure S51. HSQC NMR spectrum (400 MHz) of **12**.

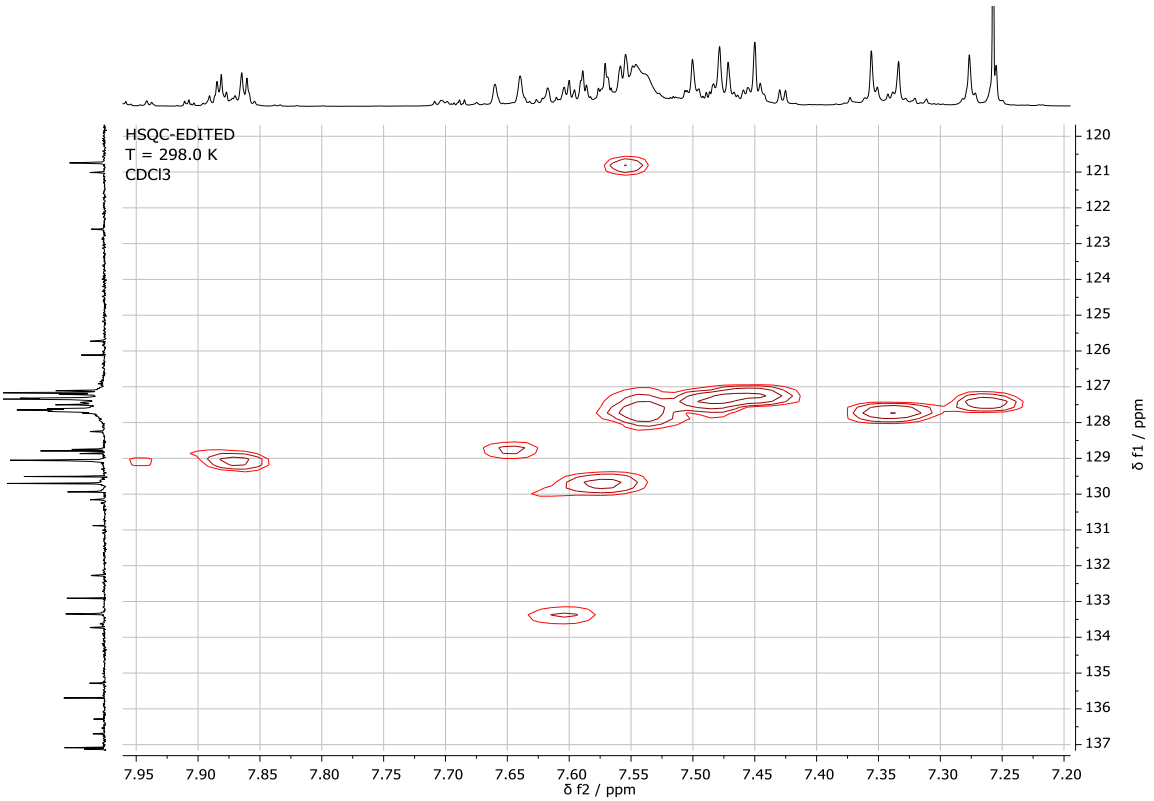

Figure S52. HSQC NMR spectrum (400 MHz) of **12**.

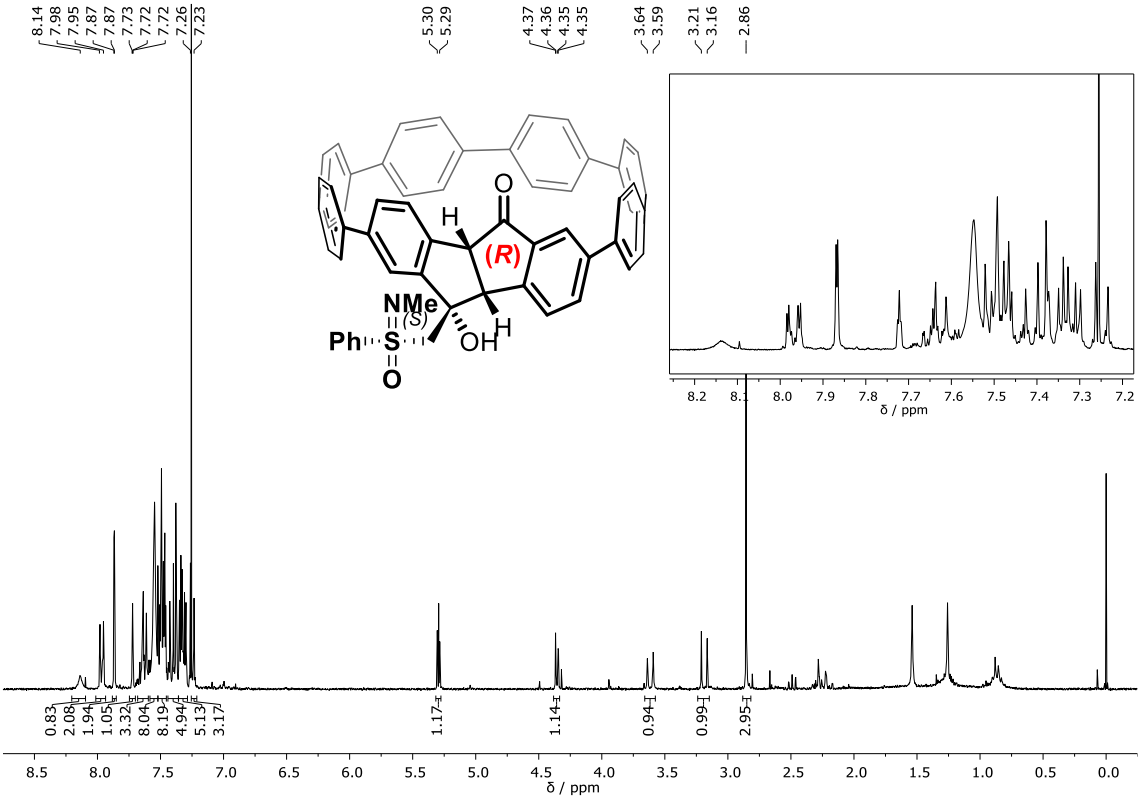

Figure S53. ^{1}H NMR spectrum (300 MHz) of **14**.

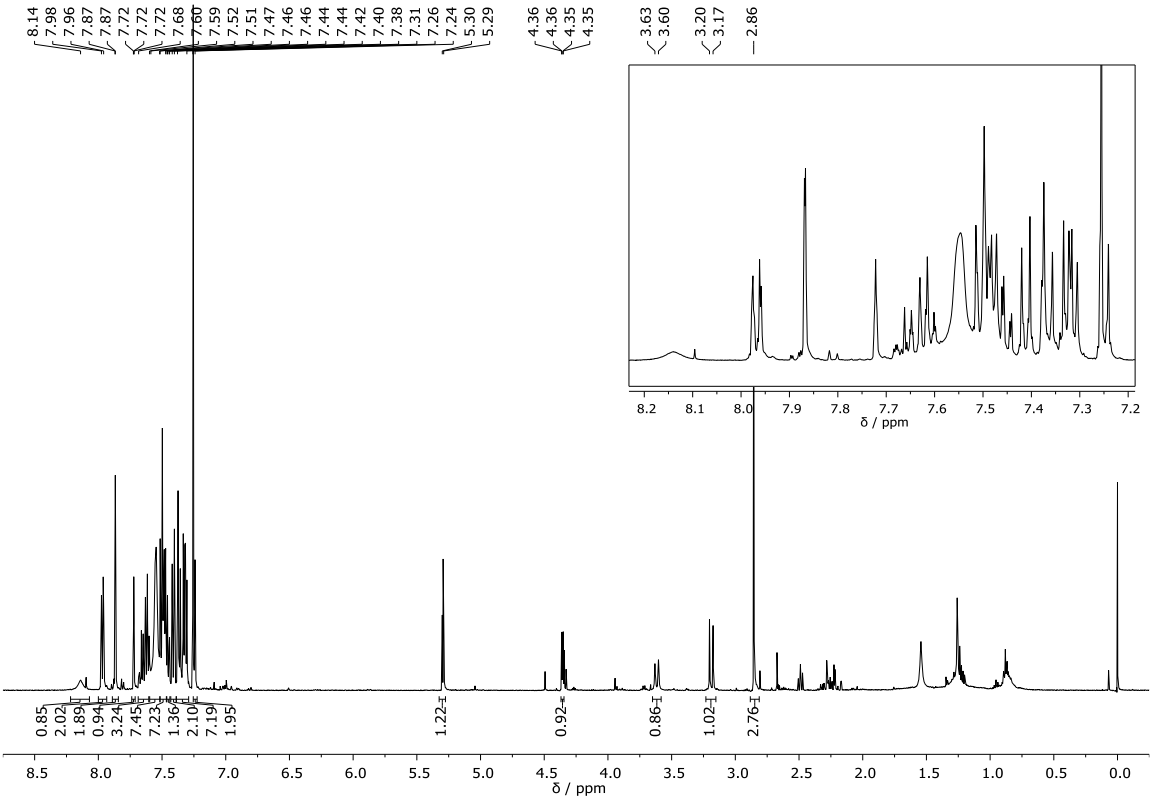

Figure S54. ^{1}H NMR spectrum (500 MHz) of **14**.

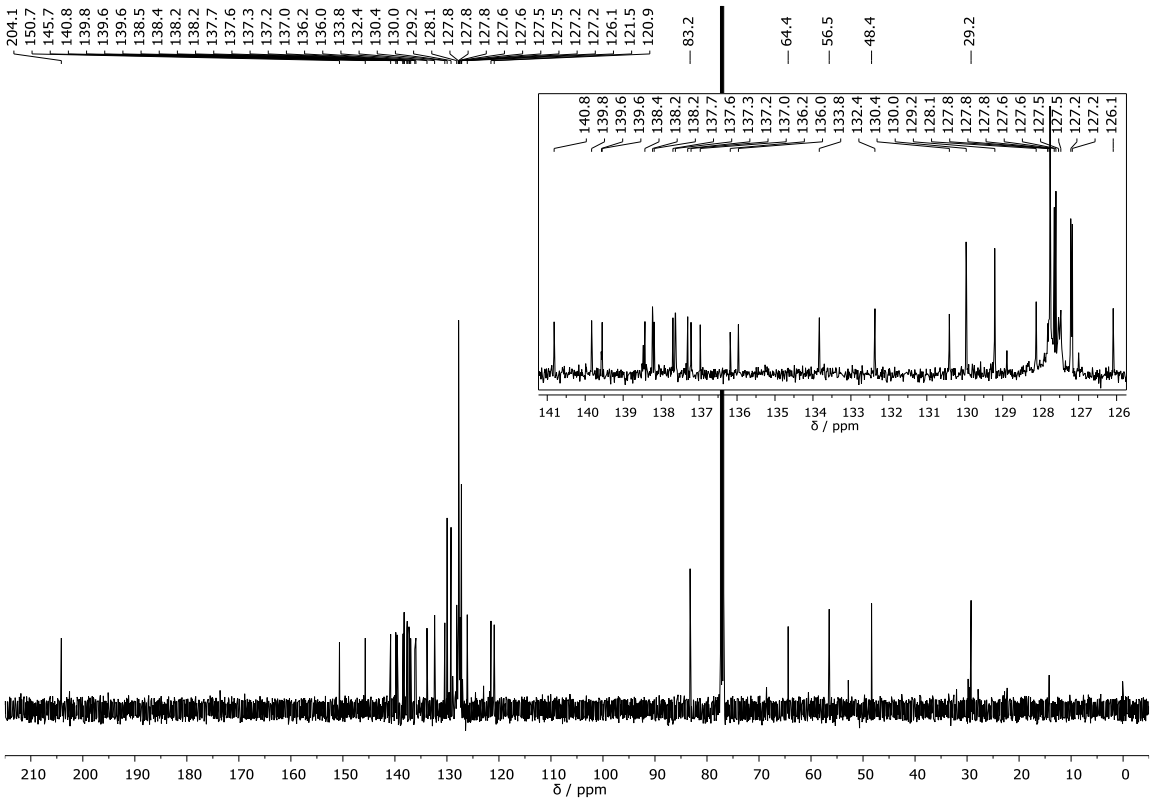

Figure S55. ^{13}C NMR spectrum (500 MHz) of **14**.

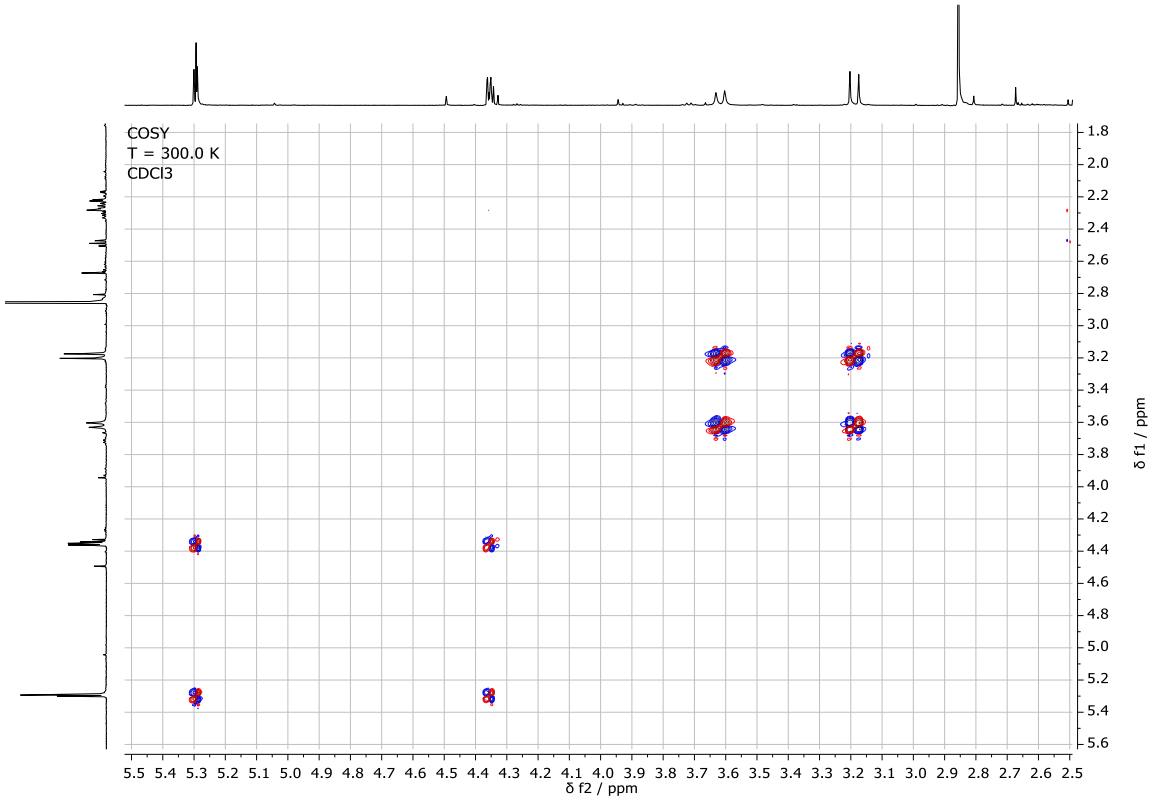

Figure S56. ^{1}H-^{1}H COSY NMR spectrum (500 MHz) of **14**.

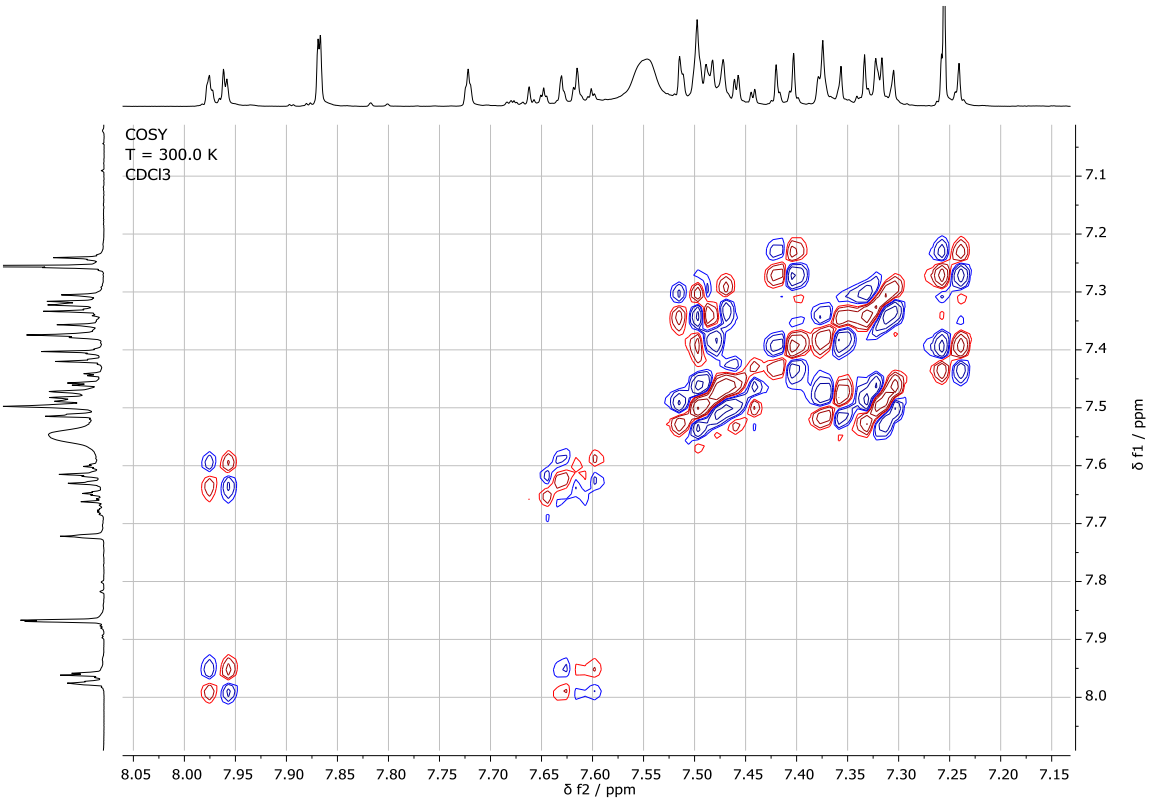

Figure S57. ^{1}H-^{1}H COSY NMR spectrum (500 MHz) of **14**.

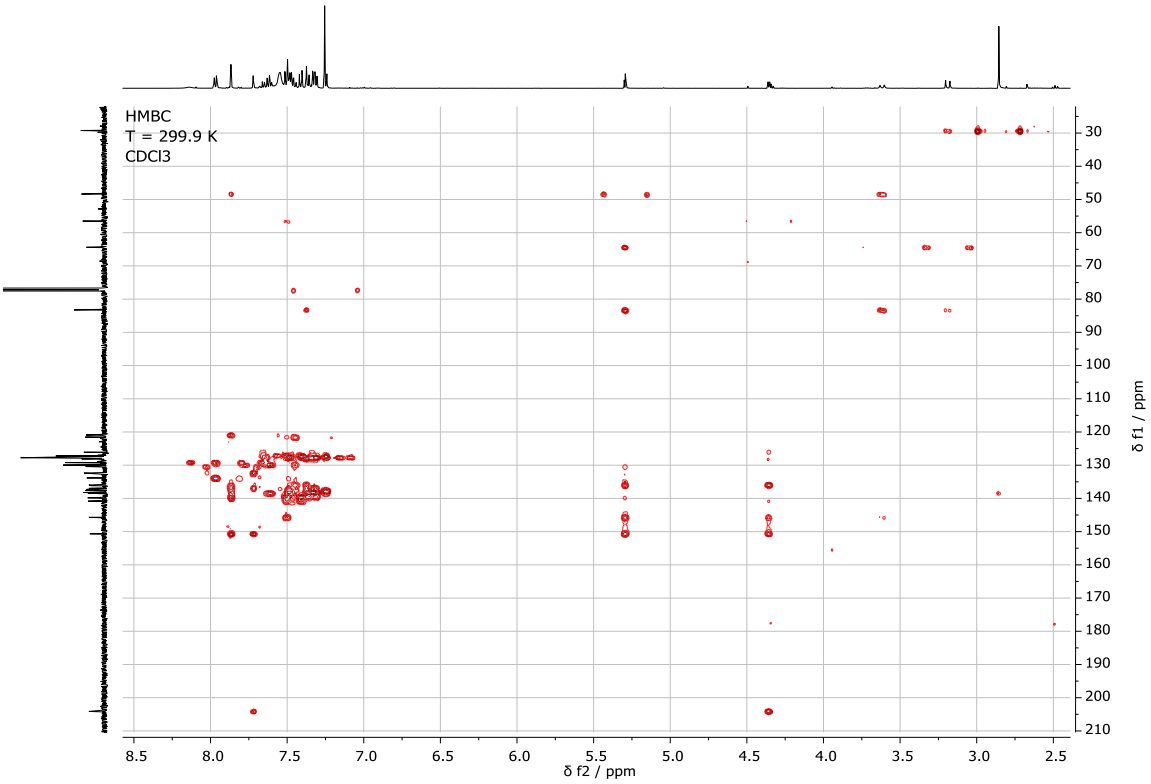

Figure S58. ^{1}H-^{13}C HMBC NMR spectrum (500 MHz) of **14**.

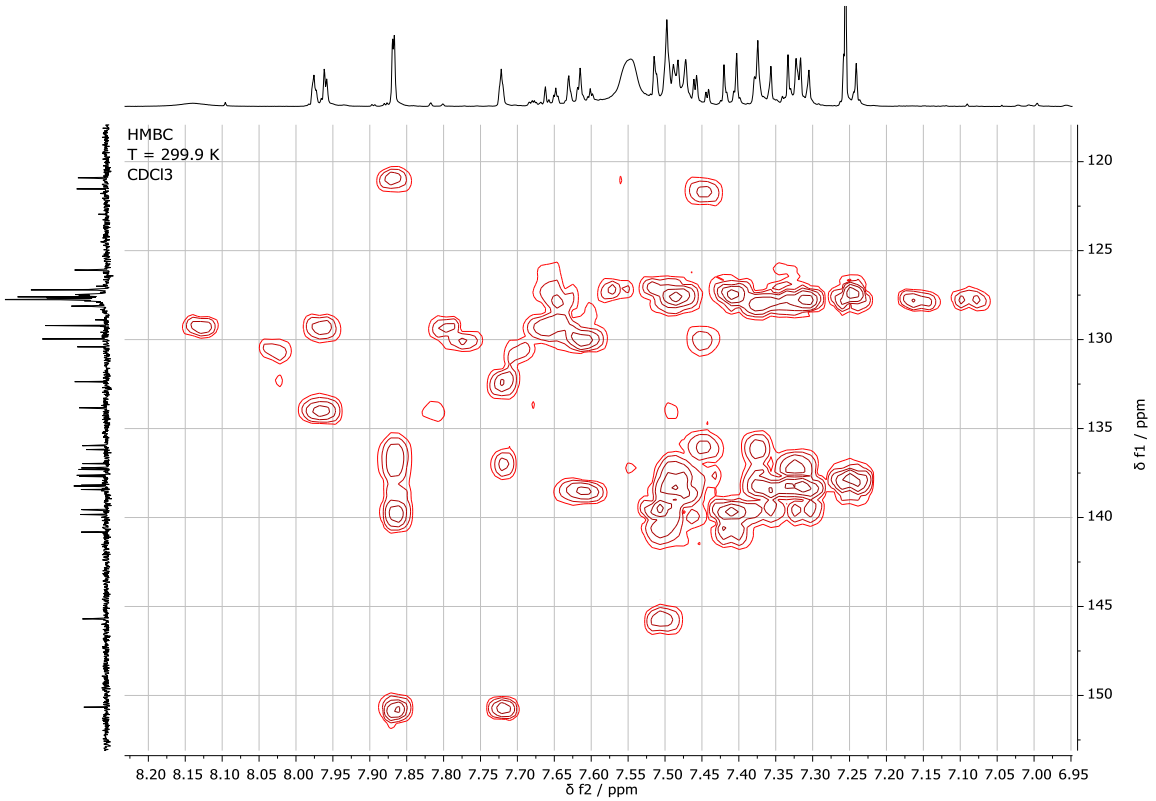

Figure S59. ^{1}H-^{13}C HMBC NMR spectrum (500 MHz) of **14**.

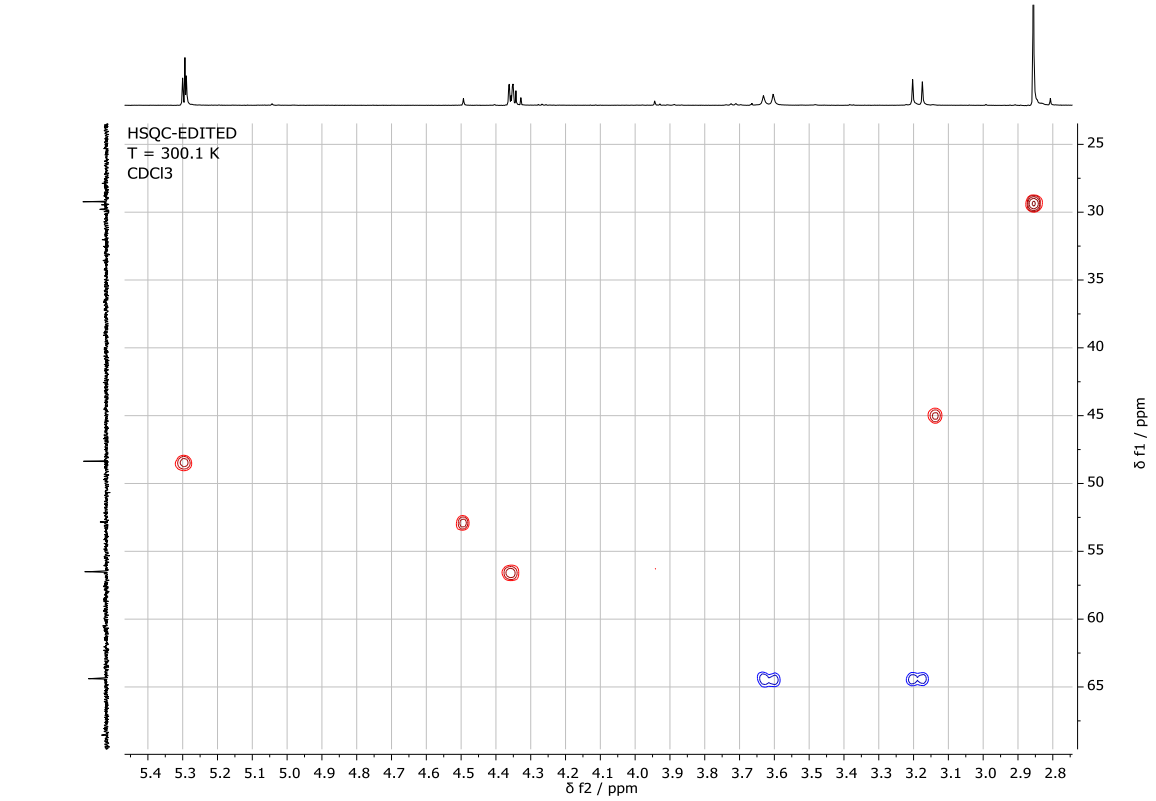

Figure S60. HSQC NMR spectrum (500 MHz) of **14**.

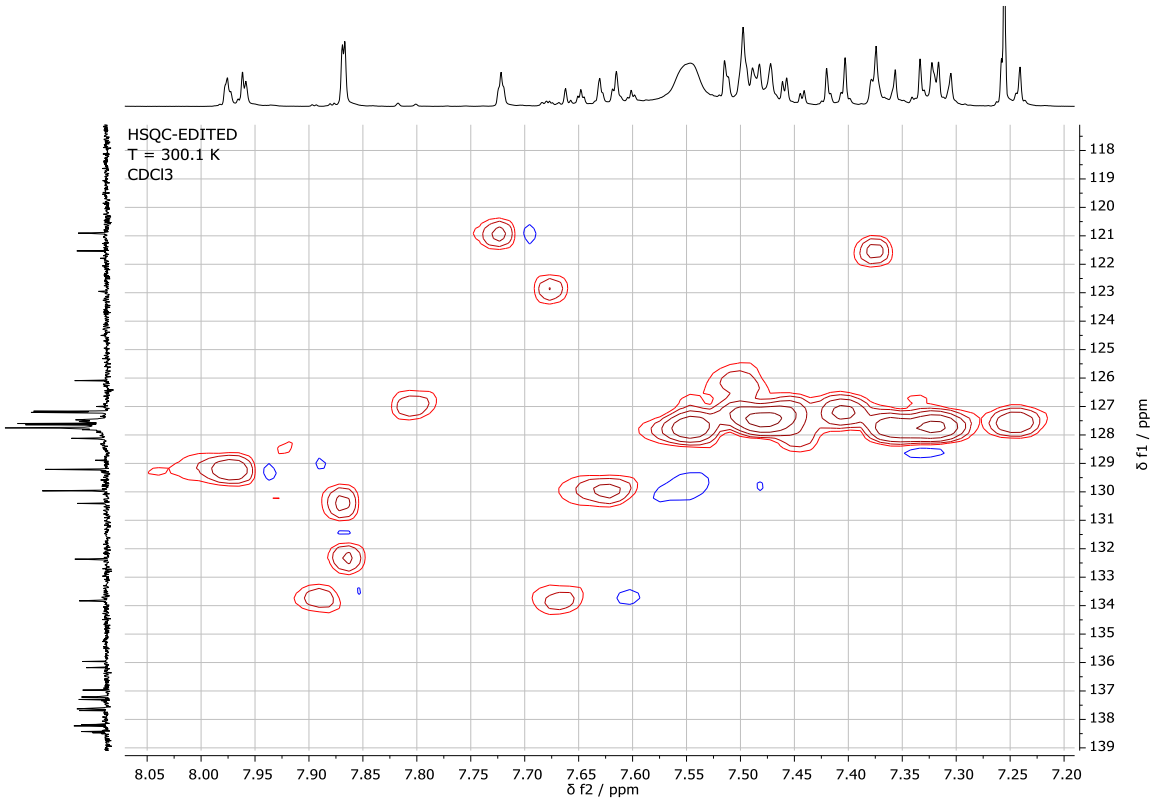

Figure S61. HSQC NMR spectrum (500 MHz) of **14**.

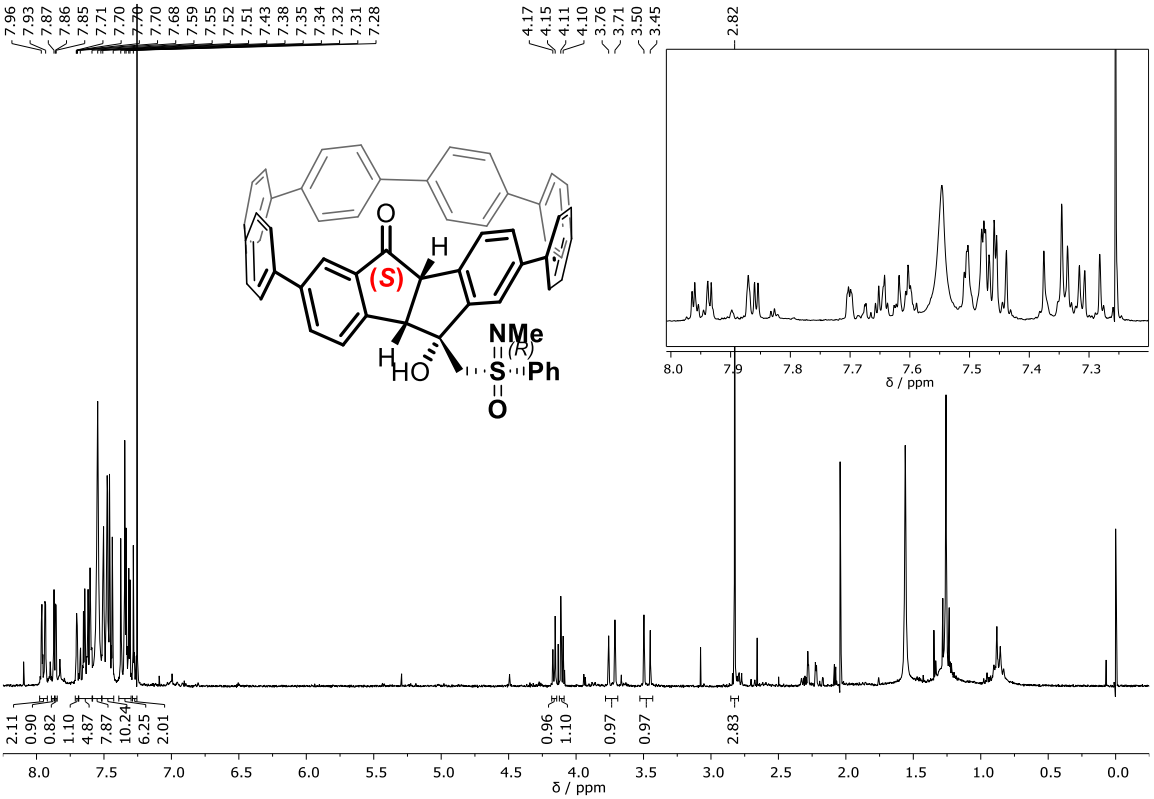

Figure S62. ^{1}H NMR spectrum (300 MHz) of **13**.

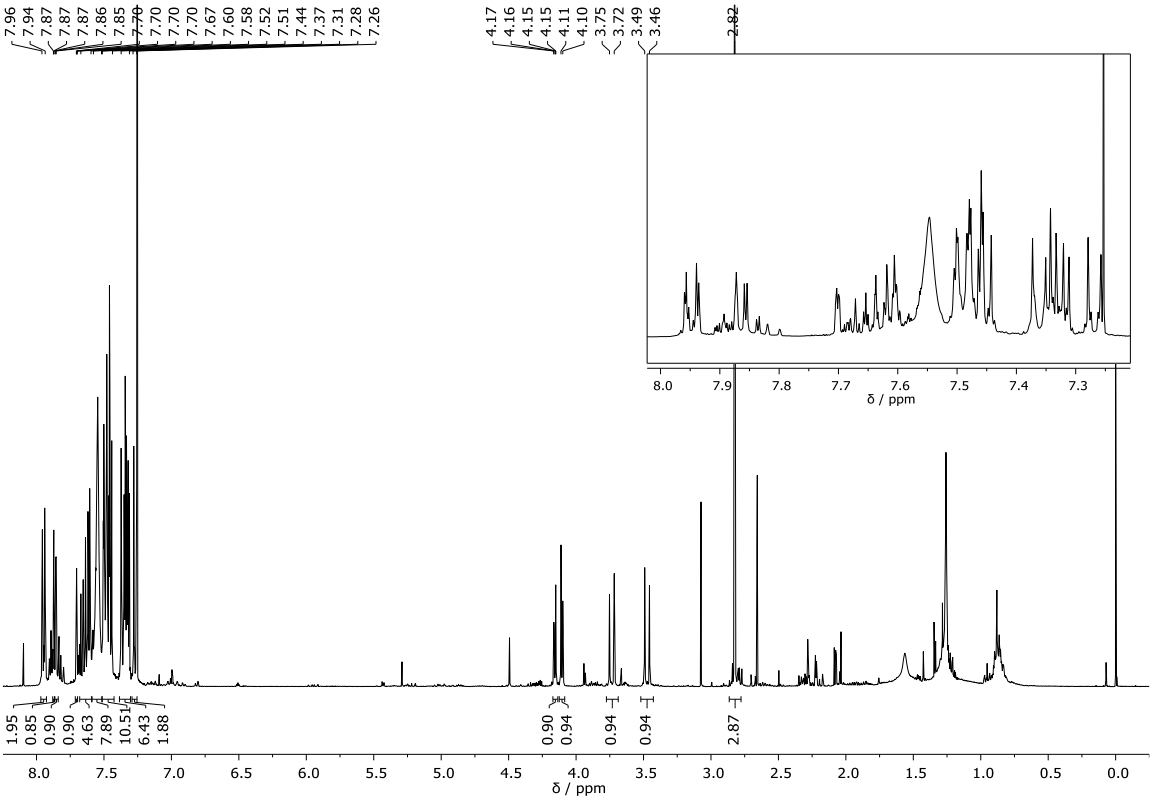

Figure S63. ^{1}H NMR spectrum (400 MHz) of **13**.

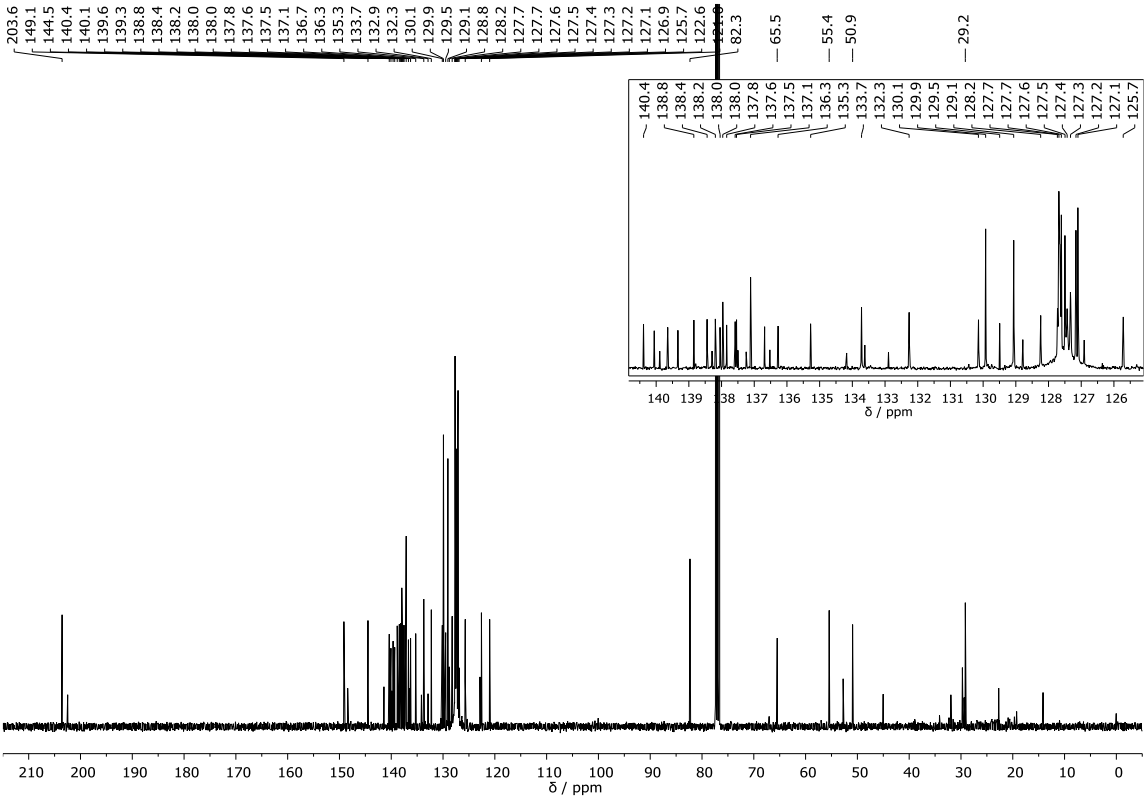

Figure S64. ^{13}C NMR spectrum (400 MHz) of **13**.

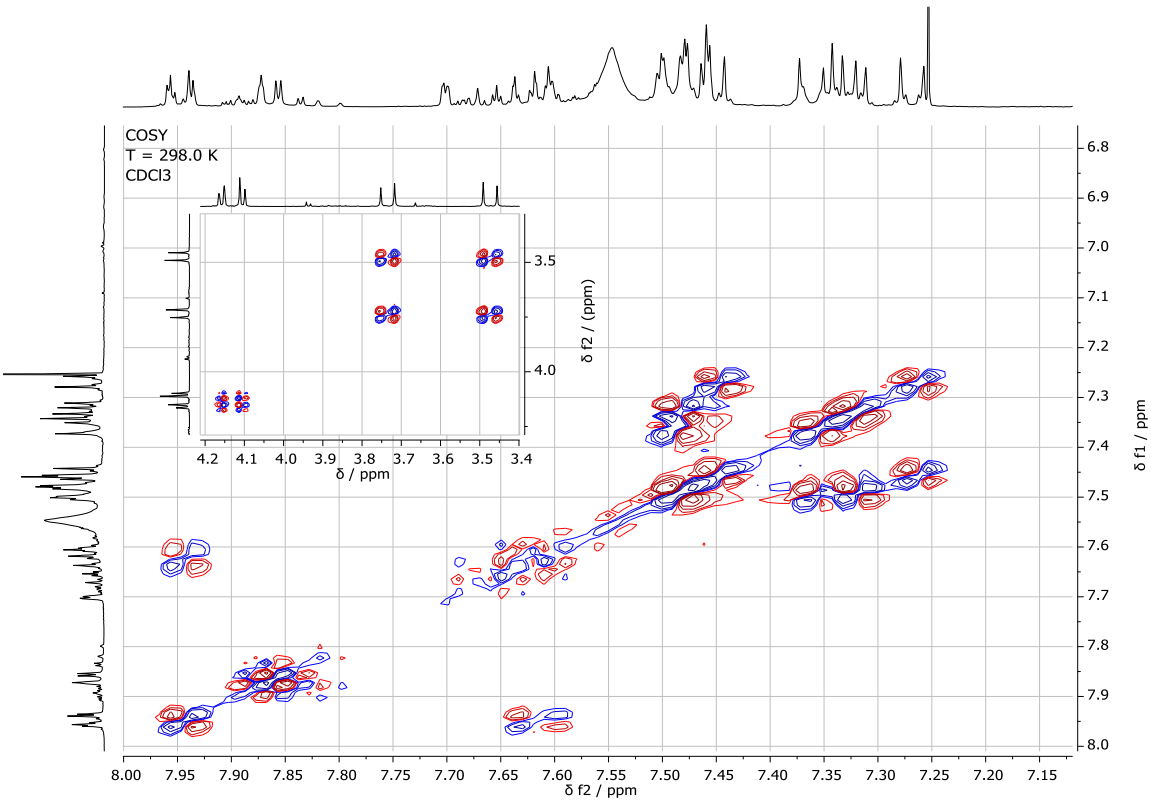

Figure S65. ^{1}H-^{1}H COSY NMR spectrum (400 MHz) of **13**.

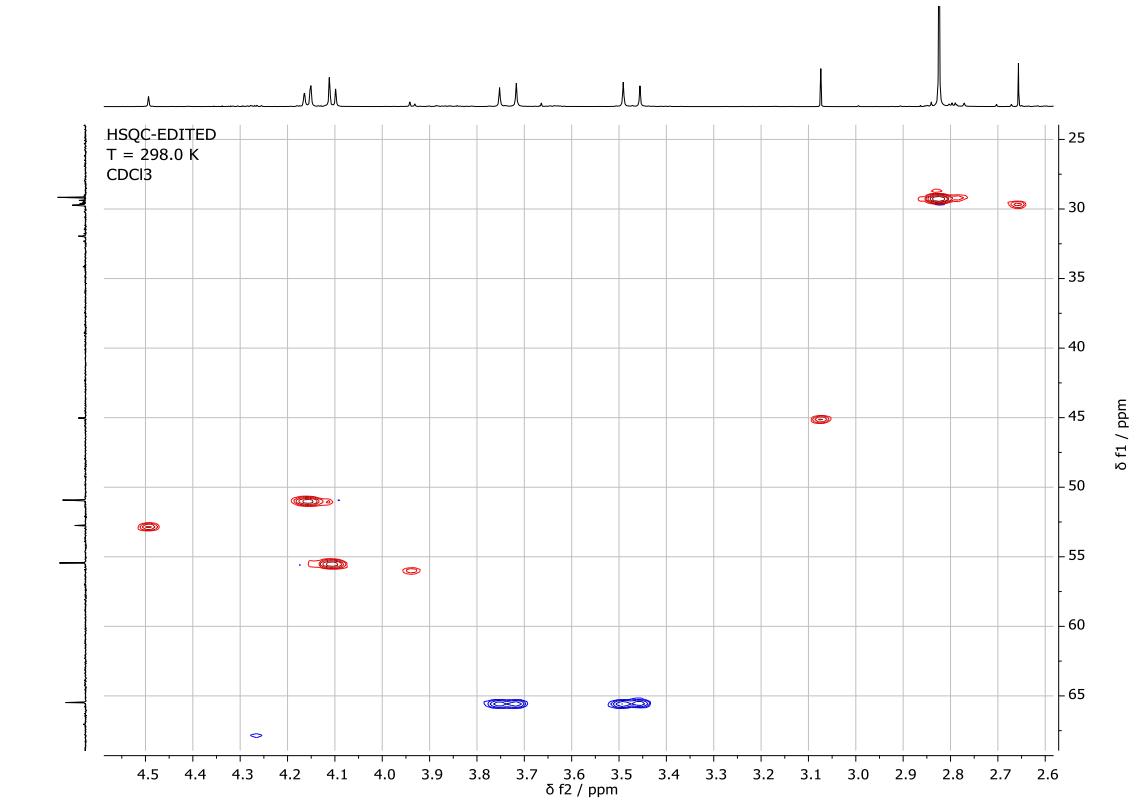

Figure S66. HSQC NMR spectrum (400 MHz) of **13**.

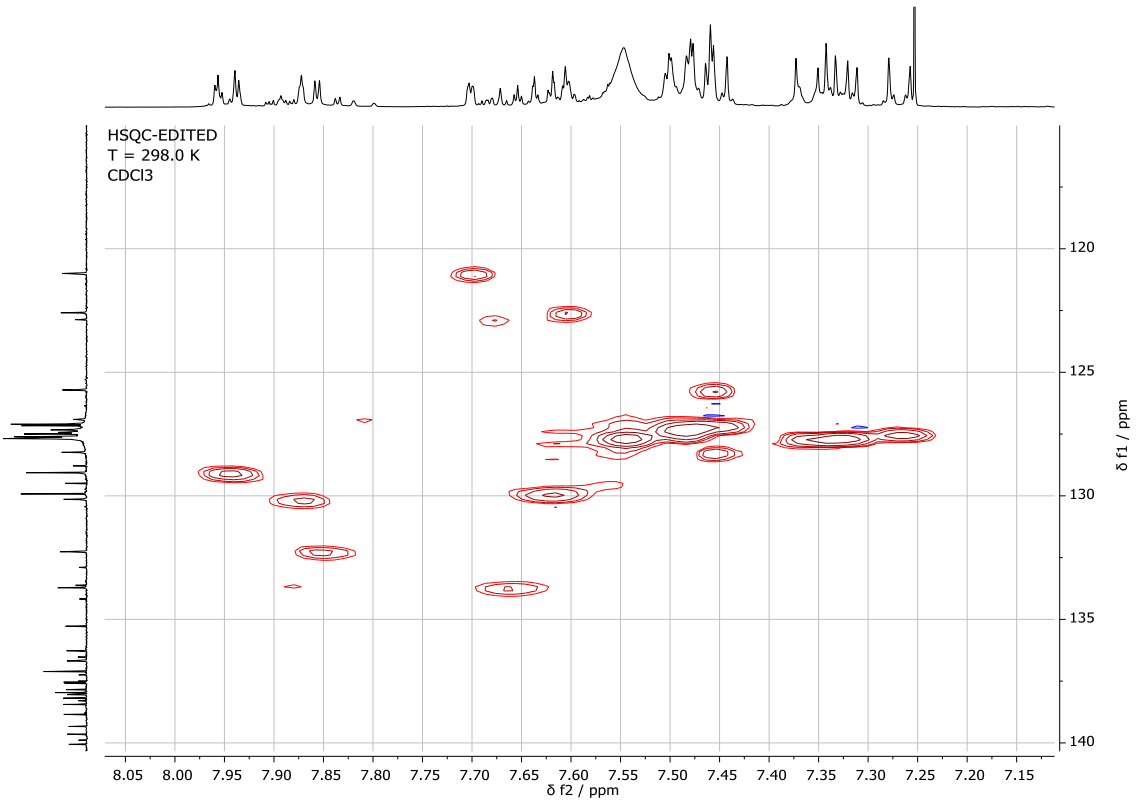

Figure S67. HSQC NMR spectrum (400 MHz) of **13**.

4 Mass Spectrometry

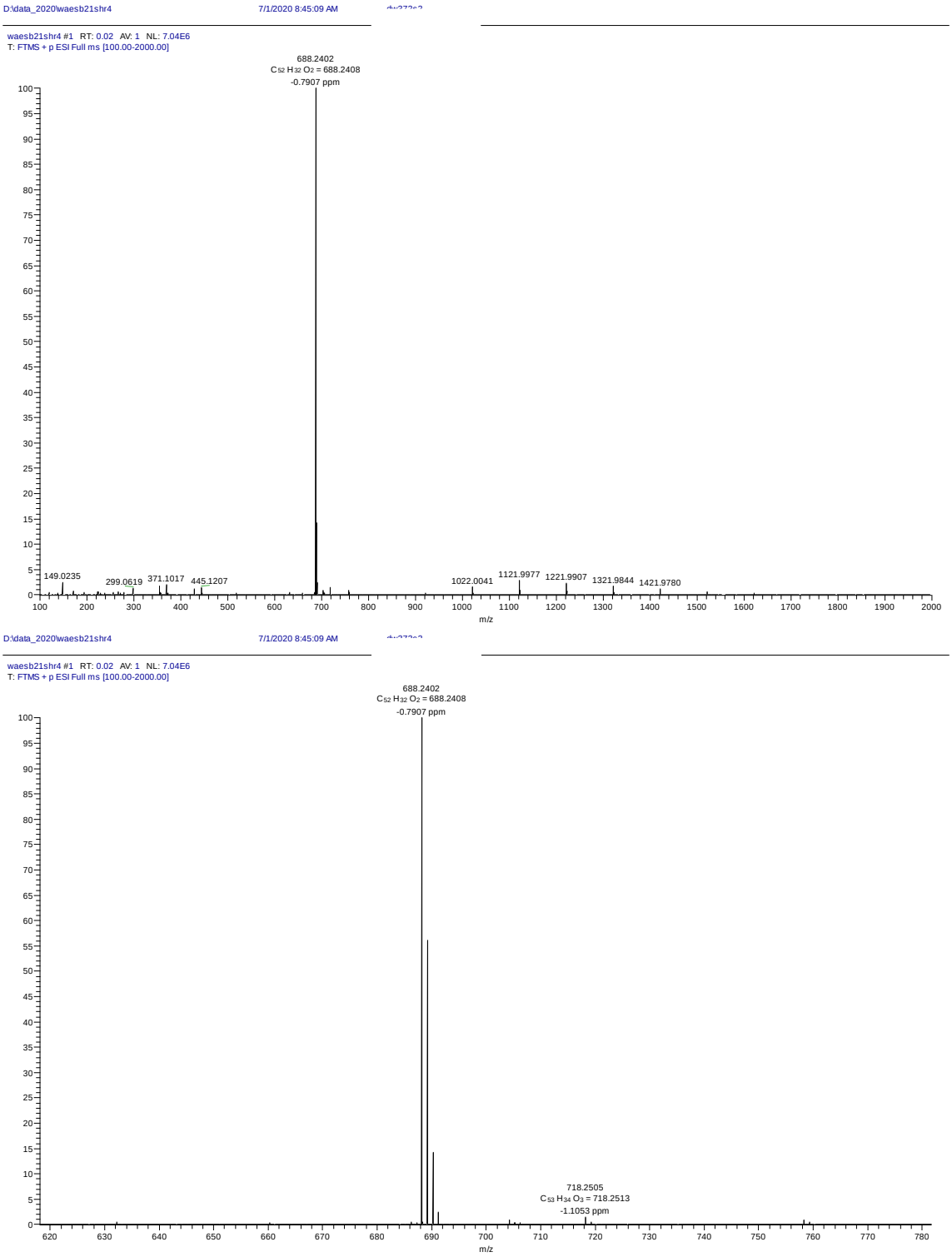

Figure S68. HR-MS spectrum of **3**. Ionization method: ESI, positive mode.

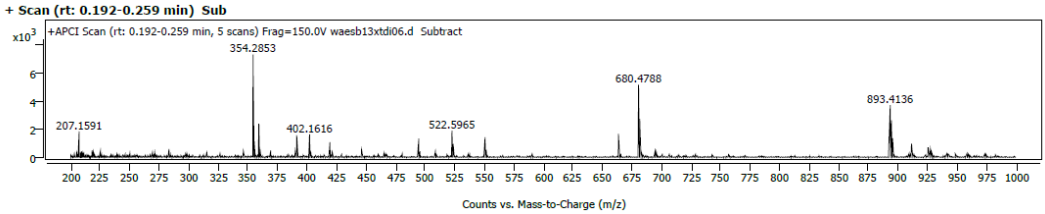

Spectrum Peaks

m/z	Z	Abund	Abund %	m/z (Calc)	Diff (ppm)	Ion Species	Formula
207.1591	1	1851	25.34	207.1591	0.27	(M+H)+	C10 H22 O4
354.2853	1	7305	100.00	354.2850	0.69	(M+NH4)+	C17 H36 O6
355.2881	1	1183	16.20	355.2883	-0.73	(M+NH4)+	C17 H36 O6
893.4136	1	3803	52.06	893.4142	-0.69	(M+H)+	C70 H52
894.4167	1	2685	36.76	894.4176	-0.99	(M+H)+	C70 H52
895.4188	1	1362	18.64	895.4209	-2.35	(M+H)+	C70 H52
359.2037		2399	32.83				
391.2295		1626	22.26				
402.1616	1	1632	22.34	402.1614	0.48		
419.3145	1	1093	14.97	419.3156	-2.48		
494.5660		1346	18.43				
522.5965		1920	26.28				
550.6290		1422	19.47				
663.4533		1700	23.27				
680.4788	1	5214	71.38				
681.4838	1	2755	37.72				

Figure S69. HR-MS spectrum of **1**. Ionization method: APCI, positive mode.

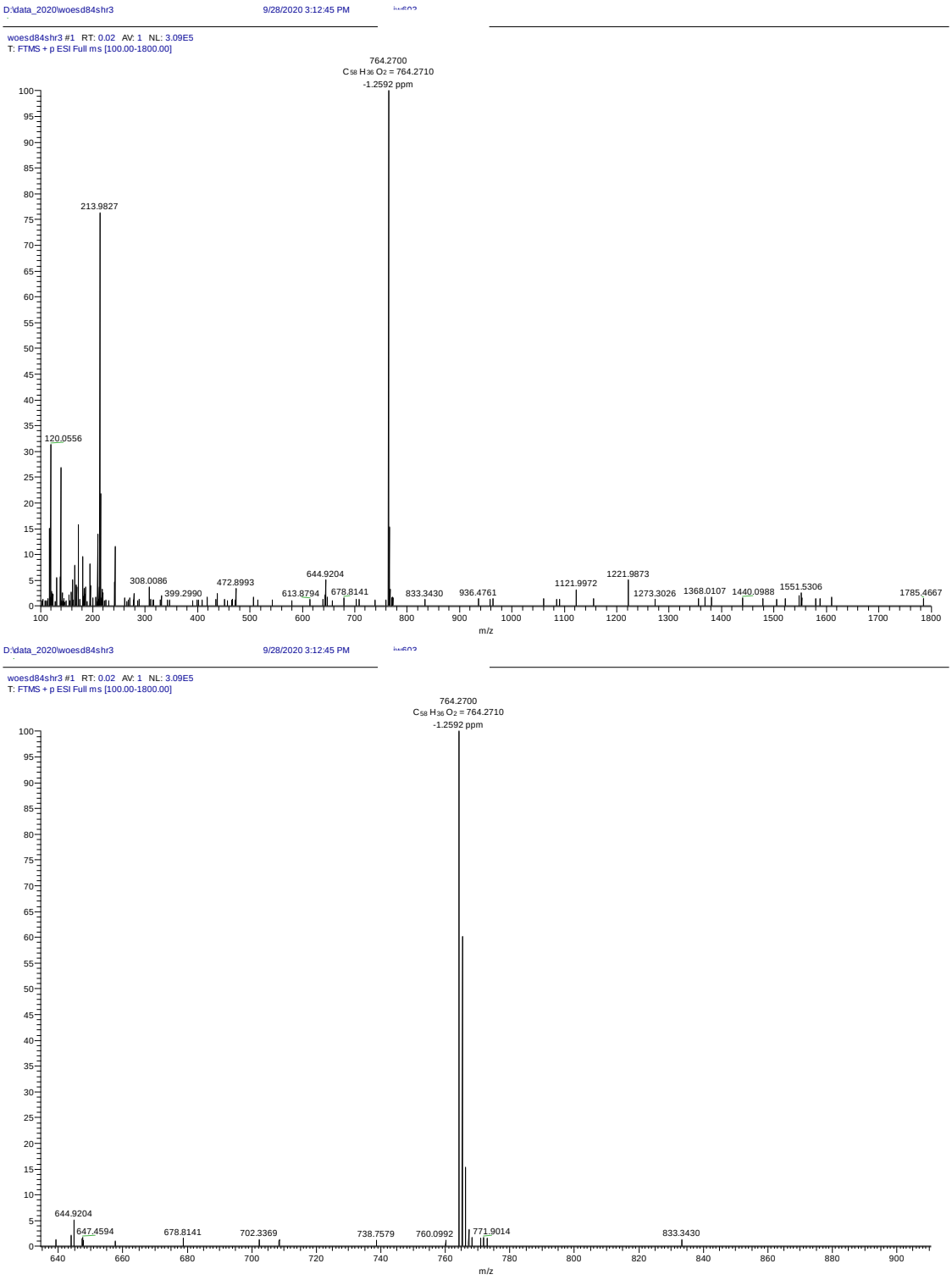

Figure S70. HR-MS spectrum of **4**. Ionization method: ESI, positive mode.

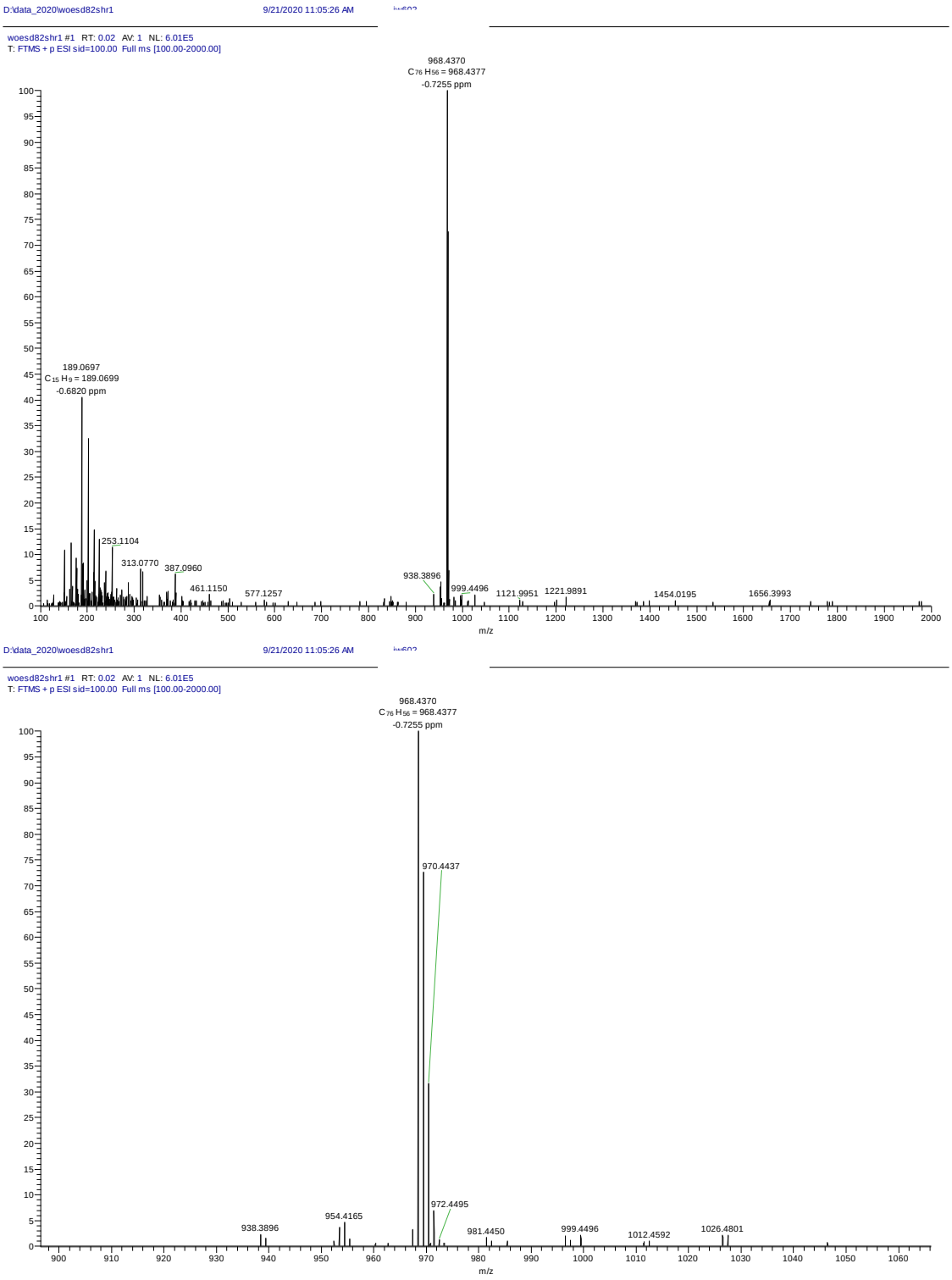

Figure S71. HR-MS spectrum of **2**. Ionization method: ESI, positive mode.

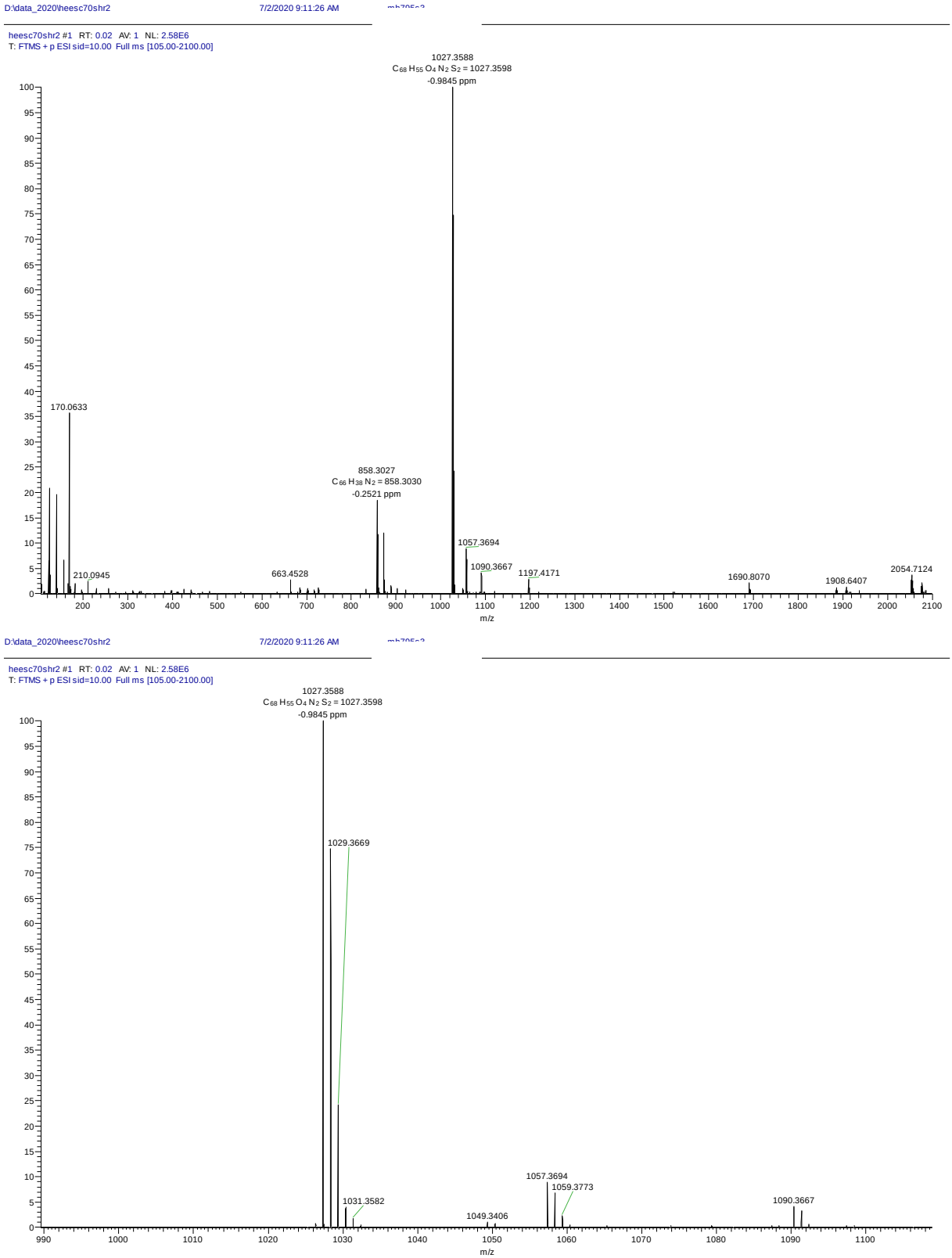

Figure S72. HR-MS spectrum of **12**. Ionization method: ESI, positive mode.

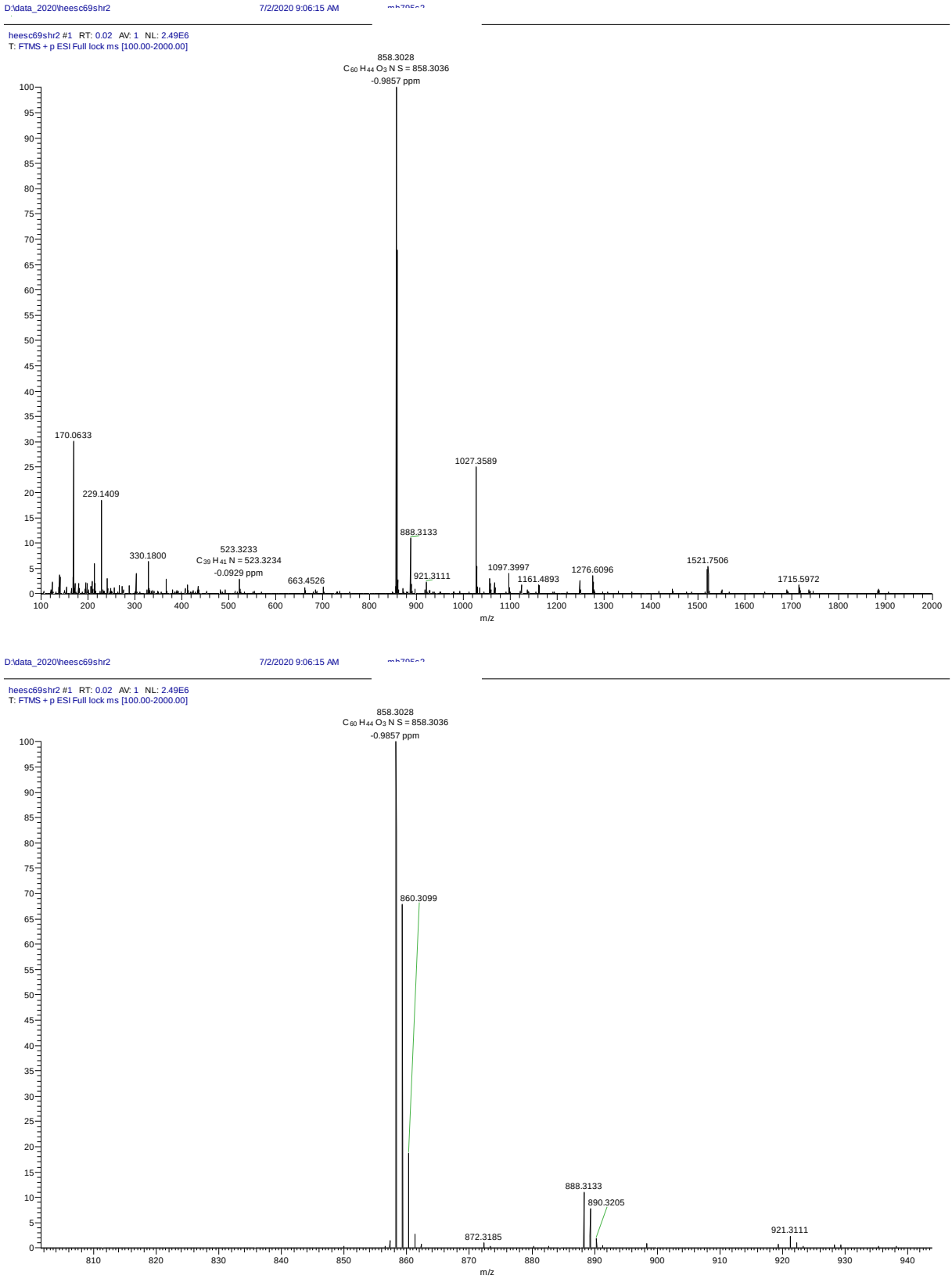

Figure S73. HR-MS spectrum of **13**. Ionization method: ESI, positive mode.

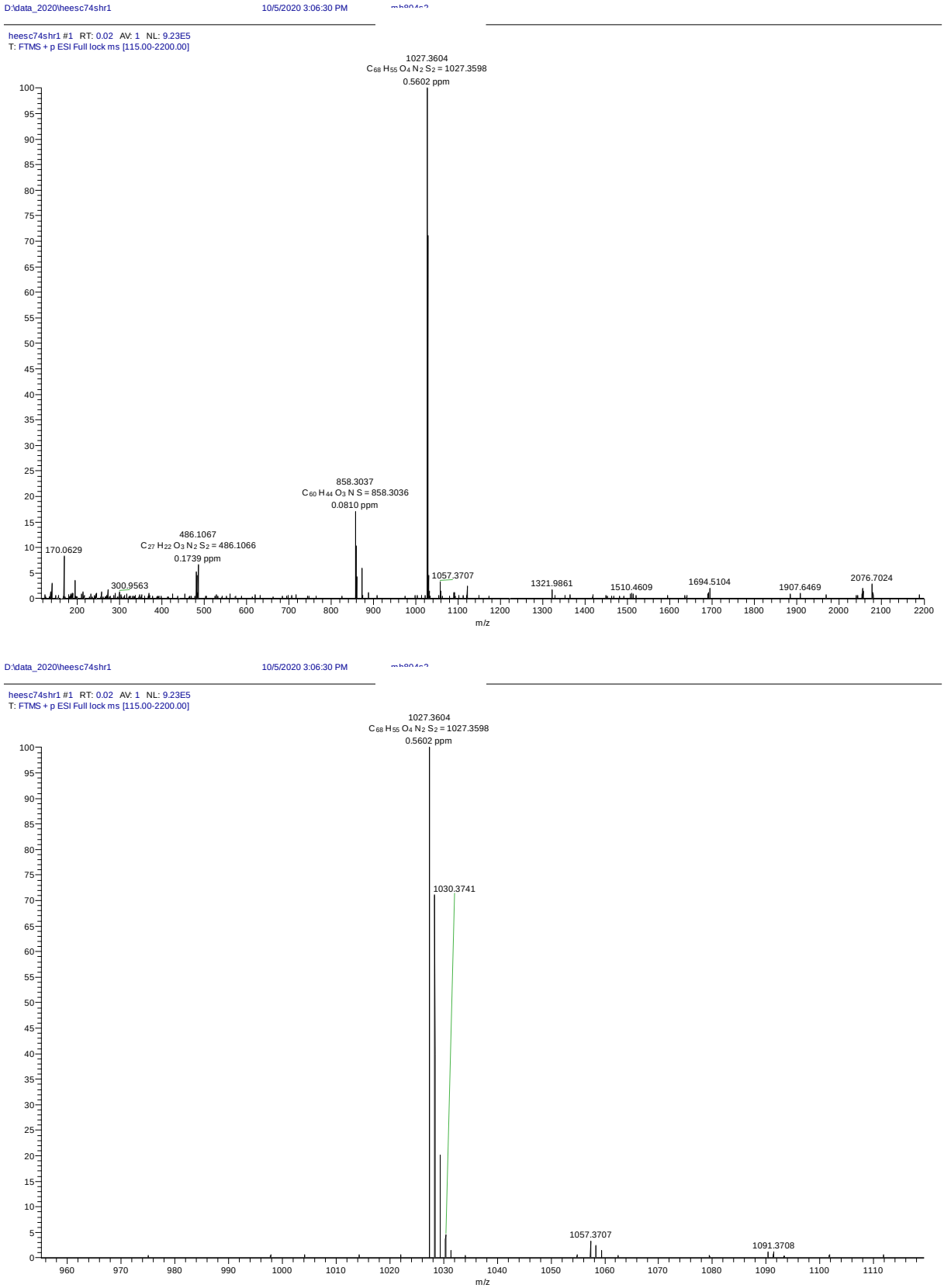

Figure S74. HR-MS spectrum of **15**. Ionization method: ESI, positive mode.

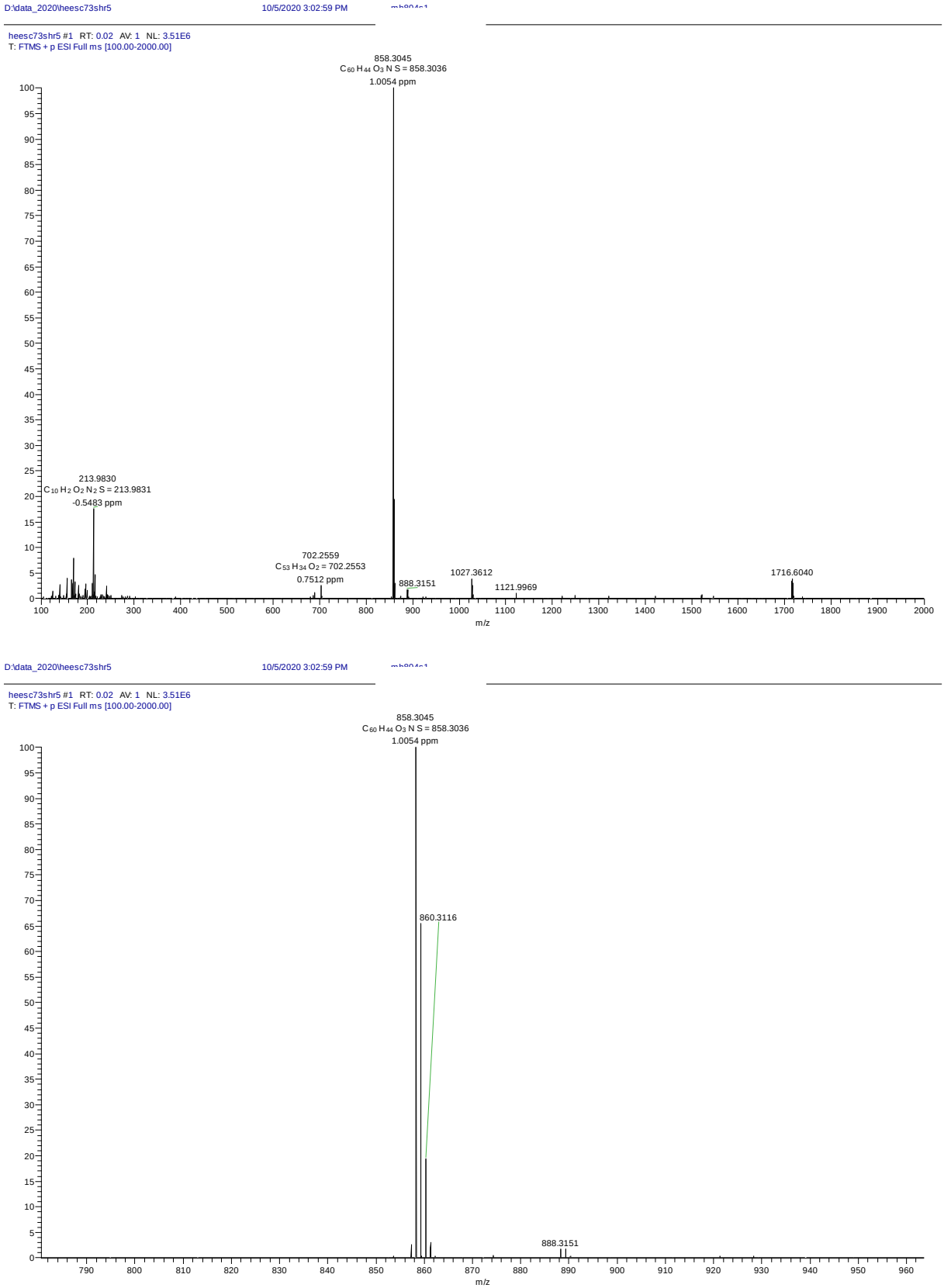

Figure 75. HR-MS spectrum of **14**. Ionization method: ESI, positive mode.

5 Absorption Spectra

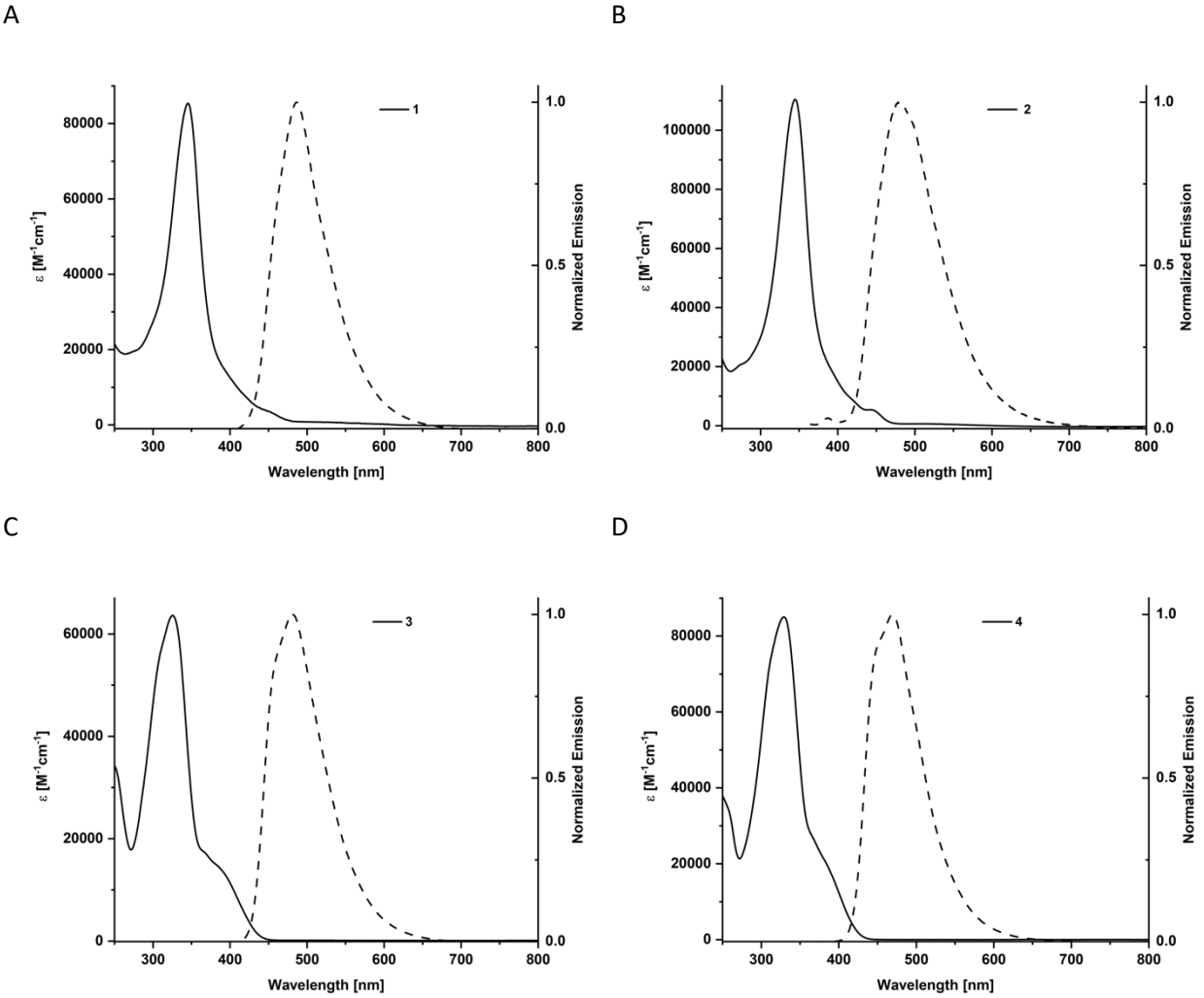

Figure S76. Absorption and emission spectra of target compounds **1** (A), **2** (B), **3** (C) and **4** (D) measured in CH_2Cl_2. Wavelength plotted versus extinction coefficient for the absorption.

6 Solvatochromic Effects in Emission Spectra

Emission spectra of **3** (A) and **1** (B) were measured in solvents of varying polarity.

A

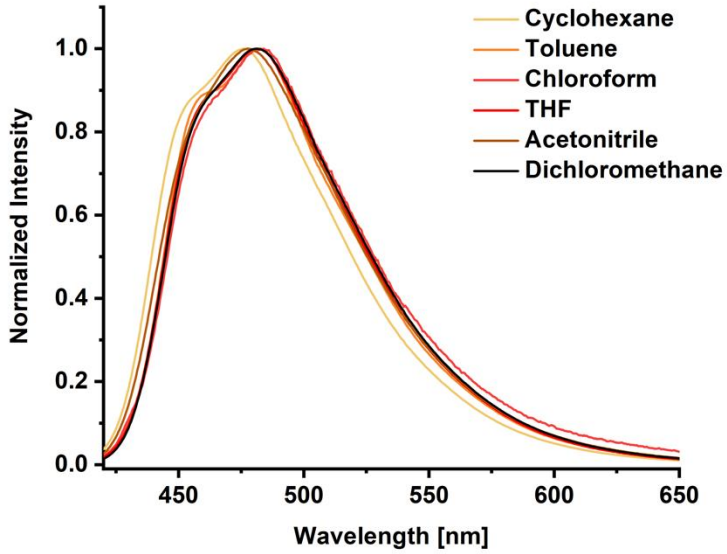

B

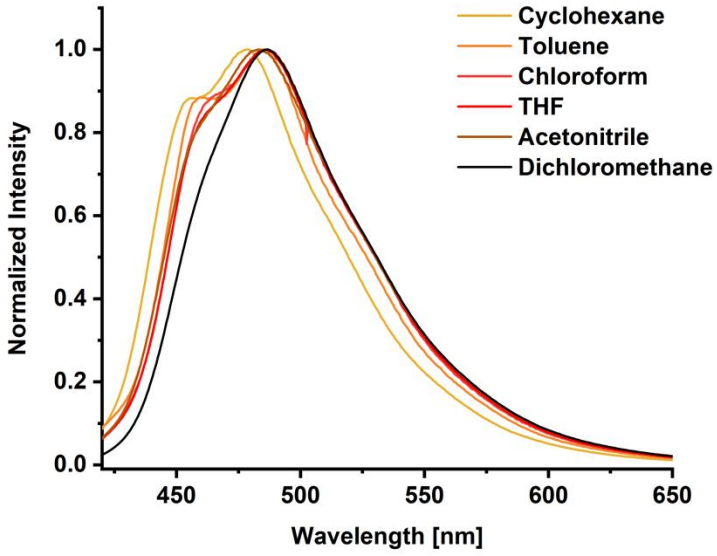

Figure S77. Emission spectra of **3** (A) and **1** (B).

7 Cyclic Voltammograms

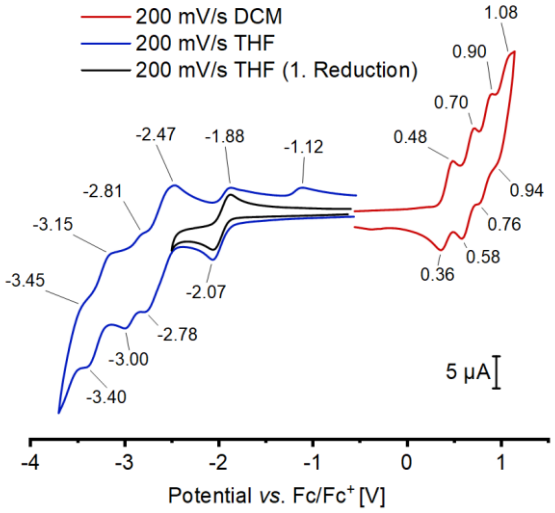

Figure S78. CV of **1** (Reduction in THF, Oxidation in CH_2Cl_2, 1 mM analyte concentration, 0.1 M *n*-Bu_4NPF_6 concentration, glassy carbon electrode, potentials plotted *vs*. Fc/Fc^+ as internal standard, 200 mV/s scan rate).

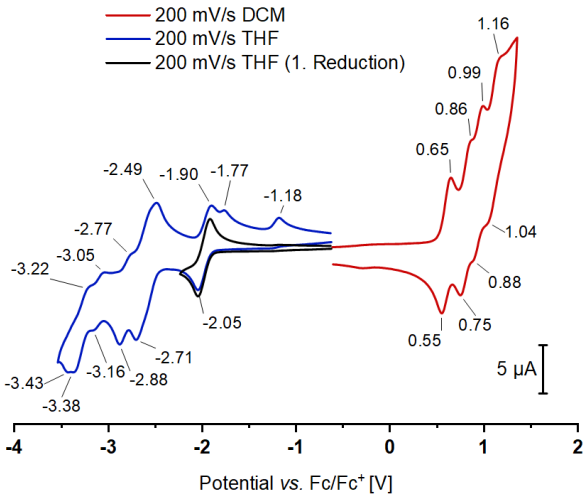

Figure S79. CV of **2** (Reduction in THF, Oxidation in CH_2Cl_2, 1 mM analyte concentration, 0.1 M *n*-Bu_4NPF_6 concentration, glassy carbon electrode, potentials plotted *vs*. Fc/Fc^+ as internal standard, 200 mV/s scan rate).

8 Circular Dichroism and Circularly Polarized Luminescence

In addition to the spectra in toluene shown in the manuscript, ECD spectra of **(*R*,*R*)-3** and **(*S*,*S*)-3** and of **(*M*)-** and **(*P*)-1** were also measured in CH_2Cl_2.

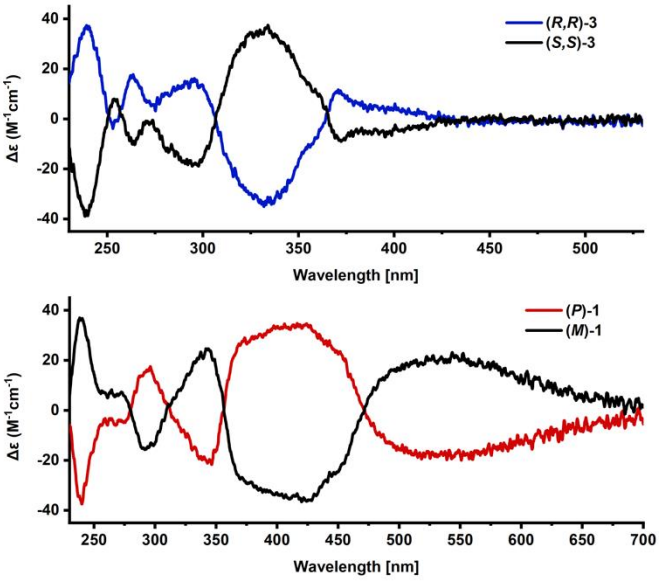

Figure S80. ECD spectra of **(*R*,*R*)-3** and **(*S*,*S*)-3** and of **(*M*)-** and **(*P*)-1** in CH_2Cl_2 (c = 10^{-4} M).

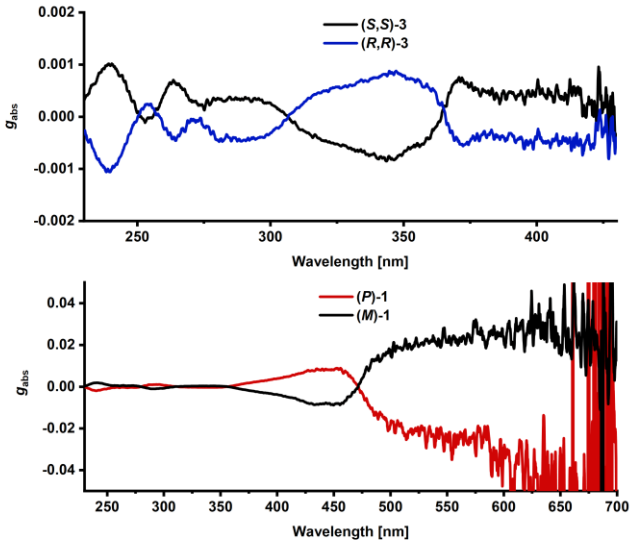

Figure S81. ECD spectra (g_{abs}) of **(*R*,*R*)-3** and **(*S*,*S*)-3** and of **(*M*)-** and **(*P*)-1** in CH_2Cl_2 (c = 10^{-4} M).

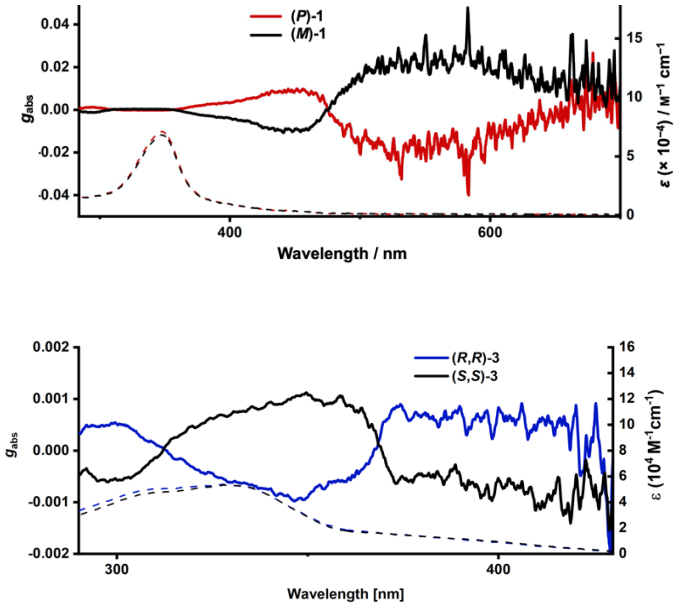

Figure S82. ECD spectra (g_{abs}, straight lines) and absorption (ε, dotted lines) of **(*R*,*R*)-3** and **(*S*,*S*)-3** in toluene (c = 0.5 x 10^{-4} M).

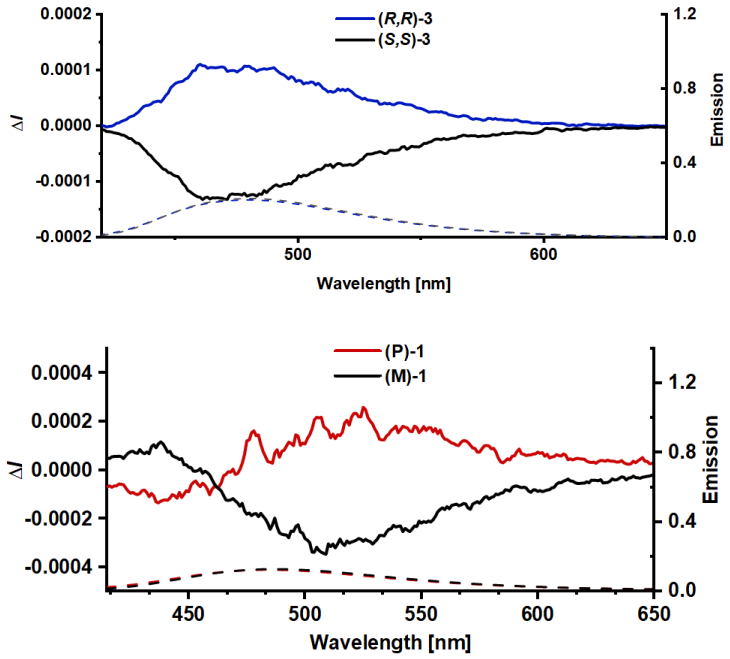

Figure S83. CPL (Δ*I*) spectra with fluorescence spectra for **(*R*,*R*)-3** and **(*S*,*S*)-3** and for **(*M*)-** and **(*P*)-1** (dotted lines) in toluene at 20 °C.

Due to the low quantum yields (Φ_F = 0.06) of **(*M*)-** and **(*P*)-1**, CPL signals had to be collected at rather high concentrations leading to a high optical density of the sample (and potential reabsorption of the emitted

light). Thus the presented data might not solely reflect the emission of circularly polarized light of compound **(*M*)-** and **(*P*)-1.**

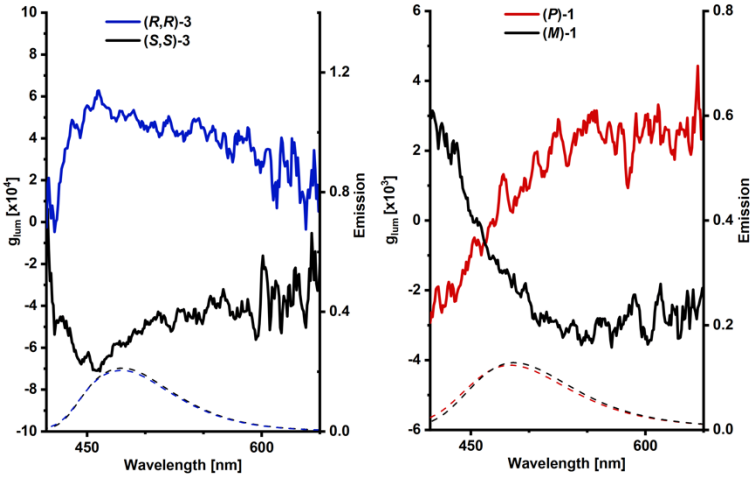

Figure S84. CPL (g_{lum}, straight lines) with fluorescence spectra for **(*M*)-** and **(*P*)-1** and **(*R*,*R*)-3** and **(*S*,*S*)-3** in toluene (20 °C).

The unusual shape of the CPL signal for **(*M*)-** and **(*P*)-1** might be rationalized with the help of the following graph combining CPL and ECD spectra, which illustrates the overlap of absorption and emission spectra with their chiroptical counterparts.

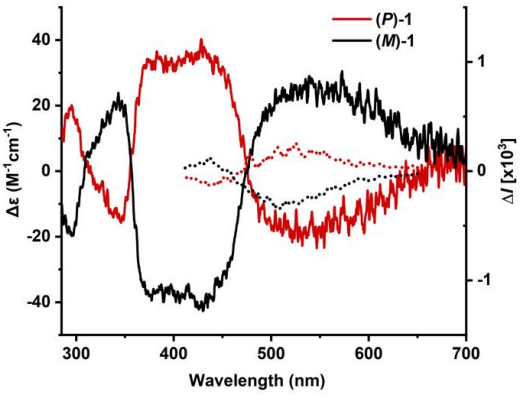

Figure S85. CPL (Δ*I*, dotted line) and ECD (Δε, straight line) spectra of **(*M*)-** and **(*P*)-1**.

The bisignate signals (Δ*I* and g_{lum}) in the CPL spectra occur at around 450 nm, which coincides with the onset of the longest wavelength polarized absorption band of these hoops. Hence it can be proposed that a part of the (CP-)light emitted by an isolated molecule is reabsorbed by the neighbouring molecules leading to this unusual bisigned signals. Thus, in those conditions, it is impossible to conclude about the emission of circularly polarized light of **(*M*)-** and **(*P*)-1**.

9 Thermodynamics of *ortho*-Tolyl-Rotation at the 5,10-Positions of DBP

To quantify the thermodynamic barrier for the rotation of sterically hindered mesityl substituents at the 5,10-positions of DBPs we conducted variable temperature-NMR measurements with a bis-*ortho*-tolyl-substituted DBP. With a coalescence temperature of 353 K we calculated the Free-Gibbs-Energy to be 18.9 kcal mol^{-1}. The two rotational isomers were also observed in the solid-state structure of **S7** (see chapter 10.2.9).

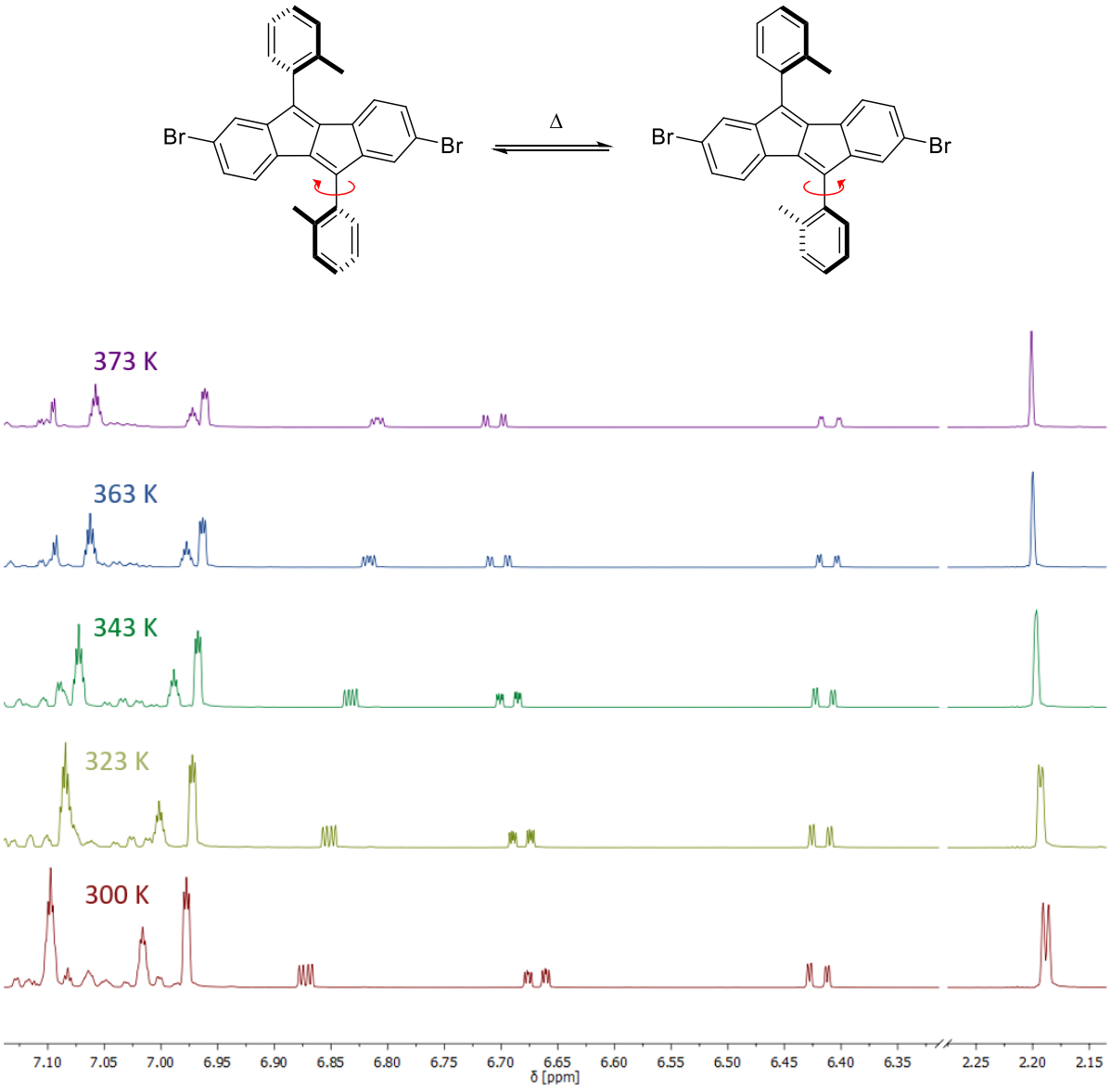

Figure S86. VT-NMR measurements (500 MHz) of bis-*ortho*-tolyl-DBP (**S7**) in toluene-d_8.

10 Single Crystal X-Ray Diffraction

10.1 General Experimental Setup and Solution

The crystals were mounted on a MITIGEN holder in perfluoroether oil. X-ray diffraction data were collected using a Bruker APEX2 QUAZAR three-circle diffractometer with a microfocus sealed X-ray tube using mirror optics as monochromator and a Bruker APEXII detector using MoK_α radiation (λ = 0.71073 Å) or a Bruker D8 VENTURE dual wavelength Mo/Cu three-circle diffractometer with a microfocus sealed X-ray tube using mirror optics as monochromator and a Bruker PHOTON III detector using CuK_α radiation (λ = 1.54184 Å). The diffractometers were equipped with an Oxford Cryostream 800 low temperature device and operating at T = 100 K. Data were measured using ω and ϕ scans scans.

All data were integrated with SAINT[9] and a multi-scan absorption correction using SADABS was applied.[10] The structures were solved by direct methods using SHELXT (2014/5)[11] and refined by full-matrix least-squares methods against F^2 by SHELXL-2018/3[12] using ShelXle (Rev 1172).[13] All non-hydrogen atoms were refined with anisotropic displacement parameters. The hydrogen atoms were refined isotropically on calculated positions using a riding model with their U_{iso} values constrained to 1.5 times the U_{eq} of their pivot atoms for terminal sp^3 carbon atoms and 1.2 times for all other carbon atoms. Disorder models were introduced by the program DSR.[14,15] Crystallographic data for the structures reported in this paper have been deposited with the Cambridge Crystallographic Data Centre.[16] These data can be obtained free of charge from The Cambridge Crystallographic Data Centre via www.ccdc.cam.ac.uk/structures. The CIF files were generated using FinalCif (v84).[17]

Table S1. Structural parameters.

Compound	**1•(CyH)(pentane)**	**2•(pentane)**	**2•$(PhCl)_2$ (i-PrOH)$_{0.5}$**	**(*S*,*S*)- 3•(PhCl)**
CCDC number	2057460	2055867	2057160	2057251
Empirical formula	$C_{81}H_{76}$	$C_{81}H_{68}$	$C_{179}H_{137}Cl_4O$	$C_{58}H_{37}ClO_2$
Formula weight	1049.41	1041.35	2445.68	801.32
Temperature [K]	100(2)	100(2)	100(2)	100(2)
Crystal system	orthorhombic	orthorhombic	monoclinic	monoclinic
Space group (number)	$Pbca$ (61)	$P2_12_12_1$ (19)	$C2/c$ (15)	$P2_1$ (4)
a [Å]	17.0179(16)	8.025(2)	55.534(5)	14.086(3)
b [Å]	18.630(2)	26.772(7)	8.9142(9)	13.495(3)
c [Å]	38.286(9)	27.166(7)	28.068(3)	22.525(5)
α [Å]	90	90	90	90
β [Å]	90	90	107.883(5)	106.657(9)
γ [Å]	90	90	90	90
Volume [Å^3]	12138(3)	5837(3)	13223(2)	4102.0(14)
Z	8	4	4	4
ρ_{calc} [g/cm^3]	1.148	1.185	1.228	1.298
μ [mm^{-1}]	0.483	0.067	1.254	1.179
F(000)	4496	2216	5148	1672
Crystal size [mm^3]	0.120×0.110×0.010	0.220×0.080×0.080	0.350×0.070×0.020	0.250×0.110×0.060
Crystal colour	red	red	red	yellow
Crystal shape	plate	block	plate	plate
Radiation	CuK_α (λ=1.54184 Å)	MoK_α (λ=0.71073 Å)	CuK_α (λ=1.54184 Å)	CuK_α (λ=1.54184 Å)
2Θ range [°]	4.62 to 109.86 (0.94 Å)	2.14 to 48.55 (0.86 Å)	6.43 to 116.88 (0.90 Å)	4.09 to 136.65 (0.83 Å)
Index ranges	−17 ≤ h ≤ 17 −19 ≤ k ≤ 19 −40 ≤ l ≤ 40	−9 ≤ h ≤ 9 −30 ≤ k ≤ 30 −31 ≤ l ≤ 31	−60 ≤ h ≤ 61 −9 ≤ k ≤ 9 −30 ≤ l ≤ 30	−16 ≤ h ≤ 14 −14 ≤ k ≤ 15 −27 ≤ l ≤ 26
Reflections collected	154610	53755	183762	111002
Independent reflections	7451 R_{int} = 0.1669 R_{sigma} = 0.0697	9430 R_{int} = 0.0587 R_{sigma} = 0.0569	9286 R_{int} = 0.0728 R_{sigma} = 0.0274	13955 R_{int} = 0.0506 R_{sigma} = 0.0363
Completeness	98.0 %	99.9 %	99.4 %	98.6 %
to θ =	54.928°	24.275°	58.439°	67.684°
Data / Restraints / Parameters	7451/307/787	9430/0/738	9286/1104/980	13955/1669/1099
Goodness-of-fit on F^2	1.060	1.057	1.070	1.039
Final R indexes [I≥2σ(I)]	R_1 = 0.0990 wR_2 = 0.2441	R_1 = 0.0529 wR_2 = 0.1153	R_1 = 0.0689 wR_2 = 0.1916	R_1 = 0.0502 wR_2 = 0.1170
Final R indexes [all data]	R_1 = 0.1683 wR_2 = 0.2878	R_1 = 0.0757 wR_2 = 0.1249	R_1 = 0.0810 wR_2 = 0.2016	R_1 = 0.0659 wR_2 = 0.1263
Largest peak/hole [eÅ^3]	0.42/–0.27	0.23/–0.22	0.60/–0.51	0.43/–0.35
Flack X parameter	–	–2.5(10)	–	0.020(5)
Extinction coefficient	0.00040(6)	–	–	–

Compound	**9**	**8a**	**5**
CCDC number	2043958	1965552	2036550
Empirical formula	$C_{48}H_{46}Br_2O_6$	$C_{64.79}H_{63.90}Cl_{0.10}N_{0.95}O_{10}$	$C_{28}H_{32}B_2O_6$
Formula weight	878.67	1019.52	486.15
Temperature [K]	100(2)	100(2)	100(2)
Crystal system	monoclinic	triclinic	triclinic
Space group (number)	$P2_1/c$ (14)	$P\overline{1}$ (2)	$P\overline{1}$ (2)
a [Å]	45.887(6)	13.254(7)	10.6190(7)
b [Å]	6.8800(8)	14.439(8)	11.0730(8)
c [Å]	12.5759(16)	15.761(8)	11.4420(9)
α [Å]	90	82.961(14)	88.121(3)
β [Å]	91.572(2)	67.977(10)	83.773(3)
γ [Å]	90	67.682(11)	83.522(3)
Volume [Å^3]	3968.8(8)	2586(2)	1328.63(17)
Z	4	2	2
ρ_{calc} [g/cm^3]	1.471	1.309	1.215
μ [mm^{-1}]	2.094	0.093	0.083
F(000)	1808	1082	516
Crystal size [mm^3]	0.15×0.11×0.03	0.160×0.120×0.040	0.320×0.300×0.070
Crystal colour	colourless	colourless	colourless
Crystal shape	needle	block	block
Radiation	MoK_α (λ=0.71073 Å)	MoK_α (λ=0.71073)	MoK_α (λ=0.71073 Å)
2Θ range [°]	1.78 to 55.09 (0.77 Å)	2.79 to 53.57	5.06 to 61.02 (0.70 Å)
Index ranges	–59 ≤ h ≤ 58 –8 ≤ k ≤ 8 –16 ≤ l ≤ 16	–16 ≤ h ≤ 16 –18 ≤ k ≤ 18 –19 ≤ l ≤ 19	–15 ≤ h ≤ 15 –15 ≤ k ≤ 15 –16 ≤ l ≤ 16
Reflections collected	54616	45409	61908
Independent reflections	8353 R_{int} = 0.0518 R_{sigma} = 0.0432	10981 R_{int} = 0.0820 R_{sigma} = 0.0851	8013 R_{int} = 0.0315 R_{sigma} = 0.0171
Completeness to θ = 25.242°	99.9 %	99.90	98.7 %
Data / Restraints / Parameters	8353/0/511	10981/1220/755	8013/301/499
Goodness-of-fit on F^2	1.053	1.040	1.048
Final *R* indexes [I≥2σ(I)]	R_1 = 0.0454 wR_2 = 0.1372	R_1 = 0.0553 wR_2 = 0.1180	R_1 = 0.0433 wR_2 = 0.1119
Final *R* indexes [all data]	R_1 = 0.0623 wR_2 = 0.1454	R_1 = 0.1116 wR_2 = 0.1389	R_1 = 0.0469 wR_2 = 0.1150
Largest peak/hole [eÅ^3]	0.50/–1.13	0.24/–0.33	0.45/–0.32

Compound	**S6**	**S7**
CCDC number	2064603	1479274
Empirical formula	$C_{16}H_{10}O_2$	$C_{30}H_{20}Br_2$
Formula weight	234.24	540.28
Temperature [K]	100(2)	100(2)
Crystal system	orthorhombic	monoclinic
Space group (number)	$P2_12_12_1$ (19)	$P2_1/n$ (14)
a [Å]	10.2477(7)	11.8475(8)
b [Å]	10.2877(5)	7.3631(4)
c [Å]	10.6997(5)	12.8990(8)
α [Å]	90	90
β [Å]	90	101.211(3)
γ [Å]	90	90
Volume [Å^3]	1128.02(11)	1103.76(12)
Z	4	2
ρ_{calc} [g/cm^3]	1.379	1.626
μ [mm^{-1}]	0.091	3.689
F(000)	488	540
Crystal size [mm^3]	0.200×0.130×0.050	0.220×0.150×0.060
Crystal colour	colourless	colourless
Crystal shape	block	needle
Radiation	MoK_α (λ=0.71073 Å)	MoK_α (λ=0.71073 Å)
2Θ range [°]	5.49 to 57.39 (0.74 Å)	4.27 to 72.31 (0.60 Å)
Index ranges	−13 ≤ h ≤ 12 −13 ≤ k ≤ 13 −14 ≤ l ≤ 14	−19 ≤ h ≤ 17 −11 ≤ k ≤ 11 −20 ≤ l ≤ 19
Reflections collected	30565	19418
Independent reflections	2877 R_{int} = 0.0329 R_{sigma} = 0.0145	4425 R_{int} = 0.0231 R_{sigma} = 0.0219
Completeness	100.0 %	100.0 %
to θ =	25.242°	25.242°
Data / Restraints / Parameters	2877/0/163	4425/106/193
Goodness-of-fit on F^2	1.063	1.320
Final *R* indexes [I≥2σ(I)]	R_1 = 0.0290 wR_2 = 0.0761	R_1 = 0.0344 wR_2 = 0.0754
Final *R* indexes [all data]	R_1 = 0.0303 wR_2 = 0.0769	R_1 = 0.0395 wR_2 = 0.0765
Largest peak/hole [eÅ^3]	0.22/−0.17	0.85/−0.40
Flack X parameter	−0.01(17)	
Extinction coefficient	–	

10.2 Refinement Details for Each Crystal

10.2.1 Crystal Structure of 1•(cyclohexane) (pentane)

Crystals suitable for X-ray diffraction were obtained by slow evaporation of a solution of a mixture of *n*-pentane, cyclohexane and dichloromethane solution at rt. The data was collected from a shock-cooled single crystal at 100(2) K on Bruker D8 VENTURE three-circle diffractometer and used CuK_α radiation.

The resolution of this structure is quite low because only light, weak scattering atoms are present in the structure. Furthermore, disordered solvent molecules, as well as a quite flexible main molecule are present. The data is still sufficient for a proof of the structure and connectivity. Because of the low C-C bond precision of 0.0109 Å, precise bond lengths cannot be discussed but the overall size of the molecule can be. Disordered moieties were refined using bond lengths restraints and displacement parameter restraints. The disorder model (*n*-pentane and cyclohexane) was introduced by the program DSR.[14,15]

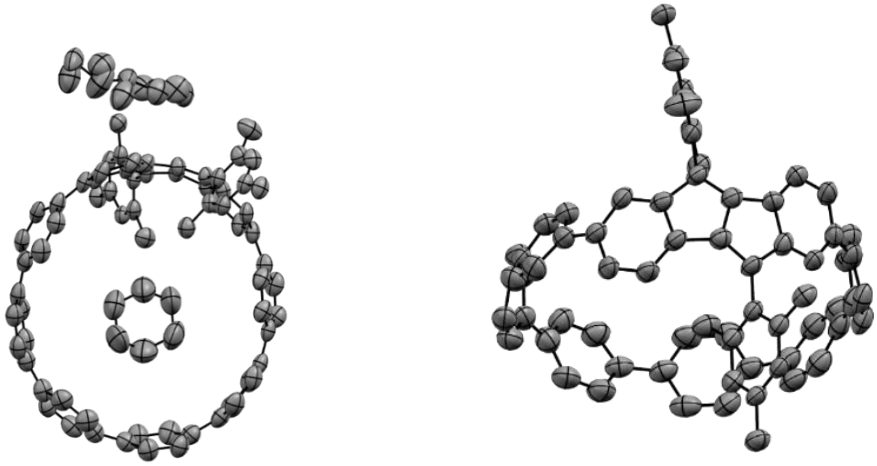

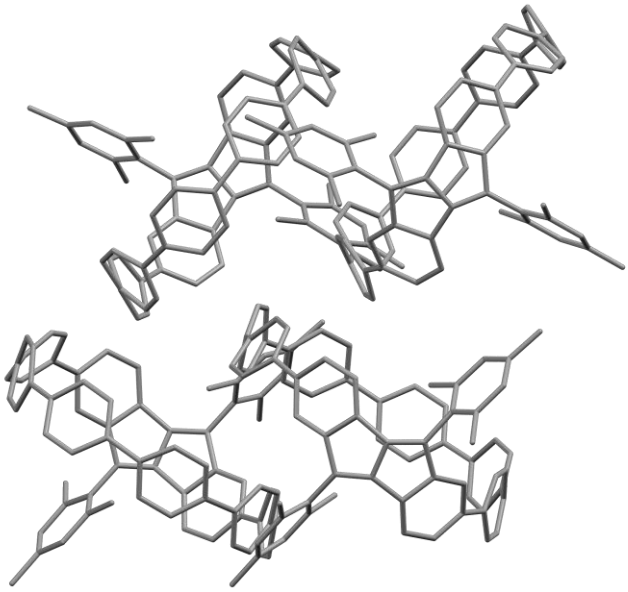

10.2.2 Crystal Structure of 2•(pentane)

Crystals suitable for x-ray diffraction were obtained by solvent layering of a $CDCl_3$ solution with *n*-pentane at rt. The data was collected from a shock-cooled single crystal at 100(2) K on a Bruker APEX2 QUAZAR three-circle diffractometer and used MoK_α radiation.

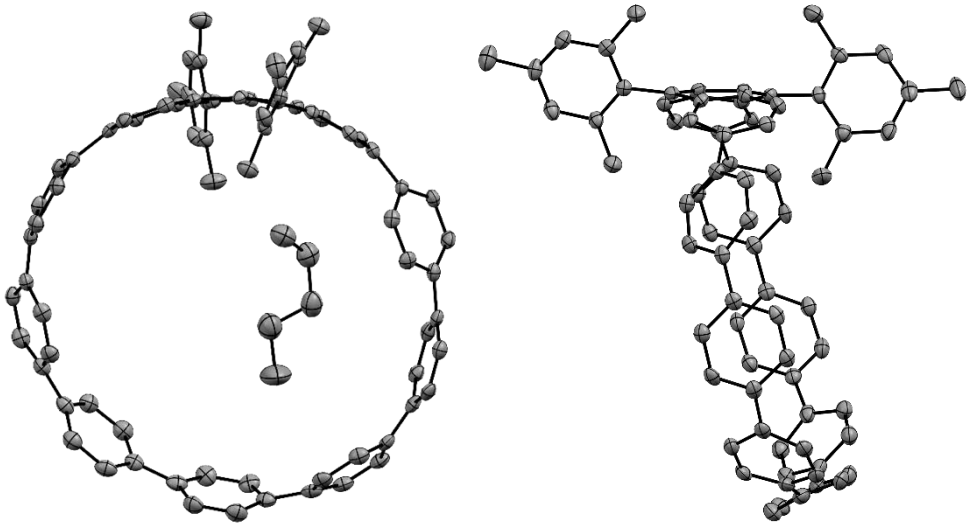

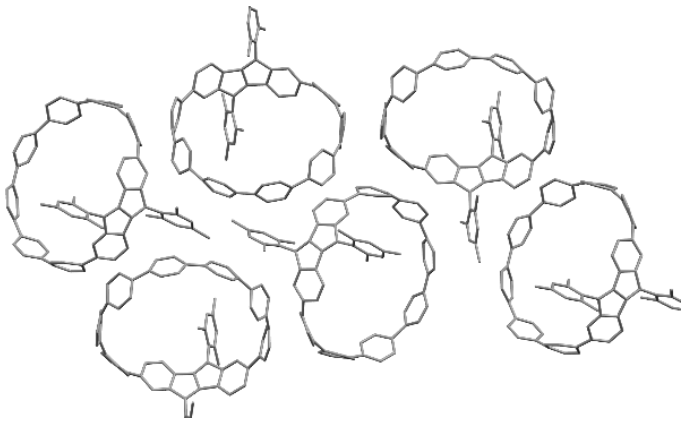

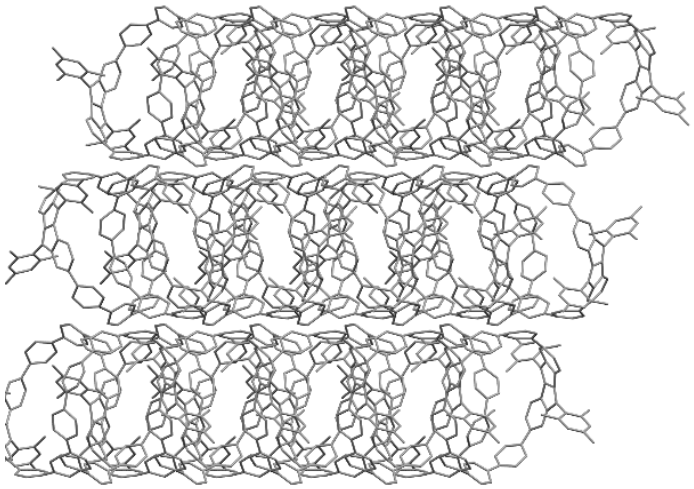

10.2.3 Crystal Structure of 2•(PhCl)2 (i PrOH)0.5

Crystals suitable for X-ray diffraction were obtained by slow diffusion of isopropanol into a chlorobenzene solution. The data was collected from a shock-cooled single crystal at 100(2) K on a Bruker D8 VENTURE three-circle diffractometer and used CuK_α radiation.

The structure contains three positions filled with solvent molecules. One chlorobenzene is located on a special position, one chlorobenzene is inside the hoop and disordered through rotation along ist long axis with 60%. The other position is occupied with chlorobenzene (50% occupation) and isopropanol (50% occupation). The hydrogen atom for the isopropanol was not modelled due to high disorder in this area. Disordered moieties were refined using bond lengths restraints and displacement parameter restraints. The disorder models were introduced by the program DSR.[14,15]

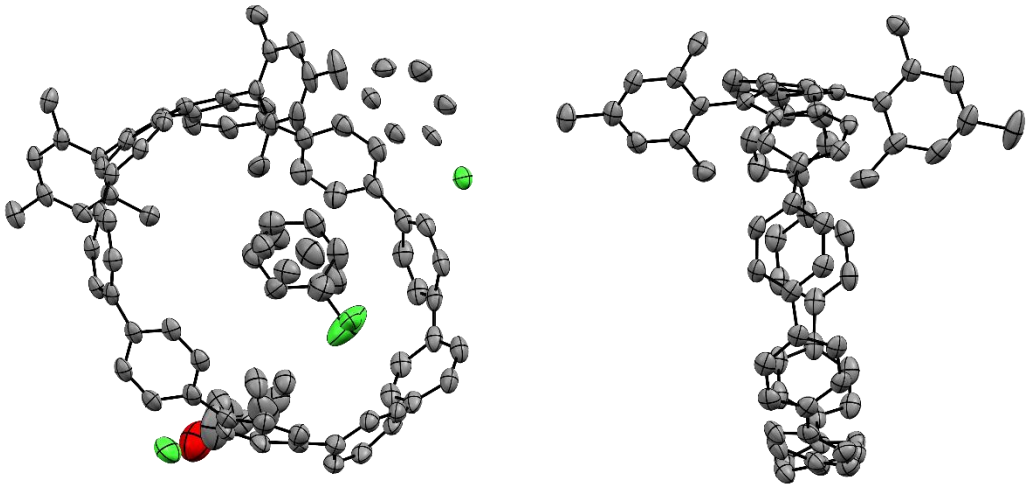

10.2.4 Crystal Structure of (S,S)-3•(PhCl)

Crystals suitable for X-ray diffraction were obtained by slow diffusion of methanol into a chlorobenzene solution. The data was collected from a shock-cooled single crystal at 100(2) K on a Bruker D8 VENTURE three-circle diffractometer and used CuK_α radiation. Displacement parameter restraints were employed for the main molecules.

There are two different molecules in the assymetric unit cell. Although the Flack X parameter is 0.020(5), the absolute structure can be assumed due to not varying too much from 0. Furthermore the enantiomeric purity of the compound was determined by chiral HPLC (see Figure S4), and the absolute structure can be assumed from the synthetic route, especially in comparison with the **compound S1** that was previously described.[4]

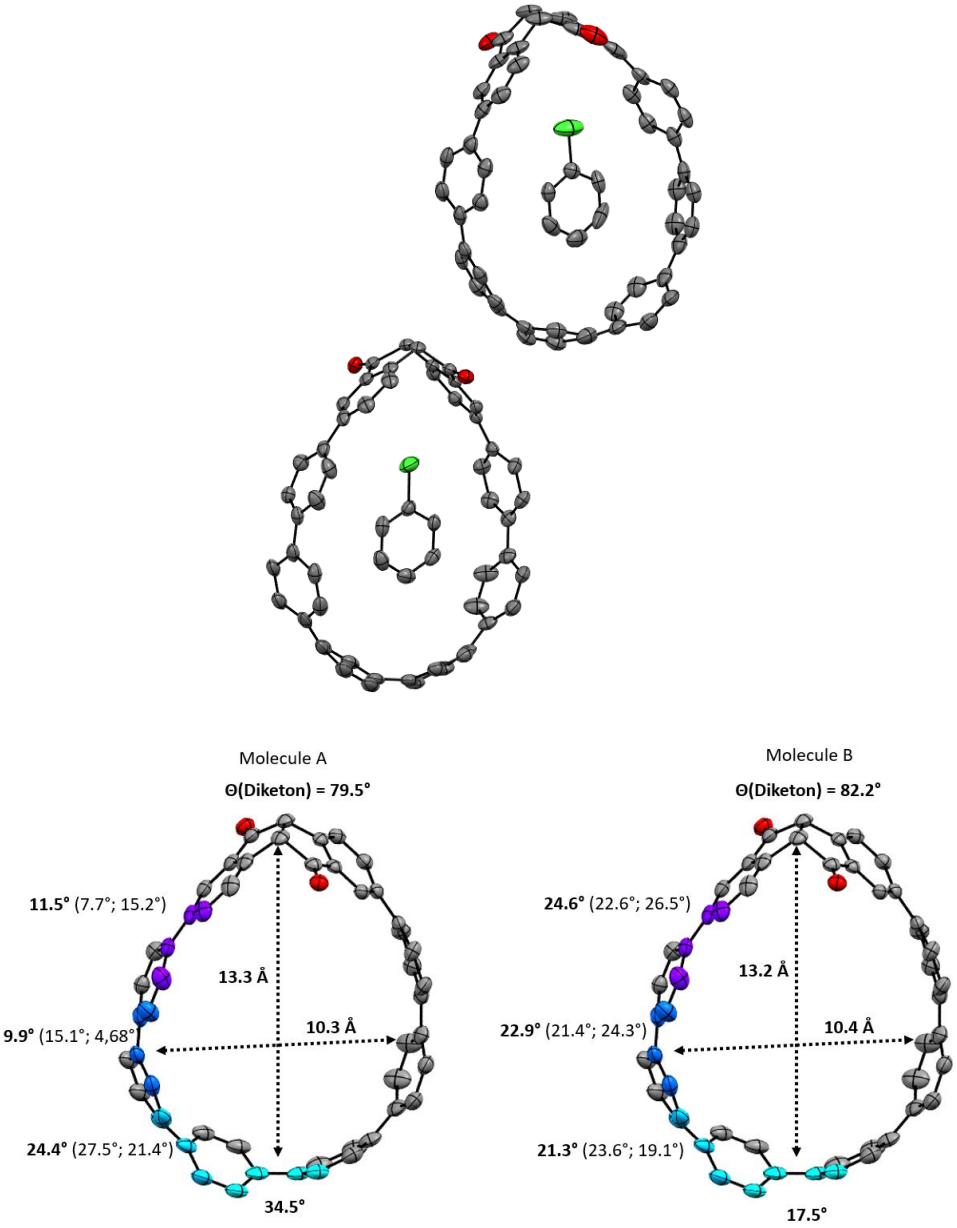

10.2.5 Crystal Structure of 9

Crystals suitable for X-ray diffraction were obtained by slow evaporation of an ethyl acetate solution. The data was collected from a shock-cooled single crystal at 100(2) K on a Bruker APEX2 QUAZAR three-circle diffractometer and used MoK_α radiation.

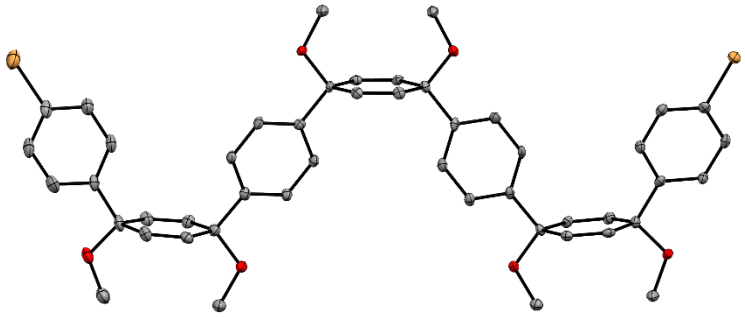

10.2.6 Crystal Structure of 8a

Crystals suitable for X-ray diffraction was obtained by slow diffusion of *n*-hexane into a chlorobenzene solution. The data was collected from a shock-cooled single crystal at 100(2) K on a Bruker APEX2 QUAZAR three-circle diffractometer and used MoK_α radiation.

One MOM group of the structure was disordered over two positions. Residual 2,2'-bipyridine from the cyclization step and CH_2Cl_2 were present in the crystal with 94.8% and 5.2% occupancy accordingly in the same position in the center of the cyclic structure. The CH_2Cl_2 molecule was heavily disordered, bond lengths were fixed with DFIX.

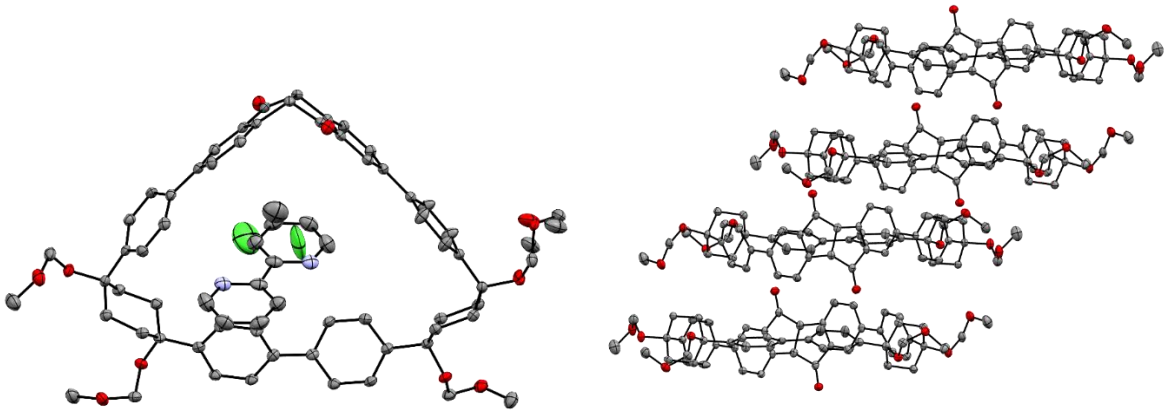

10.2.7 Crystal Structure of 5

Crystals suitable for X-ray diffraction were obtained by slow evaporation of an ethyl acetate solution. The data was collected from a shock-cooled single crystal at 100(2) K on a Bruker D8 VENTURE dual wavelength three-circle diffractometer and used MoK_α radiation. Both pinacolboron moieties were disordered and were refined using bond length restraints and displacement parameter restraints.

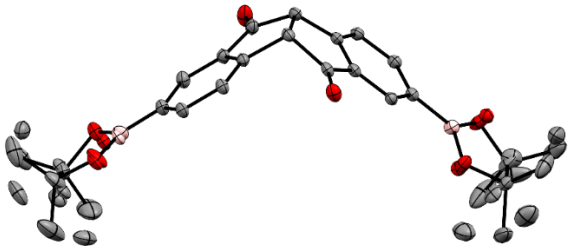

10.2.8 Crystal Structure of S6

Crystals suitable for X-ray diffraction were obtained by slow diffusion of *n*-hexane into a chlorobenzene solution. The data was collected from a shock-cooled single crystal at 100(2) K on a Bruker D8 VENTURE dual wavelength three-circle diffractometer and used MoK_α radiation.

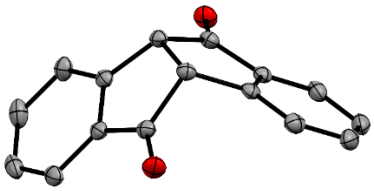

10.2.9 Crystal structure of S7

Crystals suitable for X-ray diffraction were obtained by slow evaporation of a dichloromethane solution. The data was collected from a shock-cooled single crystal at 100(2) K on a Bruker APEX2 QUAZAR three-circle diffractometer and used MoK_α radiation.

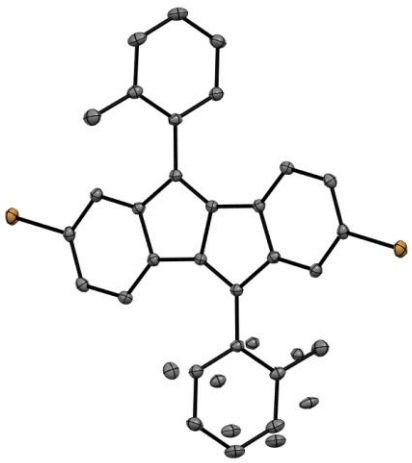

11 DFT Calculations

DFT calculations were performed with either the TURBOMOLE v7.4.1 or v7.5 program package[10], or the Gaussian 16 Rev.C.01 program package.[11] All structural modifications were done with Avogadro. Visualization and image generation of molecules were done with Avogadro, Chimera or VMD. All calculations were performed on the JUSTUS 2 High Performance Computing Cluster.[18]

The methodologies are explained in detail in the respective sub chapter alongside the used software. Initially structures of **1**, **2**, **3** and **4** were optimized on the PBEh-3c[19] level of theory without any symmetry restrictions. Stationary points on the PES were confirmed by vibrational frequency analysis (no imaginary frequency). These structures were further used to calculate frontier orbitals, theoretical UV/Vis and ECD spectra, and NICS(1)$_{iso}$ values, and as initial guess geometries for strain energy and rotational barrier calculations.

Cartesian coordinates can be found in a separate text file.

11.1 Strain Energies

Strain energies were calculated with the StrainViz[20] scheme developed by JASTI. The Gaussian program package was used applying the B3LYP[21,22] density functional and the 6-31G(d) (or 6-31G(d,p) for **1-Me-TS**) basis set.[23] The strain energies calculated for **3**, **8a**, **8b**, DBP[*n*]CPPs **1** and **2** and the rotational transition state of **1-Me** are shown in Table S2 below. Graphic representations of the localized strain energy are further given in Figure S87.

Table S2. Calculated fractional and total strain energies.

Strain[a)]	**3 (A)**	**1 (B)**	**2 (C)**	**1-Me-TS (D)**	**8b (E)**	**8a (F)**
Total	**51.7**	**68.4**	**63.4**	**100.7**	**9.3**	**11.9**
Bond	1.0	1.6	1.8	9.7	0.3	0.4
Angle	3.3	4.1	4.9	21.4	1.1	1.7
Dihedral	47.3	62.6	56.7	69.6	7.9	9.7

[a)] All energies are given in kcal·mol^{-1}

Compound **3**

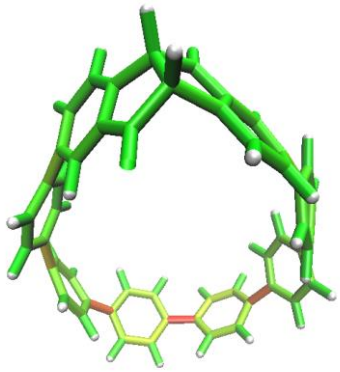

Compound **1**

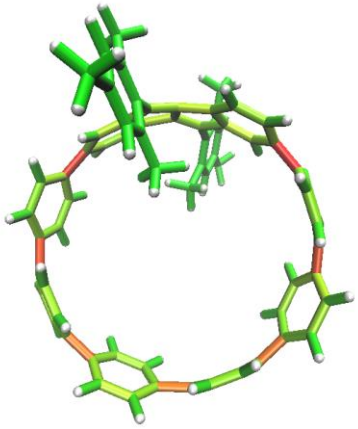

Compound **2**

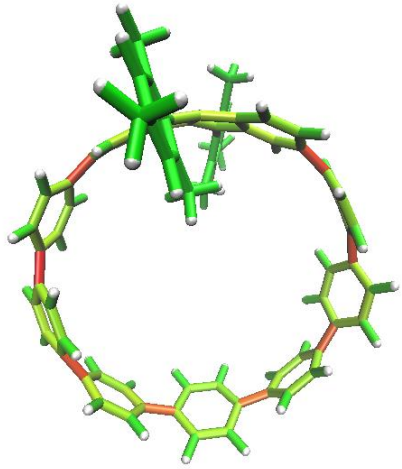

Compound **1-Me-TS**

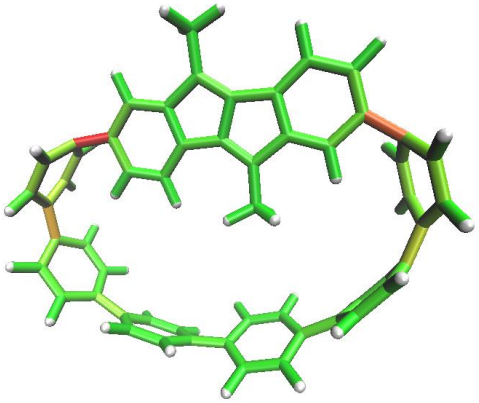

Compound **8b**

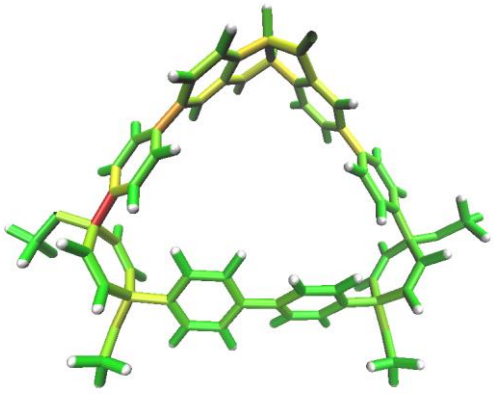

Compound **8a**

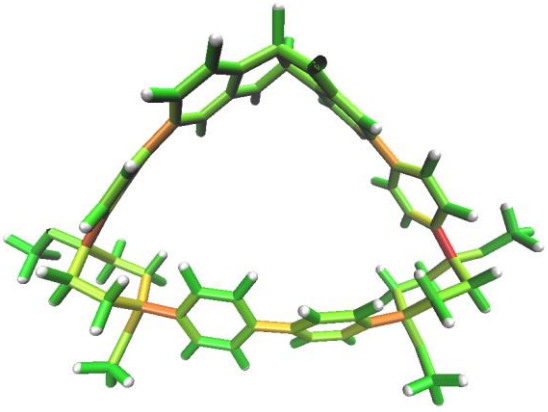

Figure S87. Graphic representations of the calculated localized strain energies.

In the figure below the strain energies of several DBP[*n*]CPP hoops plotted as a function of the respective hoop diameter. Additionally, the strain energies for [*n*]CPPs with n = 5 – 10 are shown. Values for [*n*]CPPs are taken from the literature.[20,24]

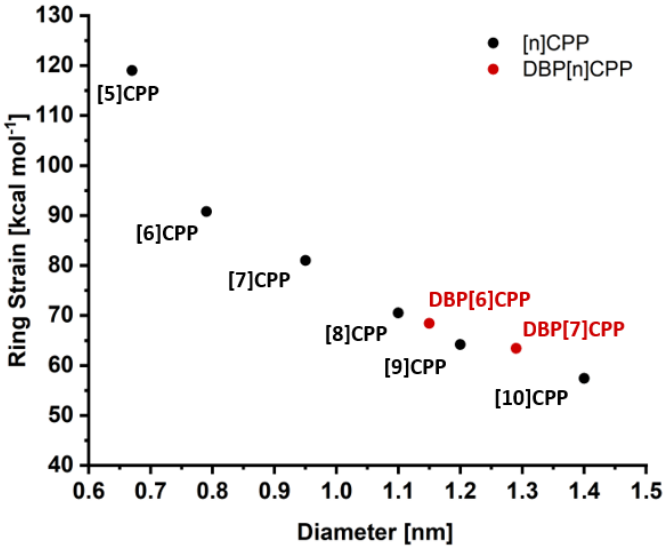

Figure S88. Correlation between calculated strain energy and hoop diameter in selected DBP[*n*]CPPs and [*n*]CPPs.

11.2 Calculation of Racemization Barriers

Calculation of transition states were done with the TS option applying the Berny algorithm as implemented in the Gaussian program package. The B3LYP[21,22] functional and the 6-31G(d,p) basis set[23] was used. Transition states were confirmed by the presence of one imaginary frequency. For the calculation of rotational barriers for **1** and **2** we replaced the mesityl with methyl groups, because the transition state search with the larger aromatic substituent did not lead to any result, most likely due to repulsion with the paraphenylene linkers.

Table S3. Calculated energies of the ground- and transition states.

	1-Me	**2-Me**
E_{TS} [Eh]	–2079.38122	–2310.47294
$ZPVE_{TS}$ [Eh]	0.72298	0.80423
Imag. Frequency [cm^{-1}]	–35.35	–31.48
E_{GS} [Eh]	–2079.44064	–2310.51699
$ZPVE_{GS}$ [Eh]	0.72426	0.80543
ΔE [Eh]	0.059413	0.044040
ΔE [kcal·mol^{-1}]	**36.5**	**26.9**

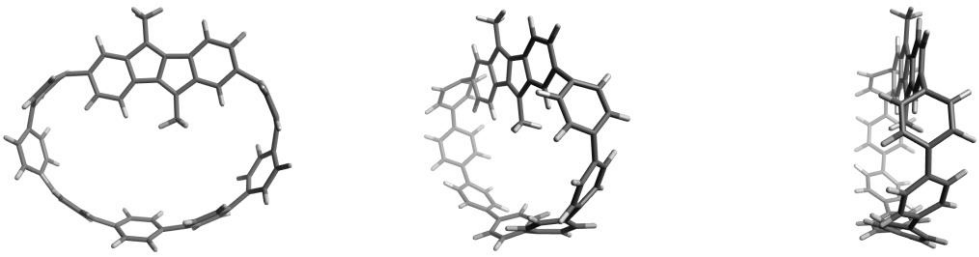

Figure S89. Representation of the transition state structure of **2-Me**.

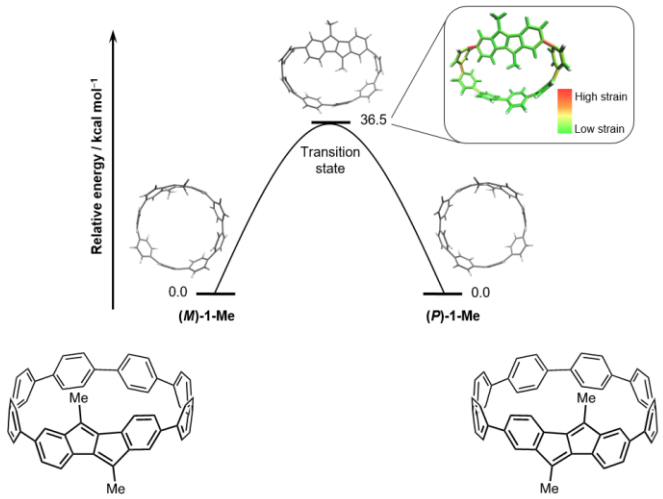

Figure S90. Calculated racemization pathway from **(*M*)-** to **(*P*)-1-Me** with StrainViz analysis of the transition state.

11.3 NICS Calculations

NICS(1)$_{iso}$ calculation were done with the GIAO method (B3LYP/6-31G(d)-SP//PBEh3c) and with dummy atoms placed 1 Å above and below the respective ring of the DBP unit. Negative NICS values indicate a diatropic ring current (associated with an aromatic character) while positive NICS values indicate a paratropic ring current (associated with an antiaromatic character). NICS(1)$_{ZZ}$ values were then calculated with the tensors from above calculation and the program Multiwfn.[25]

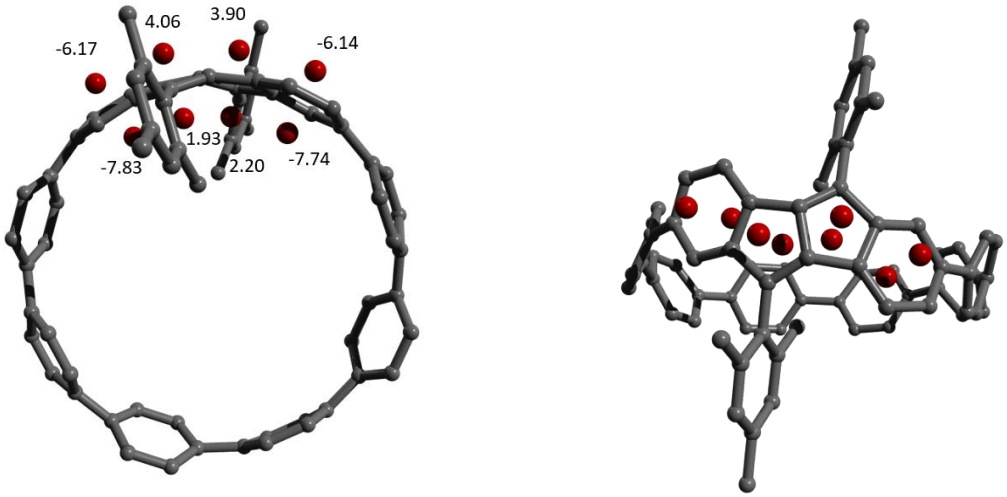

Figure S91. Representation of the placed dummy atoms used in NICS calculations with **1** as example.

Table S4. Calculated NICS(1)$_{iso}$ values (average of the two symmetrically equivalent ones each) on the B3LYP/6-31G(d) level of theory.

	6-membered ring	5- membered ring	
1	–6.2	4.0	*outside*
	–7.8	2.1	*inside*
2	–6.0	4.3	*outside*
	–7.5	2.6	*inside*

Table 5. Calculated NICS(1)$_{ZZ}$ values on the B3LYP/6-31G(d) level of theory.

	6-membered ring	5- membered ring	
1	–13.8	16.0	*outside*
	–17.9	17.3	*inside*
2	–13.2	17.4	*outside*
	–16.5	18.9	*inside*

11.4 TD-DFT Calculations

Single Point calculations of **1** – **4** were conducted with the Turbomole program package on the PW6B95[26]-D3(BJ)[27,28]/def2-QZVPP[29] level of theory. Frontier molecular orbitals of **1 and 3** are shown in the manuscript. Frontier molecular orbitals of **2** and **4** are shown below.

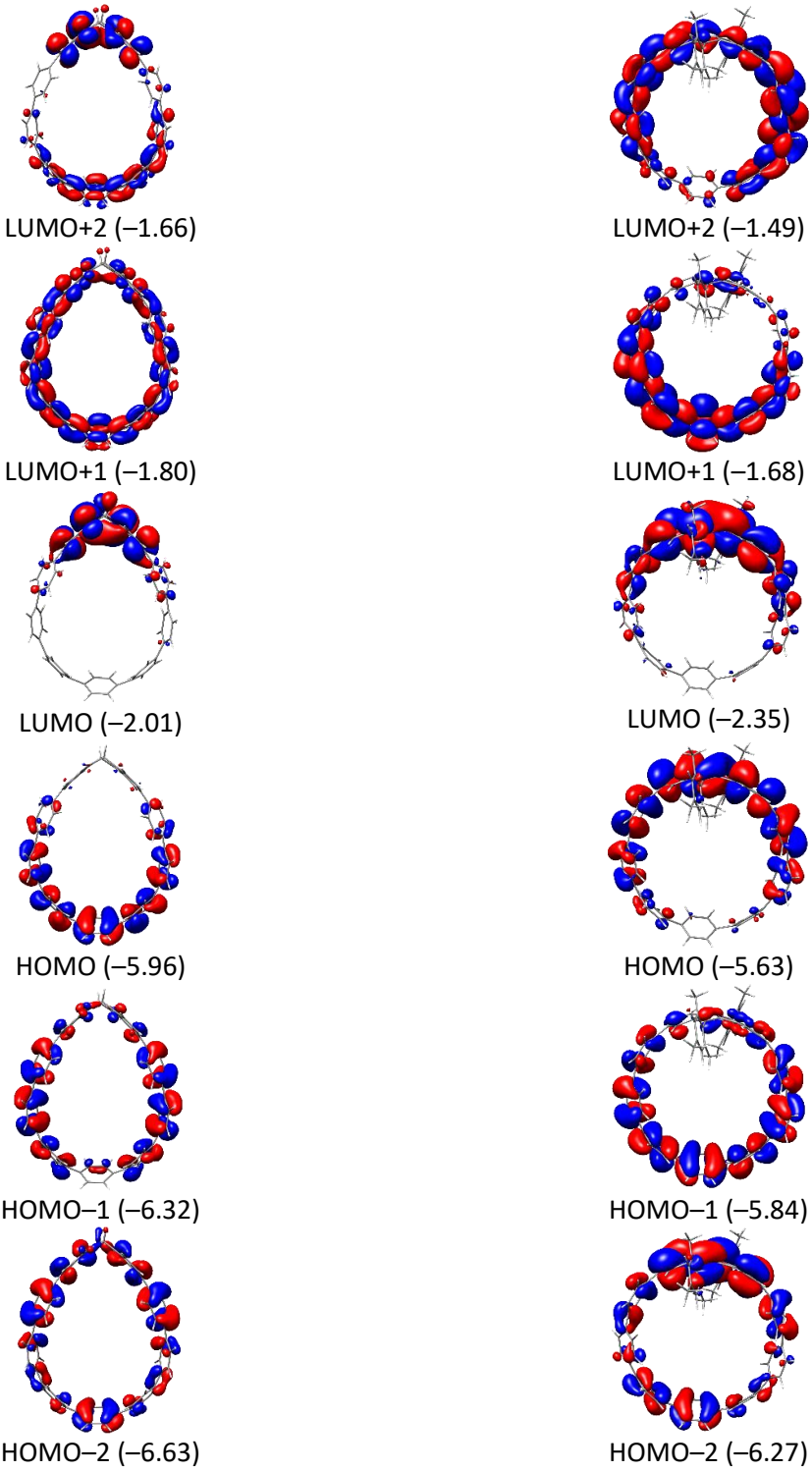

Figure S92. Frontier molecular orbitals (with energies in eV) of **4** (left) and **2** (right).

For assignment of the observed transitions in the absorption spectra we calculated the first 10 singlet excitations for **1** - **4**. These TD-DFT calculations were performed within the Gaussian program package on the CAM-B3LYP[30]/6-31G(d,p)/PCM[31](CH_2Cl_2) level of theory using the PBEh-3c optimized geometries. The calculated oscillator strengths were visualized using SpecDis v1.70 applying a gaussian band shape. In the figure below the theoretical spectra are plotted alongside the experimental spectra.

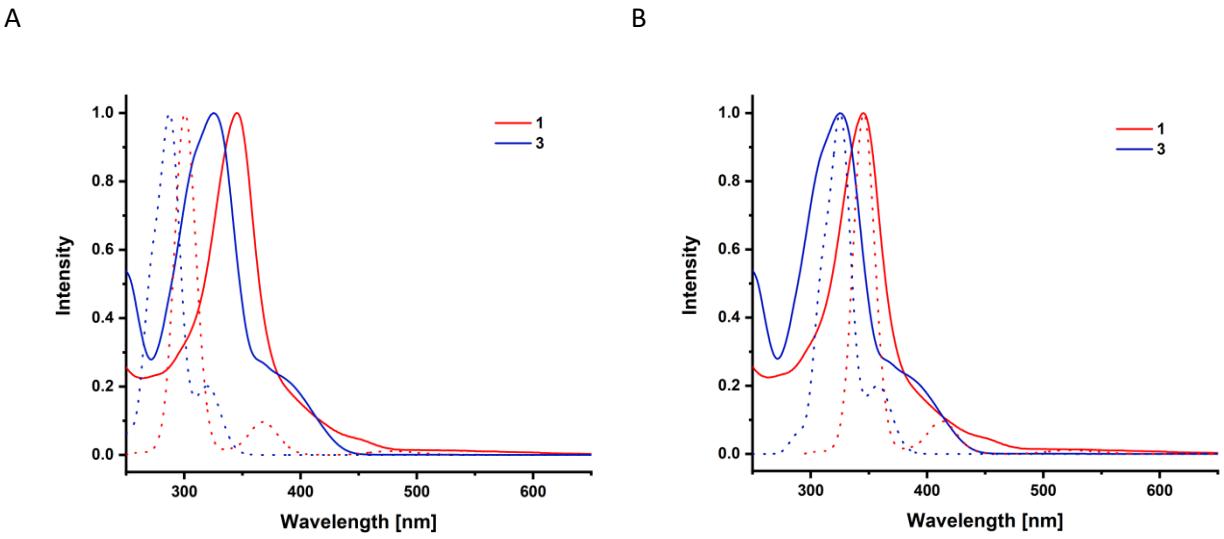

Figure S93. Theoretical (dotted lines) and experimental (straight lines) spectra of **1** and **3** (A: no referencing applied, B: referenced for the absorption maxima).

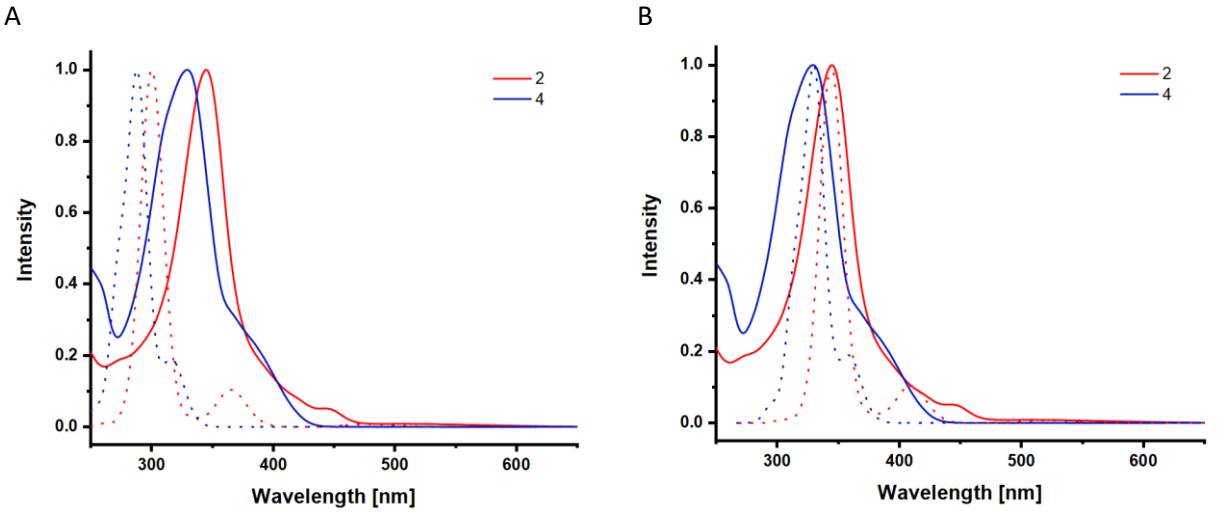

Figure S94. Theoretical (dotted lines) and experimental (straight lines) spectra of **2** and **4** (A: no referencing applied, B: referenced for the absorption maxima).

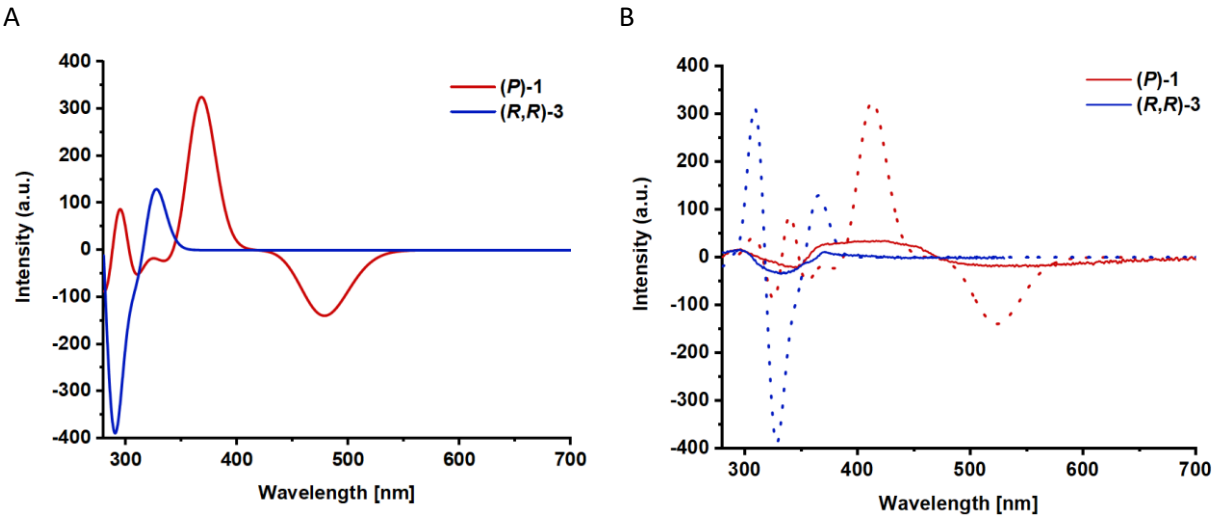

Figure S95. A) Plot of theoretical (no referencing applied) ECD spectra of **(*R*,*R*)-3** and **(*P*)-1** and B) combined plot of theoretical (dotted lines, referenced) and experimental (straight lines) spectra of **(*R*,*R*)-3** and **(*P*)-1**.

Table S6. Calculated transitions for **1**.

#	λ	f_{osc}	from	to
1	479	0.04	HOMO	LUMO
2	368	0.34	HOMO–2	LUMO
3	339	0.05	HOMO–1	LUMO
			HOMO–1	LUMO+1
			HOMO	LUMO+2
4	304	1.66	HOMO–3	LUMO
			HOMO–1	LUMO+3
			HOMO	LUMO+1
5	302	0.56	HOMO–4	LUMO
			HOMO–1	LUMO+1
6	297	1.64	HOMO	LUMO+3
			HOMO	LUMO+4
7	295	0.00	HOMO–5	LUMO
8	288	0.01	HOMO–6	LUMO
9	283	0.11	HOMO–3	LUMO
			HOMO–9	LUMO
10	265	0.01	HOMO–8	LUMO
			HOMO–2	LUMO

Table S7. Calculated transitions for **2**

#	λ	f_{osc}	from	to
1	478	0.03	HOMO	LUMO
2	365	0.41	HOMO–2	LUMO
3	333	0.09	HOMO–1	LUMO+1
			HOMO	LUMO+2
			HOMO–1	LUMO
4	304	1.83	HOMO–1	LUMO+1
			HOMO–1	LUMO+2
			HOMO–4	LUMO
			HOMO	LUMO+2
5	299	1.65	HOMO–1	LUMO+2
			HOMO–3	LUMO
			HOMO–4	LUMO
			HOMO	LUMO+1
6	297	0.02	HOMO–5	LUMO
7	294	0.92	HOMO	LUMO+2
			HOMO	LUMO+3
			HOMO–4	LUMO
8	288	0.07	HOMO–6	LUMO
			HOMO	LUMO+2
9	280	0.14	HOMO–9	LUMO
			HOMO	LUMO+1
			HOMO–3	LUMO
10	265	0.004	HOMO–8	LUMO
			HOMO–7	LUMO

Table S8. Calculated transitions for **3**.

#	λ	f_{osc}	from	to
1	324	0.26	HOMO	LUMO+1
2	316	0.12	HOMO–10	LUMO
			HOMO–13	LUMO+2
			HOMO–6	LUMO
3	311	0.10	HOMO–13	LUMO
			HOMO–10	LUMO+2
			HOMO–2	LUMO
4	289	1.66	HOMO–1	LUMO+1
			HOMO	LUMO+3
5	280	0.39	HOMO–3	LUMO+2
			HOMO–2	LUMO
			HOMO–1	LUMO+1
			HOMO	LUMO+3
6	279	0.10	HOMO–1	LUMO
7	271	0.80	HOMO–2	LUMO+1
			HOMO–1	LUMO+3
8	259	0.06	HOMO	LUMO+6
9	253	0.00	HOMO–1	LUMO+5
10	251	0.08	HOMO	LUMO+8

Table S9. Calculated transitions for **4**

#	λ	f_{osc}	from	to
1	320	0.12	HOMO	LUMO+1
2	316	0.32	HOMO	LUMO+1
			HOMO–6	LUMO
			HOMO–3	LUMO
3	309	0.07	HOMO–15	LUMO
			HOMO–4	LUMO
4	289	2.39	HOMO–1	LUMO+1
			HOMO	LUMO+3
5	280	0.14	HOMO–2	LUMO
			HOMO–3	LUMO+2
6	275	0.13	HOMO–2	LUMO+2
			HOMO–1	LUMO
			HOMO–3	LUMO
7	272	0.91	HOMO–2	LUMO+1
			HOMO	LUMO+4
			HOMO–1	LUMO+3
8	257	0.07	HOMO	LUMO+7
			HOMO	LUMO+5
9	254	0.005	HOMO	LUMO+7
			HOMO–1	LUMO+4
10	252	0.07	HOMO	LUMO+6
			HOMO	LUMO+8

12 References

1 H. E. Gottlieb, V. Kotlyar and A. Nudelman, *J. Org. Chem.*, 1997, **62**, 7512–7515.

2 B. W. D'Andrade, S. Datta, S. R. Forrest, P. Djurovich, E. Polikarpov and M. E. Thompson, *Org. Electron.*, 2005, **6**, 11–20.

3 H. Tanaka, Y. Inoue and T. Mori, *ChemPhotoChem*, 2018, **2**, 386–402.

4 M. Hermann, D. Wassy, J. Kohn, P. Seitz, M. U. Betschart, S. Grimme and B. Esser, *Angew. Chem. Int. Ed.*, 2021, DOI: 10.1002/anie.202016968.

5 H. Omachi, S. Matsuura, Y. Segawa and K. Itami, *Angew. Chem. Int. Ed.*, 2010, **49**, 10202–10205.

6 J. Wang, G. Zhuang, Q. Huang, Y. Xiao, Y. Zhou, H. Liu and P. Du, *Chem. Commun.*, 2019, 2–5.

7 Q. Huang, G. Zhuang, H. Jia, M. Qian, S. Cui, S. Yang and P. Du, *Angew. Chem. Int. Ed.*, 2019, **58**, 6244–6249.

8 G. P. Moss, *Pure Appl. Chem.*, 1996, **68**, 2193–2222.

9 *SAINT V8.37A, Bruker AXS*, Madison, Wisconsin, USA, 2015.

10 L. Krause, R. Herbst-Irmer, G. M. Sheldrick and D. Stalke, *J. Appl. Crystallogr.*, 2015, **48**, 3–10.

11 G. M. Sheldrick, *Acta Crystallogr. Sect. A Found. Adv.*, 2015, **71**, 3–8.

12 G. M. Sheldrick, *Acta Crystallogr. Sect. C Struct. Chem.*, 2015, **71**, 3–8.

13 C. B. Hübschle, G. M. Sheldrick and B. Dittrich, *J. Appl. Crystallogr.*, 2011, **44**, 1281–1284.

14 D. Kratzert, J. J. Holstein and I. Krossing, *J. Appl. Crystallogr.*, 2015, **48**, 933–938.

15 D. Kratzert and I. Krossing, *J. Appl. Crystallogr.*, 2018, **51**, 928–934.

16 C. R. Groom, I. J. Bruno, M. P. Lightfoot and S. C. Ward, *Acta Crystallogr. Sect. B Struct. Sci. Cryst. Eng. Mater.*, 2016, **72**, 171–179.

17 D. Kratzert, FinalCif, https://www.xs3.uni-freiburg.de/research/finalcif, 2020.

18 Justus II, High Performance Computing for Computational Chemistry and Quantum Sciences, State of Baden Württemberg, https://www.wiki.bwhpc.de

19 S. Grimme, J. G. Brandenburg, C. Bannwarth and A. Hansen, *J. Chem. Phys.*, 2015, **143**, 054107.

20 C. E. Colwell, T. W. Price, T. Stauch and R. Jasti, *Chem. Sci.*, 2020, **11**, 3923–3930.

21 A. D. Becke, *J. Chem. Phys.*, 1993, **98**, 5648–5652.

22 P. J. Stephens, F. J. Devlin, C. F. Chabalowski and M. J. Frisch, *J. Phys. Chem.*, 1994, **98**, 11623–11627.

23 R. Ditchfield, W. J. Hehre and J. A. Pople, *J. Chem. Phys.*, 1971, **54**, 720–723.

24 E. R. Darzi and R. Jasti, *Chem. Soc. Rev.*, 2015, **44**, 6401–6410.

25 T. Lu and F. Chen, *J. Comput. Chem.*, 2012, **33**, 580–592.

26 Y. Zhao and D. G. Truhlar, *J. Phys. Chem. A*, 2005, **109**, 5656–5667.

27 S. Grimme, J. Antony, S. Ehrlich and H. Krieg, *J. Chem. Phys.*, 2010, **132**, 154104.

28 S. Grimme, S. Ehrlich and L. Goerigk, *J. Comput. Chem.*, 2011, **32**, 1456–1465.

29 F. Weigend, *Phys. Chem. Chem. Phys.*, 2006, **8**, 1057–1065.

30 T. Yanai, D. P. Tew and N. C. Handy, *Chem. Phys. Lett.*, 2004, **393**, 51–57.

31 S. Miertuš, E. Scrocco and J. Tomasi, *Chem. Phys.*, 1981, **55**, 117–129.